

Screening for components involved in
NLR-mediated immune signalling

Inaugural-Dissertation

zur

Erlangung des Doktorgrades

**der Mathematisch-Naturwissenschaftlichen Fakultät
der Universität zu Köln**

vorgelegt von

Harald Frank Bielig

aus Neuss

Köln 2012

Berichtersteller: Prof. Dr. Jonathan Howard

Prof. Dr. Mats Paulsson

Tag der mündlichen Prüfung: 13.04.2012

Table of contents

Table of contents	I
Abbreviations	III
Symbols for amino acids	VIII
1 Introduction	1
1.1 Innate immunity and pattern recognition receptors	1
1.2 NLRs	3
1.3 NOD1 and NOD2	5
1.3.1 Signalling pathways and regulation	5
1.3.2 Bacterial sensing and physiological relevance of NOD1 and NOD2	8
1.4 Apoptosis: Programmed cell death	13
1.5 The BIRC-family: Functions beyond inhibition of apoptosis	14
1.6 RNAi and systematic screening approaches	16
1.7 Aim of the study	18
2 Materials and Methods	19
2.1 Materials	19
2.1.1 Cell lines and bacteria	19
2.1.2 Chemicals, reagents and enzymes	21
2.1.3 Kits	22
2.1.4 Plasmids	22
2.1.5 Primer	23
2.1.6 siRNAs	24
2.1.7 Antibodies	25
2.1.8 Instruments	25
2.1.9 Software	26
2.2 Methods	27
2.2.1 Cell biological methods	27
2.2.2 Screening protocols	31
2.2.3 Molecular biological methods	34
2.2.4 Biochemical methods	38
3 Results	41
3.1 High-throughput siRNA screen to identify factors involved in NOD1 signalling	41
3.1.1 Establishment of the assay system in HEK293T cells	42
3.1.1.1 Establishment of the reporter system	42
3.1.1.2 Establishment of the siRNA knock-down conditions	45
3.1.1.3 Proof of principle for the differential read-out	46
3.1.1.4 Validation of the assay principle	47
3.1.1.5 Downscaling and automation of the protocol	48
3.1.2 Pilot screen with an apoptosis library	49
3.1.3 Druggable genome screen	52
3.1.3.1 Primary druggable genome screen	52
3.1.3.2 Validation and TNF- α counter-screen	53
3.1.4 THP1-Blue validation screen	55
3.1.4.1 Assay setup, downscaling and automation	55
3.1.4.2 THP1 screen and results	59
3.1.5 Final hitlist generation	60
3.1.6 Hit validation: XIAP	62
3.1.7 Hit validation: BMPR-2	65

TABLE OF CONTENTS

3.1.8 Analysis of the roles of BIRC proteins in NOD1 signalling	68
3.2 Bacterial outer-membrane vesicles trigger NOD-mediated inflammatory responses in a quorum sensing-dependent manner	70
3.2.1 Activation of NOD1 and NOD2 by extracellular bacteria	70
3.2.2 The role of quorum sensing in subverting host-detection by NODs	73
4 Discussion	77
4.1 Screen results	77
4.1.1 Pilot screen	77
4.1.2 Druggable genome screen	78
4.1.3 Comparison with published screens	81
4.1.4 XIAP and BMPR-2 are involved in NOD1 signalling	84
4.2 Roles for BIRC proteins in NOD1 signalling	88
4.3 <i>V. cholerae</i> OMVs trigger NOD signalling in a quorum sensing-dependent manner	90
5 References	93
6 Abstract	108
7 Zusammenfassung	110
Danksagung	112
Erklärung	113
Kollaborationserklärung	114
Lebenslauf	115

Abbreviations

°C	degree Celsius
µg	microgramme
µl	microlitre
A	desoxyadenosine
A20	TNFAIP3, tumor necrosis factor, alpha-induced protein 3
AAMP	angio-associated migratory cell protein
ADP	adenosine diphosphate
AIM2	absent in melanoma 2
AMP	anti-microbial peptide
AP-1	activator protein 1
APAF1	apoptotic protease-activating factor 1
APS	ammonium persulfate
ASC	apoptosis-associated speck-like protein containing a CARD
ATG16L1	ATG16 autophagy related 16-like 1 (<i>S. cerevisiae</i>)
ATP	adenosine triphosphate
BCL-2	B cell lymphoma 2
BID	BH3 interacting domain death agonist
BIR	baculovirus inhibitory repeat
BIRC	baculoviral IAP repeat containing
BISC	BMP-induced signalling complex
BMDMs	bone marrow-derived macrophages
BMP	bone morphogenetic protein
BMPR	bone morphogenetic protein receptor
bp	basepairs
Bruce	also BIRC6, Appollon
BS	Blau syndrome
BSA	bovine serum albumin
C	desoxycytidine
CARD	caspase activating and recruitment domain
caspase	cysteine-dependent aspartate-directed proteases
CC	coiled-coil
CD	Crohn's disease
CDH1	cadherin 1, type 1; also E-cadherin
cDNA	complementary DNA
CENTB1	Centaurin beta 1
CHUK	conserved helix-loop-helix ubiquitous kinase; also IKKα
CHX	cycloheximide
cIAP	cellular inhibitor of apoptosis
CLR	C-type lectin receptor
C-terminus	carboxyl-terminus
CTNNB1	β-catenin
CUL1	cullin 1
CYLD	cylindromatosis (turban tumor syndrome)
DAMP	danger-associated molecular pattern
DAP	diaminopimelic acid
DIAP2	<i>Drosophila</i> IAP 2
DISC	death-induced signalling complex

ABBREVIATIONS

DMEM	Dulbecco's modified Eagle's medium
DMSO	dimethylsulfoxide
DNA	desoxyribonucleic acid
dNTP	desoxynucleotide triphosphate
ds	double stranded
EDTA	ethylenediaminetetraacetic acid
ELISA	enzyme-linked immunosorbent assay
EM	electron microscopy
Erbin	ErbB2 interacting protein
ERK	extracellular-signal-regulated kinase; also p44/42
<i>et al.</i>	<i>et alii</i> ; and others
FBS	fetal bovine serum
<i>g</i>	gravitational force
g	gramme
G	desoxyguanosine
GAPDH	glyceraldehyd-3-phosphat-dehydrogenase
GDF-5	growth and differentiation factor 5
GEF-H1	guanine nucleotide exchange factor H1
GO	gene ontology
GPR17	G protein-coupled receptor
GRIM-19	gene associated with retinoid-interferon-induced mortality 19
GTP	guanosine triphosphate
h	hour
HapR	hemagglutinin/protease regulatory protein (<i>V. cholerae</i>)
HEK	human embryonic kidney cells
HIN200	hematopoietic interferon-inducible nuclear antigens with 200 amino acid repeats
HtrA2	High temperature requirement protein A2
HTS	high throughput screening
HUVSMCs	human umbilical vein smooth muscle cells
HRP	horseradish peroxidase
<i>i.e.</i>	<i>id est</i> ; that is
ie-DAP	γ -D-glutamyl- <i>meso</i> -diaminopimelic acid
IBD	inflammatory bowel disease
IBM	IAP-binding motif
IFI16	interferon- γ -inducible protein 16
IFN	interferon
Ig	immunoglobulin
IKK	I κ B kinase
IL	interleukin
ILP-1	IAP-like protein 1, also BIRC4, XIAP
ILP-2	IAP-like protein 2, also BIRC8
imd	Immune deficiency pathway (<i>Drosophila</i>)
IRF	IFN regulatory factor
ITCH	itchy E3 ubiquitin ligase homolog (mouse)
I κ B α	NF- κ B inhibitor, alpha; also NFKBIA
JNK	c-Jun N-terminal kinase
kb	kilobasepairs
kDa	kilodalton
LB	Lysogeny broth

ABBREVIATIONS

LGP2	laboratory of genetics and physiology 2
LPS	lipopolysaccharide
LRR	leucine-rich repeat
M	molar
MAPK	mitogen-activated protein kinase
mc	monoclonal
MCL	Markov Cluster Algorithm
MDA5	melanoma differentiation associated gene 5
ML-IAP	melanoma-IAP, also BIRC7, Livin
MDP	muramyl dipeptide
MEF	mouse embryonic fibroblast
MEKK4	mitogen-activated protein kinase kinase kinase 4
mg	milligram
min	minute
ml	millilitre
mM	millimolar
MOI	multiplicity of infection
MOMP	Mitochondrial outer-membrane permeabilisation
mRNA	messenger RNA
MyD88	myeloid differentiation primary response gene 88
NACHT	domain present in NAIP, CIITA, HET-E and TP1
NAIP	neuronal apoptosis inhibitory protein; also BIRC1
NBD	nucleotide-binding domain
NBS-LRRs	nucleotide-binding site leucine-rich repeat
NEMO	NF- κ B essential modulator; also IKK γ
NF-AT	nuclear factor of activated T-cells
NF- κ B	Nuclear factor κ -light-chain-enhancer of activated B cells
ng	nanogram
NIK	NF- κ B-inducing kinase
NLR	nucleotide-binding domain and leucine-rich repeat containing protein
NOD	Nucleotide-binding oligomerization domain
NOS3	nitric oxide synthase 3
nRLU	normalised relative light unit
N-terminus	amino-terminus
OD	optical density
OMP	Outer membrane protein (<i>V. cholerae</i>)
OMVs	outer-membrane vesicles
ONPG	o-Nitrophenyl- β -D-galactopyranosid
PAGE	polyacrylamid gelelectrophorese
p50	NFKB1, nuclear factor of kappa light polypeptide gene enhancer in B-cells 1
PBS	phosphate buffered saline
pc	polyclonal
PCR	polymerase chain reaction
PepT	human peptide transporter
PFC	Pre-formed complex
PGN	peptidoglycan
PLK	polo-like kinase
PMA	phorbol 12-myristate 13-acetate
PRF1	perforin 1

ABBREVIATIONS

PRR	pattern-recognition receptor
PYD	pyrin domain
PYHIN	pyrin and HIN domain-containing protein
qRT-PCR	quantitative real-time PCR
RAC1	ras-related C3 botulinum toxin substrate 1
RELA	v-rel reticuloendotheliosis viral oncogene homolog A; also p65
R protein	resistance protein
RIG-I	retinoic acid-inducible gene I
RING	really interesting new gene
RIP2	receptor-interacting serine/threonine-protein kinase 2; also RIPK2, RICK
RISC	RNA-induced silencing complex
RLR	RIG-I-like receptor
RNA	ribonucleic acid
RNAi	RNA interference
RNF31	ring finger protein 31,; also HOIP
RNP	ribonucleoprotein complex
ROS	reactive oxygen species
rpm	rounds per minute
RpoS	RNA polymerase subunit sigma S
RPS-4	TIR-NBS-LRR class disease resistance protein
RT	room temperature
RT-PCR	reverse transcription PCR
SCF	Skp, Cullin, F-box containing complex
SD	standard deviation
SDS	sodium dodecyl sulphate
SEAP	secreted alkaline phosphatase
sec	seconds
shRNA	short hairpin RNA
siRNA	small interfering RNA
SMAC	second mitochondria-derived activator of caspase
SNAI1	snail homolog 1 (<i>Drosophila</i>)
SOP	standard operating procedure
ss	single stranded
SSH1	slingshot-homolog 1 (<i>Drosophila</i>)
ssRNA	single-stranded RNA
Survivin	also BIRC5
T	desoxythymidine
TAB	TAK1-binding protein
TAK1	transforming growth factor (TGF)-beta activated kinase; also MAP3K7
TβR1	TGF-beta type I receptor
TBE	TRIS-Borate-EDTA
TBK	TANK-binding kinase
TBS	TRIS buffered saline
TEMED	N,N,N',N'-Tetramethylethylendiamin
Tetra-DAP	L-Ala-D-Glu- <i>meso</i> -DAP-D-Ala (Tetra-DAP)
TGF-β	transforming growth factor (TGF)-beta
Th1, Th2	type I helper T cell, type II helper T cell
TIR	Toll-IL-1 receptor
TLR	Toll-like receptor

ABBREVIATIONS

TNFR1	TNF receptor 1, also TNFRSF1A
TNF- α	tumor necrosis factor-alpha
TRAF	TNF receptor-associated factor
Tri-DAP	L-Ala-D- γ -Glu-mDAP
TRIF	Toll/IL-1R domain containing adaptor inducing IFN- β
TRIS	Tris(hydroxymethyl)-aminomethan
Triton X-100	polyethylene glycol p-(1,1,3,3-tetramethylbutyl)-phenyl ether
Tween 20	polyoxyethylen-(20)-sorbitan monolaureate
UV	ultraviolet
V	volt
WT	wild type
XIAP	X-linked inhibitor of apoptosis; also BIRC4, ILP-1
XLP	X-linked lymphoproliferative syndrome
XPS	X-ray photoelectron spectroscopy

Symbols for amino acids

Amino acid	Three letter code	One letter code
Alanine	Ala	A
Arginine	Arg	R
Asparagine	Asn	N
Aspartate	Asp	D
Cysteine	Cys	C
Glutamate	Glu	E
Glutamine	Gln	Q
Glycine	Gly	G
Histidine	His	H
Isoleucine	Ile	I
Leucine	Leu	L
Lysine	Lys	K
Methionine	Met	M
Phenylalanine	Phe	F
Proline	Pro	P
Serine	Ser	S
Threonine	Thr	T
Tryptophane	Trp	W
Tyrosine	Tyr	Y
Valine	Val	V

1 Introduction

1.1 Innate immunity and pattern recognition receptors

All multicellular organisms are permanently challenged by pathogens, such as bacteria, viruses, fungi and protozoans. Therefore it is of crucial importance for the organism to be able to detect harmful agents and to launch a potent defence response for its own protection. All animals and plants possess an innate immune system that relies on germline encoded invariant pathogen receptors and is characterised by an instantaneous reaction. Vertebrates and jawed fish have additionally evolved an adaptive (or acquired) immune system that relies on somatic recombination of genes and clonal expansion of B- and T-lymphocytes. The adaptive immune system provides an unlimited number of receptors against all possible types of pathogens and is characterised by a delayed response.

The receptors of the evolutionary older innate immune system are invariant; they detect a limited number of conserved and mostly invariant patterns of the pathogens that are not prone to structural changes provoked by mutations, referred to as PATHOGEN-ASSOCIATED MOLECULAR PATTERNS (PAMPs) (reviewed in Medzhitov and Janeway, 1997). These patterns, also referred to as “microbial non-self”, such as bacterial cell wall components like peptidoglycan, flagellin, lipopolysaccharide (LPS) or nucleic acids, are recognised by specialised PATTERN RECOGNITION RECEPTORS (PRRs) (reviewed in Akira *et al.*, 2006) that are situated on the surface of or within the host cell. Additionally, the innate immune system surveys the integrity of cells and tissues, as it also reacts to DANGER-ASSOCIATED MOLECULAR PATTERNS (DAMPs). These are endogenous substances that are normally spatially confined from PRRs, such as cellular DNA, ATP or uric acid, or substances that are produced upon injury, such as reactive oxygen species (ROS). Upon cellular rupture, DAMPs are released and cause an innate immune reaction mediated by PRRs (Medzhitov, 2007).

PRRs are highly expressed in innate immune cells like macrophages and dendritic cells (DCs), but they are also abundant in a variety of non-professional immune cells like epithelial cells or fibroblasts and mediate the onset of immune responses (reviewed in Takeuchi and Akira, 2010).

PRRs are compartmentalised; there are specialised receptors that monitor the extracellular milieu, the vesicular compartment and the intracellular milieu. Transmembrane receptors detect extracellular pathogens and pathogens that enter the vesicular compartment. There are also PRRs that are secreted into the extracellular milieu (reviewed in Litvack and Palaniyar, 2010). Invasive pathogens that avoid detection by surface receptors can be detected by intracellular PRRs that monitor the cytoplasm.

INTRODUCTION

PRRs are evolutionary conserved. Toll-like receptors (TLRs), for example, are found in many organisms, including insects, fish and humans (reviewed in Aderem and Ulevitch, 2000). Another striking example of the conservation of PRRs among different organisms are the resistance proteins (R-proteins) of the nucleotide-binding site leucine-rich repeat (NBS-LRR) class found in plants that share high structural similarities with mammalian nucleotide binding and oligomerisation domain (NOD)-like receptors (NLRs) (reviewed in Maekawa *et al.*, 2011) (Fig. 1).

In most cases, activated PRRs trigger signalling cascades that culminate in inflammatory responses, mainly mediated by activation of the transcription factor nuclear factor κ B (NF- κ B) and of mitogen-activated protein kinases (MAPKs). That in turn leads to the onset of antimicrobial responses, such as phagocytosis, autophagy, production of reactive oxygen species (ROS), degranulation or secretion of antimicrobial peptides, which have direct antimicrobial effects. Furthermore, activation of PRRs leads to secretion of inflammatory chemokines and cytokines that mediate inflammation and recruit immune cells, such as macrophages or neutrophils, to the site of infection. Some PRRs also induce antiviral responses by triggering type I interferon (IFN) expression (reviewed in Takeuchi and Akira, 2010). Additionally, this first defence reaction mediated by the innate immune system is essential to trigger and to direct a full adaptive immune response (Fritz *et al.*, 2007; Dabbagh and Lewis, 2003).

There are at least four classes of PRRs: TLRs and the C-type lectin receptors (CLRs), which are membrane-bound and RIG-I-like receptors (RLRs) and NLRs, which are localised in the cytoplasm. The most extensively studied PRRs are the TLRs. Receptors of that family are exclusively membrane-bound and either face the extracellular milieu or the vesicular compartment. Pattern recognition is mediated by leucine-rich repeats (LRRs) pointing to the extracellular milieu, whereas the intracellular Toll/IL-1R homology (TIR) domain serves intracellular downstream signalling. In humans, there are 10 TLRs known so far, conferring protection against a wide variety of bacteria and viruses. They display a very broad substrate specificity reaching from cell wall components, such as lipopolysaccharide (LPS), lipoproteins or flagellin to nucleic acids, such as CpG DNA, double-stranded RNA (dsRNA) and single stranded RNA (ssRNA). Upon activation, TLRs trigger NF- κ B- and MAPK-mediated expression of pro-inflammatory cytokines and interferon response factor (IRF) 3/IRF7-mediated expression of type I IFNs via the adaptor proteins MyD88 (myeloid differentiation primary response gene 88) and TRIF (Toll/IL-1R domain containing adaptor inducing IFN- β), respectively (reviewed in Akira and Takeda, 2004).

Similar to the TLRs, CLRs are also membrane-bound. They sense carbohydrates present on fungi, viruses and bacteria through a carbohydrate-binding domain and trigger MAPK-, NF- κ B- and NF-AT (nuclear factor of activated T-cells)-mediated expression of pro-inflammatory cyto-

kines upon activation. CLRs also seem to be involved in the regulation of TLR-mediated responses (reviewed in Geijtenbeek and Gringhuis, 2009).

RLRs, in contrast, are localised in the cytoplasm. They contain one or two N-terminal caspase activation and recruitment (CARD) domains, a central DEAD box helicase/ATPase domain and a C-terminal regulatory domain. Thus far, there are three known members: RIG-I (retinoic acid inducible gene 1), MDA5 (melanoma-differentiation associated gene 5) and LGP2 (laboratory of genetics and physiology 2). RIG-I and MDA5 confer protection to viruses through recognition of viral nucleic acids via their C-terminal domains. LGP2, in contrast, might not recognise nucleic acids directly, but was shown to negatively regulate RIG-I and MDA5 signalling. Activation of RIG-I and MDA5 triggers IRF3/IRF7-dependent type I IFN production and expression of inflammatory cytokines (reviewed in Takeuchi and Akira, 2010).

Recently, a novel class of PRRs has been discovered. The pyrin and HIN200 (hematopoietic interferon-inducible nuclear antigens with 200 amino acid repeats) domain containing proteins absent in melanoma 2 (AIM-2) and interferon- γ -inducible protein 16 (IFI-16) have been shown to be sensors for cytoplasmic foreign DNA. Engagement of these receptors triggers inflammatory responses, such as pro-IL-1 β processing and IFN signalling through formation of multi-protein complexes termed INFLAMMASOMES (Unterholzner *et al.*, 2010; Burckstummer *et al.*, 2009).

1.2 NLRs

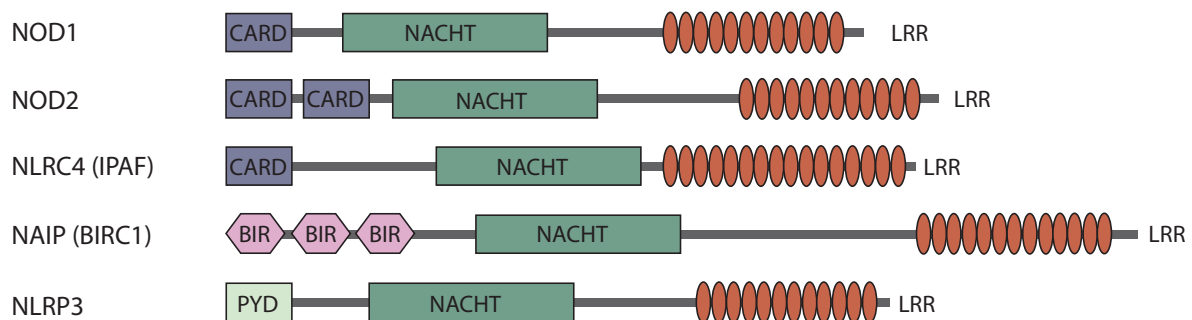
In humans, there are 23 NLR members identified so far; many of these act as cytoplasmic PRRs. They are expressed in various cell types, including myeloid and epithelial cells. Characteristic for NLRs is a tripartite domain structure similar to the structure of the apoptotic protease-activating factor 1 (APAF-1) (Fig. 1). The C-termini of NLRs consist of leucine-rich-repeats (LRRs), whereas APAF-1 contains C-terminal WD40 repeats. The LRRs are thought to mediate recognition of elicitors. Furthermore, all members contain a central oligomerisation domain referred to as present in NAIP, CIITA, HET-E and TP-1 (NACHT). NLRs are divided into sub-groups based on their N-terminal domains that consist of pyrin (PYD), baculovirus inhibitory repeat (BIR) or CARD domains (reviewed in Wilmanski *et al.*, 2008) (Fig. 1). These motifs have in common that they mediate protein-protein interactions.

NLRs can be roughly divided into two functional groups: INFLAMMASOME and NODOSOME NLRs. Some PYD-containing NLRs, such as NLRP3 and NLRP1, but also BIR-containing NLRs, such as NLRC4, are referred to as inflammasome NLRs. Upon activation, these proteins interact with the adaptor protein ASC (apoptosis-associated speck-like protein containing a

INTRODUCTION

CARD), leading to formation of large multimeric protein complexes that contain NLR proteins, ASC and pro-caspase-1. The induced proximity leads to auto-activation of caspase-1, which in turn mediates processing and secretion of the pro-inflammatory cytokines IL-1 β and IL-18. This inflammatory response consists of a two-step process: Expression of pro-caspase-1, pro-IL-1 β and pro-IL-18 is triggered by detection of microbial substances by TLRs, but a second signal, provided by the inflammasome, is required for maturation and secretion of the cytokines. Inflammasome NLRs display very broad substrate specificities. They can be activated by numerous bacteria and bacterial toxins and by a variety of DAMPs, but also by crystalline aggregates, such as asbestos, urea crystals or cholesterol crystals (reviewed in Schroder and Tschopp, 2010). For most cases, there is no proof for direct interactions of NLRs with their elicitors available, suggesting that their activation occurs via intermediate factors, and may not rely on direct ligand binding, analogous to the example of TOLL in *Drosophila* that recognises the ligand Spaetzle, which is proteolytically cleaved by upstream cascades upon PAMP recognition (reviewed in Valanne *et al.*, 2011).

NLR proteins



Homologues



Figure 1. Domain architecture of several NLR proteins and homologues. The NLR family is characterised by a tripartite domain composition similar to that of the pro-apoptotic factor APAF-1. The C-termini consist of leucine-rich repeats (LRRs) involved in detection of pathogens, the central parts contain so-called present in NAIP, CIITA, HET-E and TP1 (NACHT) domains that mediate oligomerisation. The N-termini consist of effector domains, such as caspase activation and recruitment (CARD), pyrin (PYD) or baculovirus inhibitory repeat (BIR) domains. NLR proteins share close homology with plant NBS-LRR R-proteins, such as RPS-4 (based on Fritz *et al.*, 2006; Meylan *et al.*, 2006).

A sub-group of CARD domain containing NLRs, namely NOD1 and NOD2, are referred to as nodosome NLRs. NOD1 and NOD2 detect bacterial peptidoglycan (PGN) fragments with different substrate specificities, upon activation they trigger signalling cascades that culminate in activation of NF- κ B and MAPKs. This mediates expression of pro-inflammatory cytokines, chemokines and anti-microbial peptides (Fig. 2) (reviewed in Kufer, 2008).

1.3 NOD1 and NOD2

1.3.1 Signalling pathways and regulation

Human NOD1 is encoded by the *CARD4* gene (Bertin *et al.*, 1999), NOD2 by the *CARD15* gene (Ogura *et al.*, 2001). NOD1 and NOD2 share the typical tripartite domain structure common to all NLR proteins consisting of C-terminal LRRs, a central NACHT domain and N-terminal effector domains consisting of one or two CARD domains, respectively (Fig. 1).

NOD1 and NOD2 show a predominantly cytoplasmic localisation, however, recent reports indicate that they also localise to the plasma membrane upon activation (Zurek *et al.*, 2012; Travassos *et al.*, 2010; Kufer *et al.*, 2008; Barnich *et al.*, 2005a; McDonald *et al.*, 2005). The exact role of this membrane-association still remains elusive, however, it seems to be dependent on actin and actin remodelling enzymes, such as RAC1 (ras-related C3 botulinum toxin substrate 1) (Eitel *et al.*, 2008; Legrand-Poels *et al.*, 2007).

NOD1 and NOD2 were the first NLR proteins that were described to detect microbial PAMPs. In recent years, a multitude of publications elucidated the main signalling cascades employed by these proteins. Recognition of PGN by NOD1 and NOD2 is thought to occur through the LRRs, as mutants lacking this domain proved to be incapable of PGN-sensing (Girardin *et al.*, 2005; Tanabe *et al.*, 2004). However, there is no solid evidence for a direct interaction of the LRRs with PGN so far. There is also the possibility that NOD1 and NOD2 might act as downstream adaptors of so far unidentified PRRs, as this is the case for NLRC4 that acts downstream of the actual PRR NAIP (Kofoed and Vance, 2011; Zhao *et al.*, 2011). A similar mechanism has been proposed for NLRP3, as there is evidence that NLRP3-mediated responses to PGN require upstream activation of NOD2 (Pan *et al.*, 2007). However, this important issue still needs clarification.

Under normal conditions, NOD1 and NOD2 are thought to be kept in an inactive state. Following recognition of PGN, these molecules likely undergo conformational changes that render them active by exposing the NACHT-domains that mediate homo-oligomerisation of the molecules. The exact nature of such conformational changes has not been worked out so far; the

INTRODUCTION

presumed model is based on structural information on the activation of APAF-1 (reviewed in Riedl and Salvesen, 2007), which is closely related to NLRs (Fig. 1). Oligomerisation leads to recruitment and activation of the serine-threonine kinase RIP2 (Receptor interacting protein 2) via homophilic CARD-CARD interactions (Inohara *et al.*, 2000). This creates a molecular signalling platform. RIP2 thereby acts as a molecular scaffold for the recruitment of downstream components. The kinase activity of RIP2 itself is not essential for this function, but it is required to stabilise the protein (Hasegawa *et al.*, 2008; Windheim *et al.*, 2007). NOD1- as well as NOD2-mediated recruitment of RIP2 promotes conjugation of RIP2 with K63-linked ubiquitin within the kinase domain at lysine 209. In contrast to K48-linked ubiquitination, K63-linked ubiquitination does not target proteins for proteasomal degradation, but serves as a regulatory mechanism, especially in NF- κ B signalling (reviewed in Chen, 2005). K63-linked ubiquitin chains on RIP2, possibly attached by the E3 ligases TRAF2, TRAF5 (TNF receptor associated factor) and ITCH (itchy E3 ubiquitin ligase homolog (mouse)) (Tao *et al.*, 2009; Hasegawa *et al.*, 2008), serve as docking sites for TAK1 (transforming growth factor- β activated kinase 1) (Hasegawa *et al.*, 2008). Recruitment of TAK1 is mediated by the ubiquitin-binding proteins TAB1 (TAK binding protein) and TAB2 that form a complex with TAK1 (Hasegawa *et al.*, 2008; Abbott *et al.*, 2007). Polyubiquitinated RIP2 also serves as a docking site for the IKK-complex by direct interaction with the regulatory subunit IKK γ (NEMO, NF- κ B essential modifier). In NOD2 signalling, IKK γ itself gets conjugated with K63-linked ubiquitin chains at lysine 399 in a RIP2-dependent manner (Abbott *et al.*, 2004). The interactions of RIP2 with IKK γ and TAK1 establish a close proximity between the IKK complex and the TAB/TAK complex, thus mediating TAK1-dependent activation of IKK α and IKK β . The activated IKK complex phosphorylates the NF- κ B inhibitory protein inhibitor of κ B (I κ B) that sequesters NF- κ B in the cytoplasm. Phosphorylation of I κ B triggers its proteasomal degradation, causing NF- κ B to translocate to the nucleus and activate its target genes (reviewed in Hayden and Ghosh, 2008). Additionally, there is evidence that NOD2 can also activate the alternative NF- κ B pathway by interaction with the NF- κ B-inducing kinase (NIK) in a RIP2-independent manner (Pan *et al.*, 2006).

Interestingly, the TLR pathways leading to NF- κ B activation utilise partly the same ubiquitination mechanisms as the NOD1/2 pathway, for example, ubiquitination of IKK γ at the same site is essentially involved (reviewed in Akira and Takeda, 2004). NOD1- and NOD2-dependent activation of TAK1 via RIP2 also induces c-Jun N-terminal kinase (JNK) and p38 MAPK-pathways (da Silva Correia *et al.*, 2007; Windheim *et al.*, 2007; Opitz *et al.*, 2006; Girardin *et al.*, 2001). The molecular mechanisms of NOD-mediated MAPK activation are not well under-

INTRODUCTION

stood, but there is evidence that the protein CARD9 is essentially involved at least in NOD2-mediated p38 activation (Hsu *et al.*, 2007) (Fig. 2).

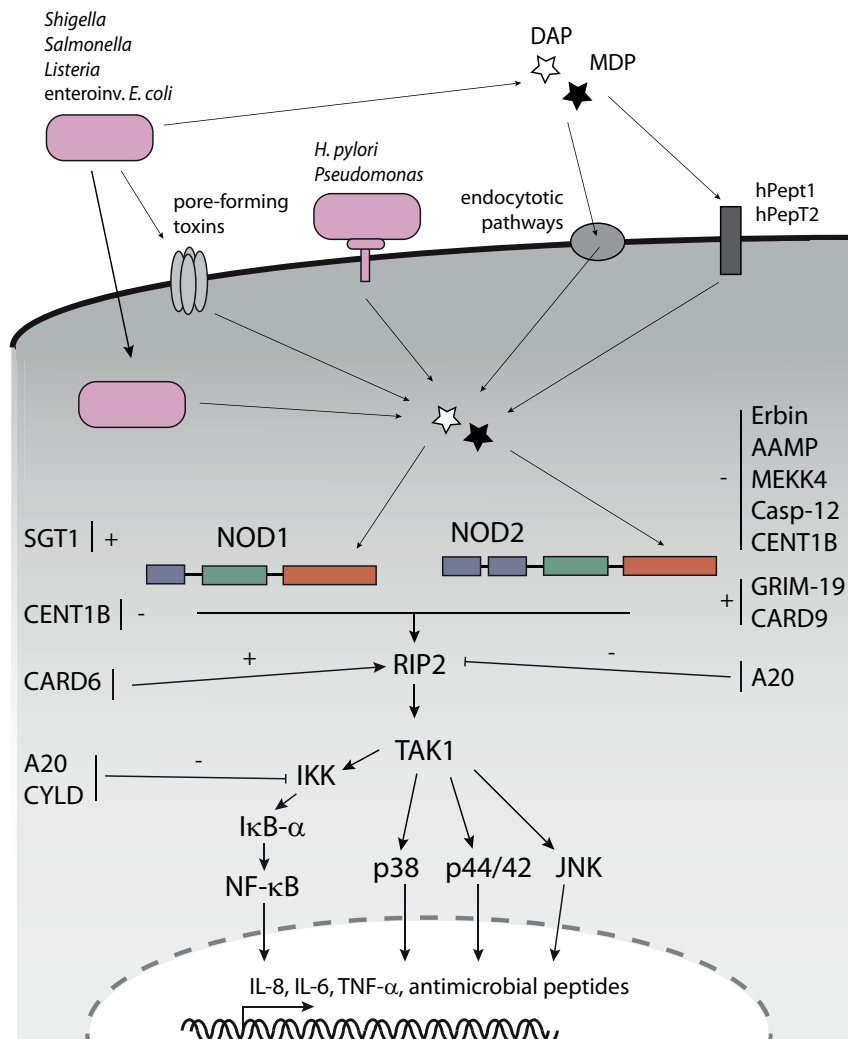


Figure 2. Uptake of PGN triggers NOD1- and NOD2-dependent signalling cascades. Bacterial PGN can gain access to the cytoplasm by invasion of bacteria, by injection via bacterial secretion systems, by pH-dependent endocytotic events and by the transmembrane translocators hPepT1 and hPepT2. Intracellular PGN fragments trigger NOD1 and NOD2 signalling cascades that involve RIP2 and TAK1, leading to expression of pro-inflammatory cytokines, chemokines and antimicrobial peptides. Factors that are known to regulate NOD signalling are indicated. For further information please refer to the main text (based on Le Bourhis *et al.*, 2007).

Overwhelming inflammatory responses can be detrimental to the host, therefore the NOD1 and NOD2 signalling cascades have to be tightly controlled. Even though NOD1 and NOD2 share the same core signalling cascade, they appear to be partly differentially regulated by accessory proteins (Fig. 2).

INTRODUCTION

A common factor that dampens NF- κ B activation in NOD1 and NOD2 signalling, but also in TLR signalling, is the de-ubiquitinating enzyme A20 (also known as TNFAIP3; tumor necrosis factor, alpha-induced protein 3), which reverses K63-linked ubiquitination of RIP2 (Hasegawa *et al.*, 2008; Hitotsumatsu *et al.*, 2008). NOD2-specific K63-linked ubiquitination of IKK γ can also be reversed by A20 and the deubiquitinating enzyme CYLD (cylindromatosis (turban tumor syndrome)) (Zhang *et al.*, 2006; Boone *et al.*, 2004). There are more examples of factors that uniquely regulate NOD2 signalling. For instance, it has been shown that MEKK-4 (mitogen-activated protein kinase kinase kinase 4) and caspase-12 down-regulate NOD2-mediated responses by interfering with the NOD2/RIP2 interaction (Clark *et al.*, 2008; LeBlanc *et al.*, 2008). Furthermore, it was reported that the protein Erbin (erbb2 interacting protein) binds NOD2 and exerts a negative regulatory function on NOD2 signalling (Kufer *et al.*, 2006; McDonald *et al.*, 2005). Recently, we discovered that the angio-associated migratory cell protein (AAMP) also interacts with NOD2 and negatively influences NOD2-mediated NF- κ B activation (Bielig *et al.*, 2009). GRIM19 (gene associated with retinoid-IFN-induced mortality-19), in contrast, has been described to positively contribute to NOD2-mediated NF- κ B activation (Barnich *et al.*, 2005b).

The regulation and fine-tuning of NOD1 signalling, in contrast, is less well characterised. Thus far, it has only been shown that the GTPase-activating protein centaurin- β 1 (CENTB1) negatively regulates NOD1 and also NOD2 signalling (Yamamoto-Furusho *et al.*, 2006). Furthermore, CARD6 exerts positive effects on NOD1-mediated NF- κ B activation by interaction with RIP2. However, these effects are not very strong and CARD6 also seems to act on NF- κ B pathways triggered by other stimuli (Dufner *et al.*, 2006).

The regulatory networks that control positive- and negative-regulation of NOD1 and NOD2 are still very poorly defined. For Erbin and CENT1B there is evidence that they serve as feedback inhibitors, as their expression is up-regulated following NOD1 and NOD2 stimulation (Kufer *et al.*, 2006; Yamamoto-Furusho *et al.*, 2006). Given the potentially dangerous effects of overwhelming inflammation, it can be assumed that NOD signalling is tightly regulated, as this is the case for TLR signalling (reviewed in Akira and Takeda, 2004). However, to date it is still not known how detection of elicitors occurs, or how NOD-mediated inflammatory responses are terminated, for example.

1.3.2 Bacterial sensing and physiological relevance of NOD1 and NOD2

Peptidoglycan (PGN) is present in the cell wall of nearly all bacteria and is essential for constructing the cell shape. PGN is constantly remodeled during cell-growth and -division (re-

INTRODUCTION

viewed in Park and Uehara, 2008). There are recycling mechanisms, but at least some PGN and degradation products are shed by growing bacteria (reviewed in Boneca, 2005).

NOD1 specifically recognises diaminopimelic acid (DAP)-containing PGN fragments that are produced as breakdown-products during growth of Gram-negative bacteria. The minimal structural motif required for NOD1-activation was identified to be γ -D-glutamyl-*meso*-diaminopimelic acid (ie-DAP), a dipeptide that serves to crosslink the carbohydrate-backbones of Gram-negative PGN (Chamaillard *et al.*, 2003; Girardin *et al.*, 2003c). Human NOD1 preferentially recognises L-Ala-D-Glu-*meso*-DAP (Tri-DAP) containing PGNs. Of note, murine NOD1 has a different substrate specificity as it is activated better by L-Ala-D-Glu-*meso*-DAP-D-Ala (Tetra-DAP) than by ie-DAP (Girardin *et al.*, 2003a). Thus NOD1 should provide protection primarily against Gram-negative bacteria. Consistently, it has been shown that NOD1 detects the invasive Gram-negative pathogens *Shigella flexneri* (Girardin *et al.*, 2001), enteroinvasive *Escherichia coli* (Kim *et al.*, 2004) and *Chlamydia spp.* (Welter-Stahl *et al.*, 2006; Opitz *et al.*, 2005), among others. It has also been shown that NOD1-deficient mice have a higher bacterial burden after infection with the Gram-negative pathogen *H. pylori* compared to WT mice (Viala *et al.*, 2004). In addition, NOD1 also recognises some Gram-positive bacteria that contain DAP-type PGNs, such as *Bacillus spp.* or *Listeria monocytogenes* (Hasegawa *et al.*, 2006; Opitz *et al.*, 2006).

NOD2, in contrast, recognises the PGN-moiety MurNac-L-Ala-D-*iso*Gln (MDP, for muramyl dipeptide), the minimal motif common to all PGNs that is conserved in Gram-negative as well as in Gram-positive bacteria (Girardin *et al.*, 2003b; Inohara *et al.*, 2003). Due to its ability to sense MDP, NOD2 should be able to detect a very broad spectrum of bacteria. Indeed, it has been shown that NOD2 detects a variety of Gram-positive and Gram-negative bacteria, such as *Streptococcus pneumoniae*, *Salmonella typhimurium* and *Mycobacterium tuberculosis* (Ferwerda *et al.*, 2005; Opitz *et al.*, 2004; Hisamatsu *et al.*, 2003). NOD2 also detects a huge variety of PGNs of heat killed bacteria *in vitro* (Hasegawa *et al.*, 2006). Furthermore, it has been shown that NOD2 is essentially involved in protection against *L. monocytogenes* in the intestine of mice (Kobayashi *et al.*, 2005).

Bacterial pathogens can be roughly divided into two groups: Extracellular bacteria, which evade phagocytic uptake and/or subsequent lysosomal degradation and invasive bacteria, which actively enter host cells. The latter either reside freely within the cytosol or stay entrapped and replicate within altered compartments of the host's endocytic pathway (so-called "pathogen-containing vacuoles") (reviewed in Raupach and Kaufmann, 2001).

Due to their cytoplasmic localisation, NOD1 and NOD2 are able to detect invasive bacteria, such as *S. flexneri* or *L. monocytogenes* that invade host cells and reside freely within the cytosol. It

INTRODUCTION

has been shown that PGN fragments derived from invasive *Shigella* activate NOD1-signalling in epithelial cells (Nigro *et al.*, 2008). Furthermore, MDP can potentially be generated by secreted bacterial autolysins in cells infected with *L. monocytogenes* (Lenz *et al.*, 2003). There is also evidence that NOD1 and NOD2 detect bacteria that normally reside within intracellular vacuoles, such as *Legionella pneumophila* (Berrington *et al.*, 2010; Frutuoso *et al.*, 2010), *S. typhimurium* (Le Bourhis *et al.*, 2009) or *Mycobacterium tuberculosis* (Brooks *et al.*, 2011; Pandey *et al.*, 2009). However, it is not well understood how in general PGN is translocated from the vesicular compartment to the cytosol where it is sensed by NOD1 and NOD2, although translocation via pore-forming toxins and peptide transporters is involved in some cases (see below).

Initially, it has been presumed that only bacteria colonising intracellular niches are recognised by intracellular PRRs and that extracellular bacteria are detected by cell surface receptors, for example by TLRs. Nowadays there is increasing evidence that extracellular bacteria can also be detected by intracellular PRRs. This raises the question how the hydrophilic PGN fragments shed by extracellular bacteria are delivered into the host cells. One possibility is delivery via bacterial secretion systems, as it has been shown that *H. pylori* can deliver PGN fragments into the cytosol of host cells via its type IV secretion system encoded by the *cag* pathogenicity island (Viala *et al.*, 2004). It is also possible that pore-forming toxins secreted by some bacteria facilitate entry of PGN to host cells, as it has been observed that NOD1 activation by PGN derived from *Haemophilus influenzae* required the pore-forming toxin pneumolysin from *S. pneumoniae*. Similar effects were observed for pore-forming toxins from *Bacillus anthracis* and *Staphylococcus aureus* (Ratner *et al.*, 2007).

Host cell factors might contribute to uptake of PGN as well, as it has been shown that clathrin- and dynamin-dependent pathways mediate an active uptake of PGN to the cytosol in a pH-dependent manner (Lee *et al.*, 2009; Marina-Garcia *et al.*, 2009). Moreover, the NOD2-elicitor MDP can specifically be taken up into the cytosol via the plasma membrane-located peptide transporter hPepT1 (human peptide transporter 1), whereas NOD1-elicitors can be taken up by hPepT2 (Swaan *et al.*, 2008; Ismail *et al.*, 2006; Vavricka *et al.*, 2004) (Fig. 2). However, these mechanisms are still not fully worked out and there are very likely further mechanisms that contribute to PGN uptake.

Whereas NOD1 is widely expressed in many tissues of the stromal and haematopoietic compartments, NOD2 shows the highest expression in immune cells like macrophages and dendritic cells and in paneth cells in the intestinal crypts, but it is also expressed in epithelial cells of the intestine and the lung (Hitotsumatsu *et al.*, 2008; Uehara *et al.*, 2007; Tada *et al.*, 2005; Ogura *et al.*, 2003; Ogura *et al.*, 2001; Inohara *et al.*, 1999). NOD1 and NOD2 are indispensable for intestinal

INTRODUCTION

homeostasis and pathogen recognition. As there are myriads of commensals in the gut, expression of TLRs in the adult is restricted in intestinal epithelial cells to prevent constant inflammation (Abreu *et al.*, 2001). Moreover, TLR signalling can be rendered anergic due to constant exposure to PAMPs (Shahin *et al.*, 1987). This prevents harmful overwhelming immune reactions to commensals. Pathogens rupturing the epithelial barrier or invading the host cells are subsequently recognised by cytoplasmic NLRs. There is a close cross-talk between NLRs and TLRs ensuring a proper distinction between commensals and pathogens. NOD1 and NOD2 are essential to trigger anti-microbial responses in cells that are anergic for TLR signalling *in vivo* (Kim *et al.*, 2008). Furthermore, there are strong synergistic effects between NOD1 and NOD2 elicitors and agonists of various TLRs (Fritz *et al.*, 2005; Uehara *et al.*, 2005; van Heel *et al.*, 2005; Traub *et al.*, 2004).

Activation of NOD1 and NOD2 in epithelial and endothelial cells by bacteria induces expression of pro-inflammatory cytokines and chemokines, such as IL-8 (CXCL-8), a chemokine that mediates the recruitment of neutrophils (Opitz *et al.*, 2006; Kim *et al.*, 2004; Viala *et al.*, 2004). Furthermore, activation of NOD1 and NOD2 in macrophages and dendritic cells induces the release of IL-8 and the cytokines IL-6, IL-1 β and TNF- α (reviewed in Fritz *et al.*, 2006). The important chemo-attractant RANTES (regulated upon activation, normal T-cell expressed and secreted/CCL5) is secreted by primary murine macrophages *in vivo* following stimulation with NOD agonists, underlining the importance of NOD signalling in co-ordinating innate immune responses (Werts *et al.*, 2007). Importantly, stimulation of NOD1 and NOD2 additionally leads to secretion of anti-microbial peptides (AMPs) in the gut. AMPs are secreted short peptides that kill bacteria by forming pores in bacterial cell membranes; they are the key effectors in cell autonomous immunity, *i.e.* defence mechanisms that are executed by the attacked cell itself that do not rely on the recruitment of immune cells. They are not only produced by professional immune cells, but also by epithelial cells. Secretion of AMPs is important to control the numbers of commensal bacteria and is thus essential for maintaining intestinal homeostasis (reviewed in Auvynet and Rosenstein, 2009; Selsted and Ouellette, 2005). Especially in intestinal crypts, a compartment that is likely kept sterile, NOD2 seems to play a pivotal role in the protection against pathogens. NOD2 is highly expressed in the AMP-secreting paneth cells in the crypts and it triggers secretion of AMPs upon pathogen intrusion (Petnicki-Ocwieja *et al.*, 2009; Kobayashi *et al.*, 2005). Furthermore, NOD2 controls the expression of the AMP human β -defensin in epithelial cells (Voss *et al.*, 2006).

NOD1 as well is crucial for the regulation of intestinal homeostasis. It is required for production of human and murine β -defensins in response to *H. pylori* infection (Boughan *et al.*, 2006; Hamanaka *et al.*, 2001) and has been shown to mediate lymphoid tissue genesis induced by com-

INTRODUCTION

mensals in the intestine of mice. Formation of intestinal B-cell containing isolated lymphoid follicles (ILFs) is essentially regulated by recognition of Gram-negative bacteria by NOD1 (Bouskra *et al.*, 2008).

Of note, NOD1 and NOD2 have also been shown to contribute to autophagy by recruiting ATG16L1 (ATG16 autophagy related 16-like 1 (*S. cerevisiae*)) to the plasma membrane. Autophagy is a process that serves to maintain cellular homeostasis and mediates degradation of intracellular pathogens (reviewed in Ramjeet *et al.*, 2010).

Within the last years, it became clear that NOD1 and NOD2 also contribute to the induction of adaptive immune responses. NOD1 and NOD2 elicitors, in particular in synergy with TLR agonists, have been shown to induce Th1- and Th2-type immune responses (Fritz *et al.*, 2007; Kobayashi *et al.*, 2005; Tada *et al.*, 2005). Furthermore, it has been demonstrated that administration of NOD1 elicitors restored neutrophil function in mice depleted in intestinal microbiota. Consistently, NOD1 deficient mice proved to be more susceptible to early pneumococcal sepsis due to inefficient neutrophil activation (Clarke *et al.*, 2010).

Taken together, innate immune mechanisms involving NOD1 and NOD2 counter-act bacterial infections by the release of anti-microbial factors, recruitment of phagocytes and by mediating the onset of adaptive immune responses. Furthermore, NOD1 and NOD2 are crucial for the regulation of the intestinal homeostasis by mediating interactions with the commensal microbiota.

Consistently, mutations in the *CARD4* and *CARD15* genes are linked to a variety of inflammatory disorders. Polymorphisms in the NOD1 gene *CARD4* have been associated to the onset of inflammatory bowel disease (McGovern *et al.*, 2005). A different polymorphism in *CARD4* seems to increase the susceptibility to asthma and allergy (Eder *et al.*, 2006; Hysi *et al.*, 2005). Frameshift mutations in the NOD2 gene *CARD15* strongly increase the susceptibility to Crohn's disease (CD), which is a severe form of chronic inflammatory bowel disease (reviewed in Hruz and Eckmann, 2010). Other mutations in *CARD15* are associated with the chronic inflammatory barrier diseases Blau syndrome and early onset sarcoidosis (reviewed in Rosenstiel *et al.*, 2007).

Of note, NOD1 has also been linked to events leading to cell death. In the first description of NOD1 it was reported that NOD1 binds several caspases and specifically activates caspase-9-mediated apoptosis (Inohara *et al.*, 1999). Later, it has been shown that NOD1 induces apoptosis by RIP2-dependent activation of caspase-8 as well, contributing to the control of tumour growth (da Silva Correia *et al.*, 2007; da Silva Correia *et al.*, 2006). However, the putative functions of NOD1 in apoptosis are far from being understood.

1.4 Apoptosis: Programmed cell death

Apoptosis, often referred to as programmed cell death, is an evolutionary conserved process in which proteolytic cascades lead to the degradation of cells in a controlled manner. In contrast to necrotic cell death, a toxic process induced by extrinsic factors or injury, apoptosis does not cause an immune reaction. Apoptosis is required for many processes, such as normal cell turnover, embryonic development and for a proper function of the immune system.

The hallmarks of apoptosis are cell shrinkage, nuclear fragmentation, protein-crosslinking, and chromatin condensation and degradation. The degraded cellular material is engulfed in vesicular structures consisting of intact cellular membranes, whereby mitochondria and other organelles stay intact within the apoptotic vesicles. The vesicles are quickly phagocytosed by macrophages and other surrounding cells. As cell membrane integrity is not affected, there is no release of cellular constituents into the extracellular milieu and no immune response following apoptotic cell death (reviewed in Elmore, 2007).

Cellular events that lead to the aforementioned biochemical changes are mediated by a family of aspartate-specific cysteine proteases termed caspases (cysteine-dependent aspartate-directed proteases) (Alnemri *et al.*, 1996). Caspases are ubiquitously expressed as inactive pro-forms and get activated by various apoptotic stimuli. This leads to proteolytic cascades that amplify the initial signals and ensure a rapid degradation of cells by selective cleavage of hundreds of target proteins (Nicholson, 1999).

There are two major pathways that trigger apoptosis: The extrinsic pathway and the intrinsic pathway. The extrinsic pathway relies on activation of tumor necrosis factor receptor (TNFR) family transmembrane receptors by extracellular ligands. Ligand binding induces formation of a multimeric protein complex termed DEATH-INDUCED SIGNALING COMPLEX (DISC) that recruits pro-caspase-8. The induced proximity leads to trans-autoactivation of caspase-8, triggering proteolytic cascades by activating effector caspases (Muzio *et al.*, 1998; Kischkel *et al.*, 1995).

The intrinsic pathway is activated by numerous non-receptor stimuli, such as deprivation of growth factors or cytokines, or by intrinsic cues like DNA damage, endoplasmic reticulum (ER) stress, free radicals, radiation, UV light, viral infection or toxins. This leads to MITOCHONDRIAL OUTER-MEMBRANE PERMEABILISATION (MOMP) and subsequent release of pro-apoptotic factors into the cytosol. This process is tightly regulated by complex interactions between pro- and anti-apoptotic members of the B cell lymphoma 2 (BCL-2) protein family (reviewed in Cory and Adams, 2002). MOMP leads to secretion of the pro-apoptotic molecules cytochrome c, second mitochondria-derived activator of caspase (SMAC) and high temperature requirement protein A2 (HtrA2). SMAC and HtrA2 inhibit anti-apoptotic factors of the BIRC-family. Cytochrome c, in contrast, triggers the activation of APAF-1. Activated APAF-1 forms a

heptameric complex termed APOPTOSOME that mediates activation of caspase-9, which in turn cleaves and activates effector caspases, thereby initiating the proteolytic cascades that finally lead to cell death (reviewed in Yuan *et al.*, 2011; Riedl and Salvesen, 2007).

1.5 The BIRC-family: Functions beyond inhibition of apoptosis

Members of the BIRC-family (baculovirus IAP repeat containing; also termed IAPs, for inhibitors of apoptosis) have mainly been investigated in respect of their roles in counter-acting apoptosis. BIRC proteins were initially found in baculoviruses and are highly conserved from viruses to yeast, nematodes and insects to humans (Uren *et al.*, 1998). In humans there are eight members, BIRC1 (NAIP), BIRC2 (c-IAP1), BIRC3 (c-IAP2), BIRC4 (XIAP, ILP-1), BIRC5 (Survivin), BIRC6 (Bruce, Apollon), BIRC7 (Livin, ML-IAP) and BIRC8 (ILP-2). Members of the BIRC family are characterised by the presence of 1-3 tandem baculovirus inhibitory repeat (BIR) domains (Fig. 3) (reviewed in Gyrd-Hansen and Meier, 2010). The BIR domain is a zinc-binding fold containing ~70 amino acid residues that is known to promote protein-protein interactions. Most members also contain a really interesting new gene (RING) finger motif that has E3 ubiquitin ligase function (Vaux and Silke, 2005). BIRC2 and BIRC3 additionally contain a CARD domain of yet unknown function.

BIRC proteins are known to inhibit apoptosis either by direct binding of active caspases (Riedl *et al.*, 2001; Deveraux *et al.*, 1997), or by indirect means. Initially, it was thought that all BIRCs inhibit caspases by direct binding, as overexpression of BIRCs effectively protects cells against apoptotic stimuli. Nonetheless, recent studies indicate that only XIAP (BIRC4) is able to inhibit caspases by direct binding under physiological conditions (Eckelman and Salvesen, 2006; Eckelman *et al.*, 2006). BIRC8 shows a close homology to XIAP, but lacks the first two BIR-domains. In spite of its putative caspase-9 interaction domain, it is only a weak caspase-9 inhibitor on its own (Shin *et al.*, 2005). However, it has been shown that over-expression of BIRC8 potently inhibits BAX-induced apoptosis (Richter *et al.*, 2001).

Indirect means to inhibit apoptosis are thought to include mono- and polyubiquitination of caspases (Morizane *et al.*, 2005; Hao *et al.*, 2004; Suzuki *et al.*, 2001; Huang *et al.*, 2000), or of the pro-apoptotic factor SMAC (Ma *et al.*, 2006; Morizane *et al.*, 2005; Hao *et al.*, 2004; Hu and Yang, 2003; MacFarlane *et al.*, 2002), leading to proteasomal degradation of these factors. Other reports indicate that BIRC7 and BIRC8 might exert their anti-apoptotic effects by binding and neutralising SMAC, rather than by direct inhibition of caspases (Shin *et al.*, 2005; Vucic *et al.*, 2005).

INTRODUCTION

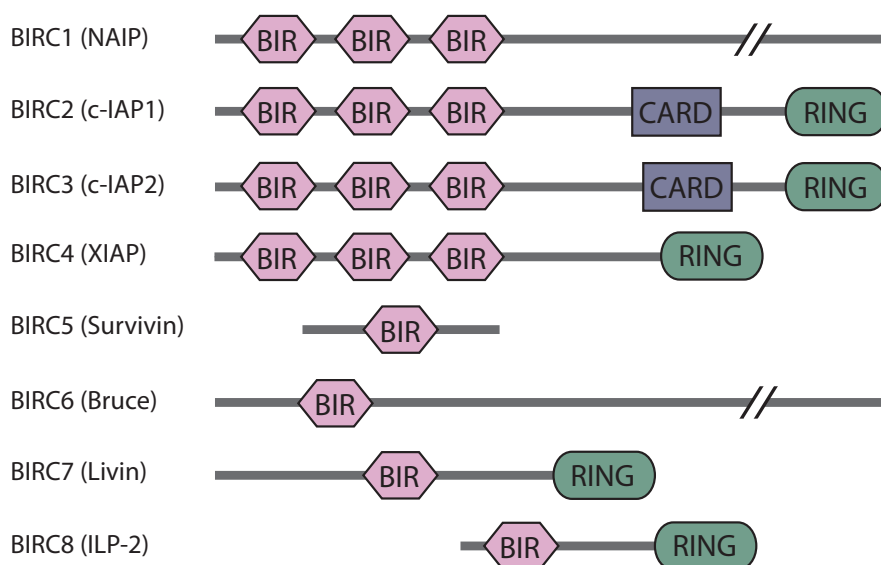


Figure 3. Domain architecture of the eight members of the BIRC family. The BIRC family is characterised by 1-3 N-terminal baculoviral inhibitory repeat (BIR) domains. Several members also contain caspase activation and recruitment (CARD) domains and/or really interesting new gene (RING) domains. For further details please refer to the main text (based on Salvesen and Duckett, 2002).

BIRC proteins are regulated by pro-apoptotic IAP-binding proteins, such as the mitochondrial proteins SMAC and HtrA2. SMAC has been shown to inhibit the association of XIAP with caspases and mediate the release of caspases to execute their downstream apoptotic functions. This may also be the case for other BIRCs (Liu *et al.*, 2000; Wu *et al.*, 2000; Deveraux *et al.*, 1997; Roy *et al.*, 1997), as SMAC also targets BIRC2 and BIRC3 for proteasomal degradation by ubiquitination (Yang and Du, 2004). Furthermore, HtrA2 has an intrinsic protease activity and can directly cleave BIRC proteins (Srinivasula *et al.*, 2003; Yang *et al.*, 2003; Hegde *et al.*, 2002; Martins *et al.*, 2002; Verhagen *et al.*, 2002).

Recent reports indicate that BIRC family members also have important functions in other cellular processes. Some members are involved in the regulation of cell division (Verhagen *et al.*, 2001), cellular signalling (Salvesen and Duckett, 2002) and in immune detection of bacterial products. BIRC1, for example, which also belongs to the NLR family (Fig. 1, Fig. 3), acts as PRR itself; it directly recognises bacterial flagellin and components of the bacterial type III secretion apparatus to mediate caspase-1 activation and IL-1 β processing via formation of a NLRC4- and ASC-dependent inflammasome (Kofoed and Vance, 2011; Zhao *et al.*, 2011). BIRC5 is involved in the segregation of chromosomes in the G2/S-phase of the cell cycle (Skoufias *et al.*, 2000; Uren *et al.*, 2000), and BIRC6 plays a role in cytokinesis (Pohl and Jentsch, 2008).

Importantly, recent studies indicate that some members of the BIRC family exert important functions in innate immunity and pro-survival signalling. BIRC2 and BIRC3 are implicated as

key players in the TNFR1 (tumor necrosis factor receptor 1) signalling pathway. They were found to be associated with the TNFR signalling complex (Rothe *et al.*, 1995) where they act as E3 ubiquitin ligases mediating TNFR1-dependent NF- κ B activation and preventing TNFR1-mediated apoptosis (Bertrand *et al.*, 2008). A recent study revealed that BIRC2 and BIRC3 play similar roles in NOD1 and NOD2 signalling (Bertrand *et al.*, 2009). Furthermore, BIRC2 and BIRC3 also seem to positively regulate MyD88-dependent TLR signalling by mediating K48-linked ubiquitination of TRAF3 (Tseng *et al.*, 2010).

XIAP was also found to be implicated in pro-survival signalling events. Through interactions of its BIR1 domain with the TAB1/TAK1 complex it participates in activation of MAPKs and NF- κ B (Lu *et al.*, 2007; Sanna *et al.*, 2002; Sanna *et al.*, 1998). Moreover, XIAP is essential for NOD2-mediated immune responses against the invasive pathogen *L. monocytogenes* (Bauler *et al.*, 2008), indicating a role in innate immunity. This raises the questions how exactly the mentioned BIRC proteins are involved in the regulation of innate immune responses, and if also other BIRC family members contribute to innate immunity.

1.6 RNAi and systematic screening approaches

The principle of RNA-interference (RNAi)-mediated gene-silencing is widely used in research to determine the function of genes in certain biological processes by loss-of-function studies. In this work, we conducted an RNAi-based high-throughput screen (HTS) to identify novel factors involved in the regulation of the NOD1 signalling cascade.

RNAi is a conserved mechanism common to eukaryotic cells. It serves to regulate gene expression by post-transcriptional gene silencing and provides protection against foreign nucleic acids, such as transposons and viruses. The first RNAi-based processes, described in the early 1990s, were gene silencing in plants (Jorgensen, 1990) and quelling in the fungus *Neurospora crassa* (Romano and Macino, 1992). Evidence for the existence of RNAi in animals was then provided by Fire and colleagues in 1998. They demonstrated that injection of long dsRNA into the nematode *Caenorhabditis elegans* triggers the degradation of complementary mRNA (Fire *et al.*, 1998). Only later it became evident that RNAi also occurs in mammalian cells (Elbashir *et al.*, 2001). Recently, a related RNA-based defence mechanism was also described for bacteria and archaea (Horvath and Barrangou, 2010), underlining the ubiquitous importance of RNA-based mechanisms as protection systems against viruses and mobile genetic elements. Today, RNAi-based methods are widely used as standard methods for reverse genetics, and also therapeutic applications are being investigated.

INTRODUCTION

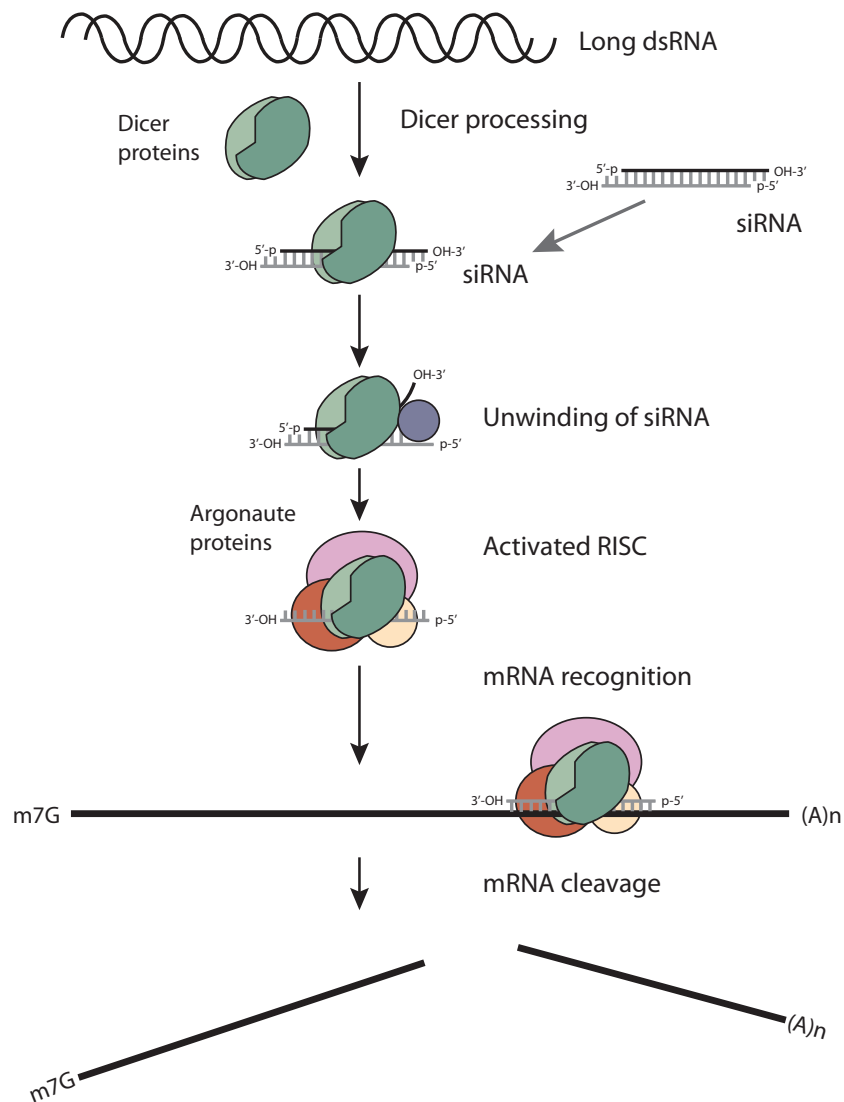


Figure 4. The molecular mechanism of RNAi. Long dsRNA is cleaved into short interfering RNAs (siRNAs) by Dicer protein complexes. Alternatively, siRNAs can directly be inserted into cells. The siRNA duplexes are unwound starting at the 5' end. The guide strand is taken up into the RNA-induced silencing complex (RISC) mediated by argonaute proteins, whereas the other strand is degraded (pre-RISC). The guide strand directs the endonuclease activity of the activated RISC (holo-RISC) to cleave homologous mRNA. For further details please refer to the main text (based on Dykxhoorn and Lieberman, 2005).

Many of the underlying mechanisms were discovered in *Drosophila*, but the involved proteins and regulatory mechanisms are believed to be very similar in mammalian cells. Degradation of mRNA by RNAi is guided by small 23-25 nucleotide dsRNA, termed small interfering RNA (siRNA). These small RNAs are produced by cleavage of long dsRNA molecules by members of the highly conserved Dicer enzyme family that possess RNase III-like properties (Myers *et al.*, 2003; Zamore *et al.*, 2000). The siRNA is subsequently passed on to the argonaute (AGO) proteins contained in a ribonucleoprotein complex (RNP) termed RNA-INDUCED SILENCING

COMPLEX (RISC), where it is unwound and cleaved, whereby the leading strand (guide strand) remains bound to the complex and the other strand gets degraded (Leuschner *et al.*, 2006; Matranga *et al.*, 2005; Liu *et al.*, 2004). The leading strand subsequently guides recognition of complementary mRNA through base-pairing, which in turn leads to incorporation of the mRNA into the RISC. The bound mRNA gets degraded by the endonuclease activity of the contained argonaute proteins. This in turn leads to silencing of the corresponding gene (reviewed in Ender and Meister, 2010) (Fig. 4).

Large-scale HTS approaches based on RNAi, often on a genome-wide scale, proved to be a very powerful tool in functional genomics (for example Sharma *et al.*, 2011; Karlas *et al.*, 2010; Muller *et al.*, 2005)). The major advantage of these automated approaches is that the functions of many thousand genes in a specific biological process can be monitored by systematic gene-by-gene knock-downs in one single screening approach under controlled conditions.

1.7 Aim of the study

The intracellular NLR-type PRR NOD1 is critically involved in innate immune responses against Gram-negative bacteria by detection of PGN fragments. Even though the main events leading to NF- κ B activation are established, the regulation and fine-tuning of this potentially harmful inflammatory signalling pathway remains largely elusive. The aim of this study was to gain a better understanding of the NOD1 signalling cascade by conducting an unbiased high-throughput siRNA screen to identify novel components of the NOD1 pathway.

Another event in NOD1 and NOD2 signalling that is still not fully understood is the uptake of PGN into the cytosol of host cells. Recent studies indicate that multiple different mechanisms in the host cell facilitate PGN translocation from the extracellular and vesicular milieu into the cytosol. Recently, it was shown that also pathogens possess factors that enable PGN uptake. Pore-forming toxins and the type IV secretion system were shown to be involved in this by enabling PGN translocation across the plasma membrane of host cells (Ratner *et al.*, 2007; Viala *et al.*, 2004). Intriguingly, many Gram negative bacteria secrete large amounts of outer-membrane vesicles (OMVs) that contain proteins from the periplasmic space and PAMPs (Kulp and Kuehn, 2010). It has been shown that OMVs purified from *Pseudomonas aeruginosa* can induce IL-8 responses in host cells (Bauman and Kuehn, 2006) and that OMVs can trigger NOD1 responses (Kaparakis *et al.*, 2009). The second part of this project aims at elucidating a possible role of OMVs as carriers of PGN fragments that might trigger NOD1 and NOD2 signalling.

2 Materials and Methods

2.1 Materials

2.1.1 Cell lines and bacteria

HEK293T cells

HEK293 (human embryonic kidney) cells are adherent human epithelial cells transformed with sheared adenovirus 5 DNA (Graham *et al.*, 1977). The derivative HEK293T is highly transfectible and additionally contains the SV40 (simian virus 40) T-antigen that allows replication of plasmids containing the SV40 origin of replication. HEK293T cells were purchased from ATCC (#CRL 11268, www.atcc.org/).

HeLa cells

HeLa cells are adherent human epithelial cells derived from a cervical carcinoma. This immortalised cell line is transformed with human papilloma virus 18 (HPV18). HeLa cells were purchased from ATCC (#CCL 2, www.atcc.org/).

HeLa shRNA cell lines

HeLa cells stably expressing shRNA (XIAP and scrambled) were provided by Hamid Kashkar and are described elsewhere (Kashkar *et al.*, 2007).

THP-1 cells

The human monocytic cell line THP-1 was first isolated from the blood of a one-year old boy with acute monocytic leukemia. During culture, THP-1 cells maintain monocytic characteristics for up to 14 months (Tsuchiya *et al.*, 1980). THP-1 cells are non-adherent, but can be differentiated into adherent macrophage-like cells with phorbol esters, such as phorbol 12-myristate 13-acetate (PMA). THP-1 cells were purchased from ATCC (#TIB 202, www.atcc.org/).

THP1-Blue cells

THP1-Blue cells are a derivative of the THP-1 cell line. They have a NF- κ B-inducible reporter-system stably integrated into the genome. The reporter expresses secreted embryonic alkaline phosphatase (SEAP) under the control of a NF- κ B inducible promoter. Cells are resistant to zeocin and were purchased from InVivoGen (#thp-sp, www.invivogen.com).

***Escherichia coli* DH5 α**

Competent *E. coli* DH5 α (F⁻ Φ 80*lacZ* Δ M15 Δ (*lacZYA-argF*)U169 *deoR recA1 endA1 hsdR17* (τ_k^- , m_k^+) *phoA supE44 thi-1 gyrA96 relA1* λ), derived from apathogenic *E. coli* K12 (purchased from Invitrogen) were used for plasmid amplifications.

***Escherichia coli* XL01-Blue**

Competent *E. coli* XL01-Blue (*recA1 endA1 gyrA96 thi-1 hsdR17 supE44 relA1 lac* [F['] *proAB lacZ* Δ M15 Tn10 (Tet^r)] (purchased from Stratagene) were used for plasmid amplifications.

***Shigella flexneri* M90T afaE⁺**

S. flexneri M90T is a wild-type (WT) invasive strain of *S. flexneri* serotype 5a derived from a clinical isolate containing the virulence plasmid pWR100. This strain additionally contains the pIL22-afaE (spectinomycin resistance) plasmid encoding the afimbrial adhesion factor afaE from uropathogenic *E. coli* to enhance the capability to invade human cells (Clerc and Sansonetti, 1987).

***Shigella flexneri* BS176 afaE⁺**

S. flexneri BS176 is an apathogenic mutant of the M90T afaE⁺ strain which lacks the virulence plasmid pWR100 and cannot invade eukaryotic cells (Clerc and Sansonetti, 1987).

2.1.2 Chemicals, reagents and enzymes

All chemicals were purchased from Merck, Sigma-Aldrich or Roth, if not otherwise stated.

Reagent	Supplier
3 mm CHR chromatography paper	Whatman
384 well cell culture plates	Corning
ATP	Sigma-Aldrich
Agarose	Sigma-Aldrich
C12-ieDAP	InVivoGen
Cell culture plastics (10cm-, 24 well-, 96 well-plates, flasks)	TRP
dNTP mix	Fermentas
D-Luciferin	Sigma-Aldrich
Dulbecco's modified Eagle's medium (DMEM)	Biochrom AG
Fetal Bovine Serum (FBS)	Gibco
Fetal Calf Serum (FCS)	Bio West
FuGENE6	Roche
GeneRuler DNA ladder, low range	Fermentas
Gentamycin	Roth
HiPerFect	Qiagen
illustra™ PuReTAq™ Ready-To-Go™ PCR beads	GE Healthcare
iQ™ SYBR® Green Supermix	Bio-Rad
Kanamycin	Roth
LPS	InVivoGen
MAXI-Sorp ELISA plates, 96 well	Nunc
MDP	InVivoGen
M-Tri-DAP	InVivoGen
Nitrocellulose Membrane (0.2 µm)	Bio-Rad
Non-essential amino acids	Biochrom AG
ONPG	Fluka
PAGE ruler prestained protein marker	Fermentas
Penicillin/Streptomycin	Biochrom AG
PBS (1x) for cell culture	Biochrom AG
PMA	Sigma-Aldrich

MATERIALS AND METHODS

Polymyxin B	Sigma-Aldrich
QUANTI-Blue™	InVivoGen
Recombinant Human BMP-2	R&D Systems
Rotiphorese® Gel 30 (37.5:1)	Roth
Spectinomycin	Fluka Biochemika
Super Signal West Femto Maximum sensitivity Substrate	Thermo Scientific
Super Signal West Pico Luminol/Enhancer Solution	Thermo Scientific
Taq DNA polymerase	Fermentas
Tri-DAP	InVivoGen
Trypsin/EDTA (10x)	Biochrom AG
Tumor necrosis factor α (TNF- α)	InVivoGen
VLE RPMI1640 medium	Biochrom AG
X-tremeGENE 9	Roche
Zeocin	InVivoGen

2.1.3 Kits

Kit	Manufacturer
Bio Rad Dc Protein Assay	Bio Rad
Cell Proliferation Kit II (XTT)	Roche
DuoSet ELISA (human IL-6 and IL-8)	R&D Systems
First Strand cDNA Synthesis Kit	Fermentas
NucleoBond PC500 (Plasmid preparation MAXI)	Macherey-Nagel
Qiagen Plasmid Giga Kit	Qiagen
Qiagen Plasmid Maxi Kit	Qiagen
RNeasy Mini Kit (RNA preparation)	Qiagen

2.1.4 Plasmids

Plasmid	Insert	Reference
pcDNA3.1	-	Invitrogen
pcDNA3.1- β -galactosidase	-	(Kufer <i>et al.</i> , 2006)

MATERIALS AND METHODS

pcDNA3.1-Myc-XIAP	human XIAP	(Seeger <i>et al.</i> , 2010)
pcDNA3.1-NOD1	human NOD1	Gift from G. Nuñez
pcDNA3.1-NOD2	human NOD2	Gift from G. Nuñez
pcDNA3.1-SMAC Δ MTS	human SMAC Δ MTS	(Kashkar <i>et al.</i> , 2006)
pGL3-IL-8-luciferase	-	(Bowie <i>et al.</i> , 2000)
NF- κ B-reporter-Ig κ -luciferase	-	(Munoz <i>et al.</i> , 1994)

2.1.5 Primer

Name	GC [%]	Length [bp]	Tm [°C]	Sequence
BIRC2_fwd	45	20	55.3	GCATTTCCCAACTGTCCAT
BIRC2_rev	50	20	57.3	GGAAACCACTTGGCATGTTC
BIRC3_fwd	45	20	55.3	CAGCCCGCTTTAAACATTC
BIRC3_rev	50	20	57.3	TGGGCTGTCTGATGTGGATA
BIRC5_fwd	55	20	59.4	GGACCACCGCATCTCTACAT
BIRC5_rev	60	20	61.4	GTCTGGCTCGTTCTCAGTGG
BIRC7_fwd	55	20	59.4	TGGCCTCCTTCTATGACTGG
BIRC7_rev	55	20	59.4	GCACCTCACCTTGCCTGAT
BIRC7_fwd2	55	20	59.4	CCATCAGGACAAGGTGAGGT
BIRC7_rev2	60	20	61.4	AGCTGGGAGTGAGTCTCCTG
BIRC8_fwd	45	20	55.3	AATCCATCCATGACGGGTTA
BIRC8_rev	50	20	57.3	CATGCTGTCCCAAGGATCT
BMPR-2_fwd	48	25	63.0	CACTGAATTGCTTGACTTCTGTGGC
BMPR-2_rev	48	25	63.0	GCTACGCATCTCCATGTTTCAGCTA
GAPDH_5	60	23	52.2	GGTATCGTGGAAGGACTCATGAC
GAPDH_3	60	23	56.5	ATGCCAGTGAGCTTCCCGTTCAG
Myco fwd	47.8	23	60.6	CACCATCTGCTACTCTGTTAACC
Myco rev	47.8	23	60.6	GGAGCAAACAGGATTAGATACCC
NOD1_fwd	42.9	21	55.9	TCCAAAGCCAAACAGAAACTC
NOD1_rev	52.6	19	56.7	CAGCATCCAGATGAACGTG
NOD2_fwd	57.9	19	58.8	GAAGTACATCCGCACCGAG
NOD2_rev	50	22	60.3	GACACCATCCATGAGAAGACAG

MATERIALS AND METHODS

XIAPfw2	52.9	17	49.4	ACACCATATACCCGAGG
XIAPrv2	56.3	16	51.2	CCAGGCACGATCACAA

2.1.6 siRNAs

Gene	Supplier	Name	Number	Target
No target	Qiagen	AllStars	SI1027281	No target
BIRC2	Qiagen	Hs_BIRC2_7	SI02654435	AACATAGTAGCTTGTTTCAGTG
BIRC2	Qiagen	Hs_BIRC2_8	SI02654442	CTAGGAGACAGTCCTATTCAA
BIRC3	Qiagen	Hs_BIRC3_5	SI00299439	AATTGGGAACCGAAGGATAAT
BIRC3	Qiagen	Hs_BIRC3_8	SI02661918	CAAGAACATGATGTTATTTAA
BIRC5	Qiagen	Hs_BIRC5_5	SI00299453	AAGCATTCGTCCGGTTGCGCT
BIRC5	Qiagen	Hs_BIRC5_6	SI00299460	TGCACCACTTCCAGGGTTTAT
BIRC7	Qiagen	Hs_BIRC7_2	SI02645111	TTGGATGCTTCTGAATAGAAA
BIRC7	Qiagen	Hs_BIRC7_3	SI02645118	ATGGCTTAACTGTACCTGTTT
BIRC8	Qiagen	Hs_BIRC8_2	SI00146202	CACGAGGTGCTCACTGCGCAA
BIRC8	Qiagen	Hs_BIRC8_4	SI00146216	AACGTTAATATTCGAGGTGAA
BMPR-2	Qiagen	Hs_BMPR-2_5	SI00604996	AAGCACCGAAGCGAAACTTAA
BMPR-2	Qiagen	Hs_BMPR-2_6	SI00605003	CTCGTAAGTATGTAAAGAAA
NOD1	Qiagen	Hs_CARD4_4	SI00084483	CACCCTGAGTCTTGCGTCCAA
NOD2	Qiagen	Hs_CARD15_3	SI00133049	CTGCCACATGCAAGAAGTATA
RELA	Qiagen	RELA	SI1027020	AAGATCAATGGCTACACAGGA
RIP2	Qiagen	Hs_RIPK2_5	SI0263200	ACGTATGATCTCTTAATAGA
XIAP	Qiagen	XIAP	custom	GGAAUAAAUUGUCCAUGC

For the pilot screen, the Apoptosis siRNA set V1 (Qiagen) consisting of 418 apoptosis-related genes was used. For the main screening project, the Human Druggable Genome siRNA Set V2.0 (Qiagen) was used. This pre-designed siRNA library includes siRNAs designed against 6992 potentially druggable targets of the human genome. An individual library for hit validation containing 535 genes was purchased from Qiagen and spotted on 384 well plates.

2.1.7 Antibodies

Primary antibodies

Antigen	Type	Clone	Dilution	Reference
GAPDH	Rabbit pc	FL-355	1:1000	Santa Cruz Biotechnology (sc-25778)
NF- κ B p65	Mouse mc	F-6	1:500	Santa Cruz Biotechnology (sc-8008)
phospho-p42/44	Rabbit mc	137F5	1:1000	Cell Signaling (#4695)
p42/44	Mouse mc	E10	1:2000	Cell Signaling (#9106)
XIAP	Mouse mc	48	1:500	BD Biosciences (#610763)

Secondary antibodies

Antigen	Type	Enzyme	Dilution	Reference
Mouse IgG	Goat	HRP	1:4000	Bio-Rad Laboratories (170-6516)
Rabbit IgG	Goat	HRP	1:4000	Bio-Rad Laboratories (170-6515)

2.1.8 Instruments

Instrument	Manufacturer
384 well pipetting head	Beckman Coulter
Biomek FX ^P laboratory automation workstation	Beckman Coulter
Centrifuge 5415R	Eppendorf
Centrifuge 5418	Eppendorf
Centro XS ³ LB960 Luminometer	Berthold Technologies
Cytomat Microplate Hotel and Incubator	Thermo Electron Corporation
Envision plate reader	Perkin Elmer
Incubator	Heraeus
Gel electrophoresis system	Bio-Rad Laboratories
iQ5 TM cyclor (qRT-PCR)	Bio-Rad Laboratories
LAS-4000 Luminescent Image Analyser	Fujifilm
Micro Centrifuge	Roth
MicroDrop MD combi	Thermo Electron Corporation

MATERIALS AND METHODS

MicroDrop MD micro	Thermo Electron Corporation
Micropipettes	Gilson, Finnzymes
Multifuge 4KR	Heraeus
Multipette plus dispenser	Eppendorf
Nano Photometer™	Implen GmbH
Neubauer counting chamber	Labor Optik
Nunc-Immuno Wash 12	Nunc
OD600 DiluPhotometer™	Implen GmbH
ORCA robot arm	Beckman Coulter
Pipetboy acu	Integra Biosciences
Primus Thermocycler	MWG Biotech
PS-M3D Orbital Shaker	Grant-bio
Research pro multichannel pipettes	Eppendorf
Steri-Cycle CO ₂ Incubator, Model 381	Thermo Forma
Sterile bench	Heraeus
Thermomixer comfort	Eppendorf
TRANS BLOT SD, Semi-Dry Transfer Cell	Bio-Rad Laboratories

2.1.9 Software

Software	Company/Source
Adobe Acrobat 9 professional	Adobe Systems Incorporated
Adobe Illustrator CS5	Adobe Systems Incorporated
Adobe Photoshop CS5	Adobe Systems Incorporated
Bioconductor	Open source (www.bioconductor.org)
Biomek Workstation Software	Beckmann Coulter
Bio-Rad iQ5 version 2.0	Bio-Rad Laboratories
CellHTS2	(Boutros <i>et al.</i> , 2006)
Endnote X	Thomson Reuters
GORilla	(Eden <i>et al.</i> , 2009; Eden <i>et al.</i> , 2007)
GraphPad Prism 5	GraphPad Software Inc.
Imagereader LAS-4000	Fujifilm

Ingenuity Pathway Analysis	Ingenuity Systems
Microwin 2000	Berthold Technologies
Microsoft Office 2003	Microsoft
Microsoft Excel 2007	Microsoft
SAMI EX Workstation Editor	Beckmann Coulter
STRING 9.0	www.string.embl.de

2.2 Methods

2.2.1 Cell biological methods

Tissue culture

HEK293T cells were grown at 37 °C with 5 % CO₂ in Dulbecco's MEM (with 3.7 g/l NaHCO₃, 4.5 g/l D-Glucose and stable glutamine, without Na-Pyruvate, low endotoxin) (in the following referred to as DMEM) containing 10 % heat-inactivated fetal calf serum (FCS) and penicillin-streptomycin (100 IU/ml and 100 mg/ml, respectively) (P/S). HeLa cells were cultured at 37 °C with 5 % CO₂ in DMEM (containing FCS and P/S). THP-1 cells were cultured in very low endotoxin RPMI1640 (containing FCS and P/S). THP1-Blue cells were maintained in very low endotoxin RPMI 1640 (containing FCS and P/S) and 100 µg/ml zeocin. Cells were continuously tested for mycoplasma contamination using PCR (see below).

Luciferase reporter gene assays

Activation of NF-κB and IL-8 was measured using a luciferase reporter gene assay as described previously (Kufer *et al.*, 2006). HEK293T cells were trypsinised, counted using a Neubauer chamber and adjusted to 3x10⁵ cells per ml in DMEM (containing FCS and P/S). Subsequently, 100 µl of the cell suspension was seeded in 96 well plates and transfected using FuGENE6. Per well, 8.6 ng β-galactosidase-plasmid, 13 ng luciferase-reporter plasmid (NF-κB or IL-8) and 0.5 ng NOD1 or 0.1 ng NOD2 expression plasmid were used, the DNA content was adjusted with pcDNA to 51 ng DNA total. The contents were diluted in 20 µl DMEM, 0.2 µl FuGENE6 was added and the mixture was incubated at RT for 20 min prior to transfection. Subsequently, cells were stimulated with 500 nM Tr-iDAP, 50 nM MDP or 0.01 µg/ml TNF-α. After 16 h of incubation, the growth medium was removed and cells were lysed in 100 µl lysis buffer.; 50 µl of the

MATERIALS AND METHODS

lysates was used to measure the luciferase activity, the remaining lysates were mixed with 100 μ l ONPG-development buffer to determine the β -galactosidase expression. Luciferase activity was normalised as a ratio to β -galactosidase activity, the mean and standard deviations were calculated from triplicates.

siRNA in HEK293T cells

Gene silencing with small interfering RNA (siRNA) was performed by transfection of siRNA using HiPerFect. HEK293T cell solution was adjusted to 2×10^4 cells/ml in DMEM (containing FCS and P/S). Subsequently, 100 μ l of the cell solution was seeded in a 96 well cell culture plate. Cells were transfected with transfection mixes containing 20 nM siRNA, 0.8 μ l HiPerFect and 20 μ l DMEM that were incubated for 10 min at RT prior to transfection. After 16 h, the growth medium was removed and replaced with 100 μ l fresh medium. 72 hours after siRNA transfection, cells were transfected with the NF- κ B luciferase reporter system and NOD1 or NOD2 expression plasmids, as described above. Subsequently, cells were stimulated with 500 nM Tri-DAP, 50 nM MDP or 10 ng/ml TNF- α . After 16 h incubation, the luciferase and β -galactosidase read-outs were performed as described above.

To monitor knock-down efficiency, cells were treated as indicated above. After 48 h to 72 h incubation, cells were lysed in 2xLaemmli buffer. For each sample, 6 wells were pooled. Samples were boiled for 10 min at 95 $^{\circ}$ C and subsequently subjected to Western blotting.

Reagents

Lysis buffer: 25 mM Tris pH 8.0, 8 mM MgCl₂, 1 % Triton, 15 % Glycerol, H₂O

Reading buffer: Lysis buffer containing 0.77 μ g/ml D-luciferin and 1.33 mM ATP

ONPG-dilution buffer: 0.06 M Na₂HPO₄, 0.04 M NaH₂PO₄, 0.01 M KCl, 0.001 M MgSO₄, pH 7

ONPG-development buffer: 4:1 ONPG-dilution buffer : ONPG stock solution (4 mg/ml) in ONPG-dilution buffer

6xLaemmli buffer: 7 ml 0.5 M Tris pH 6.8 containing 0.4 % SDS, 3 ml glycerol, 1 g SDS, 1.2 mg brom-phenol blue. 60 μ l β -mercaptoethanol was added per ml before use

THP1-Blue assay

Cells were counted using a Neubauer chamber and adjusted to 1.5×10^6 cells/ml in RPMI1640 (containing FCS and P/S). Subsequently, 100 μ l of the cell solution was seeded per well in a 96 well plate. 20 μ l of the samples was added per well including appropriate controls, such as Tri-

MATERIALS AND METHODS

DAP (10 µg/ml), MDP (10 µg/ml), LPS (0.1 µg/ml) or endotoxin free water. SEAP activity was measured after 16 h incubation at 37 °C and 5 % CO₂. For that purpose, 20 µl of the supernatant was added to 200 µl QUANTI-Blue SEAP-detection medium and incubated at 37 °C for 1-2 h. SEAP activity was measured at 620 nm. All assays were performed in triplicates.

Reagents

QUANTI-Blue SEAP-detection medium: Reconstituted in ddH₂O according to the manufacturer's manual

siRNA in THP-1 and THP1-Blue cells

THP-1/THP1-Blue cells were counted using a Neubauer chamber and adjusted to for 4x10⁵ cells/ml in RPMI1640 (containing FCS and P/S). Of this solution, 500 µl was seeded into a 24 well plate and cells were differentiated by adding 0.1 µM PMA. After 24 h of incubation, the growth medium was removed and replaced with 100 µl RPMI1640 (containing FCS and P/S). The transfection mixes containing 100 nM siRNA, 6 µl HiPerfect and 100 µl RPMI1640 were incubated for 10 min at RT and then added dropwise to the cells. After 6 h incubation at 37 °C and 5 % CO₂, 400 µl RPMI (containing FCS and P/S) was added to the cells. Cells were incubated for 48 - 72 h at 37 °C and 5 % CO₂ with continuous medium changes twice a day. After 48 - 72 h, the growth medium was replaced with 300 µl RPMI1640 (containing FCS and P/S) and the cells were stimulated with 10 µg/ml Tri-DAP, 10 µg/ml MDP, 0.1 µg/ml LPS or 0.01 µg/ml TNF-α for 16 h. Subsequently, the read-out was performed as described above (only for THP1-Blue cells). Alternatively, cytokine secretion in the supernatants was determined by ELISA. Assays were performed in duplicates. In parallel, cellular RNA was extracted to determine knock-down efficiency by RT-PCR or qRT-PCR.

siRNA in HeLa cells

HeLa cells were counted using a Neubauer chamber and adjusted to 8x10⁴ cells/ml in DMEM (containing FCS and P/S). Subsequently, 500 µl of the cell solution was seeded in a 24 well cell culture plate and incubated for 5 h at 37 °C with 5 % CO₂. After the incubation, cells were transfected with 10 nM siRNA and 4.5 µl HiPerFect in 100 µl DMEM. After 24 h, the growth medium was exchanged, 48 h later, cells were infected with *S. flexneri* BS176 afaE⁺ or M90T afaE⁺ (MOI=10), as indicated below. Supernatants were collected 6 h after infection and IL-8 levels were determined by ELISA. Assays were performed in duplicates. In parallel, cellular RNA was extracted to determine knock-down efficiency by RT-PCR.

Gene knock-down in stable HeLa shRNA cell lines

HeLa shRNA cells (HeLa shSCR or HeLa shXIAP) were counted using a Neubauer chamber and adjusted to 4×10^5 cells/ml in DMEM (containing FCS and P/S). Subsequently, 500 μ l of the cell solution was seeded in a 24 well cell culture plate and incubated for 24 h at 37 °C with 5 % CO₂. After incubation, cells were infected with *S. flexneri* BS176 afaE⁺ or M90T afaE⁺ (MOI=37.5), as indicated below. Supernatants were collected 6 h after infection and IL-8 levels were determined by ELISA. Assays were performed in duplicates.

Bacterial infection of HeLa cells with *Shigella flexneri*

S. flexneri BS176 afaE⁺ and M90T afaE⁺ from glycerol stocks were plated on congo red plates two days prior to infection and grown at 37 °C over night. One day prior infection, pre-cultures in 5 ml soy bean medium with 200 μ g/ml spectinomycin were inoculated with a single bacterial colony and grown at 37 °C over night on a shaker with 225 rpm. On the day of infection, fresh *Shigella* cultures were prepared by diluting the overnight cultures 1:20, 1:25 and 1:30 and grown to an optical density at 600 nm (OD₆₀₀) of 0.3 - 0.6. One millilitre of the solution was centrifuged at 4000 rpm for 5 min. The pellet was resuspended in DMEM to adjust the solution to an OD₆₀₀ of 0.3. In parallel, HeLa cells or HeLa cells stably expressing shRNA were washed with 1 ml DMEM, then 250 μ l of DMEM was added. After 1-2 h incubation, HeLa cells were infected with 13.3 μ l of the *Shigella*-solution (corresponds to MOI=10). Infected cells were incubated for 15 min at RT to allow sedimentation of the bacteria, then they were incubated for 30 min at 37 °C and 5 % CO₂ to allow invasion of the cells. Subsequently, the supernatants were discarded and replaced by 250 μ l DMEM containing 200 μ g/ml gentamycin to kill extracellular bacteria. Cells were incubated at 37 °C and 5 % CO₂ for 6 h, then supernatants were collected and stored at -20 °C to perform ELISA-assays. Assays were performed in duplicates. In parallel, cellular RNA was extracted to determine knock-down efficiency by RT-PCR.

Reagents

Soy Bean Medium: 30 g BLL Trypticase Soy Broth. Ad. 1 l ddH₂O, autoclaved

Congo Red plates: 25 μ l Soy Bean Medium, 1.5 % Bacto Agar, 0.01 % Congo Red. Boiled for 15 min, after cooling 200 μ g/ml spectinomycin was added and the solution was poured into a cell culture dish

Cell viability assays

For cell viability assays, 3×10^4 HEK293T cells or 1.5×10^5 THP1-Blue cells were seeded in 96 well plates and treated as indicated. After 16 h of incubation, XTT-assays (Cell Proliferation Kit II (XTT), Roche) were performed according to the manufacturer's manual. Measurements were performed in triplicates, data are presented as percent cell viability to the control (set to 100 %).

2.2.2 Screening protocols

Large scale siRNA NF- κ B luciferase screen

For the pilot screen, a library of 418 apoptosis-related genes (Qiagen) was used and each gene was targeted with two individual siRNAs. Tri-DAP and TNF- α stimulation were performed in parallel. The top 34 inhibiting and top 18 activating hits were subsequently validated with four different siRNAs. The druggable genome screen was conducted using the Qiagen druggable genome library consisting of 6992 genes. Each gene was targeted by four individual siRNAs. For validation- and TNF- α counter-screening, a subset of the druggable genome library targeting the 435 inhibiting and the top 100 activating hits from the primary druggable genome screen was used. Each gene was targeted with two individual siRNAs.

For screening, uniquely HEK293T cells with a passage number of two were used. Cells were thawed 6 days before use. The whole assay procedure was performed automatically using a Biomek FX^P laboratory automation workstation equipped with a 384 well pipetting head, an ORCA robot arm, two Multidrop (MD) dispensing devices, a Cytomat microplate hotel and incubator, and an integrated Envision plate reader operated with SAMI EX and Biomek software.

Four μ l of 200 nM siRNAs were pre-spotted on clear 384 well cell culture plates to allow reverse transfection of cells (final concentration of 20 nM). All plates contained non-targeting (AllStars) as well as RELA (p65), NOD1 and PLK (Polo-like kinase) siRNAs as internal controls. For transfection, 8 μ l medium per well were mixed with 0.25 μ l HiPerFect and added to the siRNAs. The mixtures were incubated at RT for 15 min before adding 1×10^3 HEK293T cells in 30 μ l RPMI1640 medium (containing FCS and P/S).

After 48 h of incubation to allow establishment of the knock down, and a medium change after 24 h, cells were transfected. The transfection mixtures contained 11.6 ng β -gal plasmid, 7.03 μ l NF- κ B-luciferase plasmid, 0.135 ng NOD1 expression plasmid, 8.78 ng pcDNA-plasmid

MATERIALS AND METHODS

and 0.0918 μl FuGENE6. The mixture was added up to a volume of 5 μl with RPMI and incubated at RT for max. 2 h. Subsequently, cells were stimulated with 0.5 μM Tri-DAP in a volume of 3 μl H₂O. For the TNF- α -counter-screen, 5 ng/ml TNF- α in a volume of 3 μl RPMI was added instead. After stimulation, cells were incubated at 37 °C and 5 % CO₂ for 16 h.

For read-out, cells were lysed by adding 30 μl 2xlysis buffer and subsequently mixed by pipetting. 35 μl of the lysate was then added to a white 384 well plate containing 35 μl reading-buffer. Subsequently, bioluminescence of the samples was measured using an Envision plate reader.

For β -galactosidase read-out, 35 μl of ONPG-development buffer was added to the remaining lysate. After 15 min incubation at 37 °C and 5 % CO₂, the absorbance of the samples at 405 nm was measured automatically with an Envision plate reader. Each siRNA was tested in four biological replicates.

Reagents

2xLysis buffer: 50 mM Tris pH 8.0, 16 mM MgCl₂, 2 % Triton, 30 % Glycerol, H₂O

THP1-Blue siRNA screen

For screening, uniquely THP1-Blue cells with a passage number of three were used. Cells were thawed 10 days before use. The whole assay procedure was performed automatically using a Biomek FX^P laboratory automation workstation equipped with a 384 well pipetting head, an ORCA robot arm, two Microdrop (MD) pipetting devices (MD combi and MD micro), a Cytomat microplate hotel and an Envision plate reader operated with SAMI EX workstation editor and Biomek software.

The siRNAs (200 nM) were pre-spotted on clear 384 well cell culture plates in 4 μl volume and the cells were reversely transfected. All plates contained AllStars, RELA, NOD1 and PLK siRNAs as internal controls. For transfection, 8 μl medium were mixed with 0.25 μl HiPerFect and added to the microplates containing the siRNAs using a MD micro pipetting device. The mixtures were incubated at RT for 15 min, then 8×10^3 THP1-Blue cells in 10 μl RPMI1640 medium (containing FCS and P/S) and 0.1 μM PMA were added using the MD micro pipetting device. After 6 h incubation, 20 μl medium was added.

The cells were incubated for 72 h, while the growth medium was exchanged twice a day. To prevent detachment of the cells, only 35 μl of the 42 μl total volume in the wells was aspirated and replaced with 35 μl fresh medium using the 384 well pipetting head.

After 72 h, 35 μl growth medium was replaced by 15 μl growth medium containing 10 $\mu\text{g}/\text{ml}$ Tri-DAP to stimulate the cells. The cells were incubated for 16 h before read-out. For SEAP-

detection, 10 μ l supernatant per well was transferred to a fresh plate containing 50 μ l QUANTI-Blue SEAP detection medium and incubated for 5 h. 10 μ l XTT reagent was added to the remaining 10 μ l and incubated at 37 °C for 1 h. Absorption at 632 nm and 485 nm, respectively, were measured.

Data analysis

Data was processed using the CellHTS2 package (Boutros *et al.*, 2006), Bioconductor/R, and Excel. The luciferase signal (relative light units; RLU) was normalised by division by the β -galactosidase signal (ABS405) (normalised RLU; $RLU/ABS405 = nRLU$). To exclude experimental artefacts, all those plates were excluded, where the average β -galactosidase signal of the non-targeting controls (ABS405) was >2.5 , <0.2 or had a standard deviation of $>50\%$.

Next, all wells displaying a β -galactosidase signal of $<40\%$ of the non-coding controls, supposedly due to low plasmid transfection efficiency or siRNA toxicity, were excluded from further analysis.

Subsequently, the nRLUs were normalised relative to the inhibitory effect of the RELA-control siRNAs compared to the non-targeting controls (normalised percent inhibition; NPI) and median z-scores of the 4 biological replicates were calculated using CellHTS2.

In the next step, the median z-scores of individual siRNAs were used to calculate two separate ranked gene lists, using the redundant siRNA analysis algorithm (RSA) (Konig *et al.*, 2007). These lists comprise genes leading to a decreased NF- κ B activity when knocked down (termed “inhibiting hits”), or to an increased activity (“activating hits”), respectively.

For validation and TNF- α -counter-screening in HEK293T cells, as well as for hit validation in THP1-Blue cells (only for the druggable genome screen), the top 34 (pilot screen) or 435 inhibiting (druggable genome screen) as well as the 18 (pilot screen) or top 100 activating (druggable genome screen) hits were selected. For each of these genes, both siRNAs and two new siRNAs were re-synthesised and assembled on 384 well plates for the pilot screen. For the druggable genome screen, the two siRNAs showing the strongest effect in the screen were re-synthesised and assembled on 384 well plates (“validation plates”).

To validate the results of the primary screens, the experiments were repeated as above, using the validation plates. Data analysis using CellHTS2 was performed as described above; siRNAs were selected as “inhibiting Tri-DAP-hits”, if their median Z-score exceeded the median of non-targeting controls by more than two standard deviations. To exclude unspecific hits, all siRNAs selected for validation were screened for their influence on TNF- α -induced NF- κ B

activation. Data analysis was done analogous to the Tri-DAP validation screen. “Inhibiting TNF- α -hit siRNAs” were excluded from further analysis.

Data from the THP1-blue screen consists of two parameters (QUANTI-Blue absorption at 632 nm for Tri-DAP response [QB], and XTT absorption at 485 nm for cell viability [XTT]) and was processed similar as described above: QB-signal of each well was normalised to cell viability (XTT), yielding nQB (normalised QUANTI-Blue absorption; $QB/XTT = nQB$). After quality control and outlier flagging, the three best experimental replicates were NPI-normalised to non-targeting and NOD1-control siRNAs using CellHTS2, and median Z-scores were used for hit identification. All genes with two siRNAs displaying a decrease of > 1.5 fold standard deviation compared to the non-targeting control were regarded as validated inhibiting hits.

2.2.3 Molecular biological methods

Production of competent bacteria

Approximately 10 μ l of DH5 α or XL01-Blue bacteria was taken from glycerol stocks, plated on LB agar plates and incubated at 37 °C over night. A single colony was inoculated in 5 ml liquid LB medium and incubated at 37 °C over night on a shaker with 100 rpm. Of this culture, 1.5 ml was inoculated in 500 ml LB medium and incubated at 20 °C at 225 rpm until the culture reached an OD₆₀₀ of 0.3 – 0.6. The culture was chilled on ice for 10 min and centrifuged for 15 min at 4000 rpm and 2 °C. The supernatant was discarded and the pellet was washed with 150 ml cold transformation buffer. The culture was centrifuged again for 15 min at 4000 rpm and 2 °C, the pellet was re-suspended in 40 ml transformation buffer and 3 ml DMSO and 500 μ l aliquots were frozen in liquid nitrogen and stored at -80 °C.

Reagents

LB medium: For 1 l medium, 10 g tryptone, 10 g NaCl and 5 g yeast extract were dissolved in H₂O and adjusted to 1 l volume. The solution was sterilised by autoclaving.

LB agar plates: LB medium was prepared as described above, 15 g agar powder was added per litre. After autoclaving, antibiotics were added and the liquid was poured in 10 cm petri dishes.

Transformation buffer: 15 mM CaCl₂, 250 mM KCl, 10 mM PIPES, 55 mM, MnCl₂·4 H₂O, pH 6.7; sterile filtrated.

Heat-shock transformation of *E. coli*

Chemical competent DH5 α or XL01-Blue *E. coli* cells were thawed on ice. One microlitre plasmid DNA was added to 50 μ l cell suspension and incubated on ice for 30 min. Subsequently, bacteria were subjected to a heat-shock at 42 °C for 1 min. For transformation of bacteria with plasmids containing an ampicillin resistance marker, bacteria were subsequently diluted in 1 ml LB medium and 200 μ l of the solution was directly plated on LB agar plates supplemented with 100 μ g/ml ampicillin. For transformation of plasmids containing a kanamycin resistance marker, bacteria were diluted in 1 ml LB medium and incubated for 45 min at 37°C. After incubation, 200 μ l of the solution was plated on LB agar plates supplemented with 50 μ g/ml kanamycin. Bacteria were grown overnight at 37 °C.

Isolation of DNA from *E. coli*

A single transformed *E. coli* clone picked from the appropriate LB agar plate was inoculated in 2 ml LB medium containing 100 μ g/ml ampicillin or 50 μ g/ml kanamycin and incubated at 37 °C while shaking at 225 rpm for 6 h. 100 μ l of the starter culture was then inoculated in 100 ml LB medium (for Maxi preps) or 500 ml LB medium (for Giga preps) containing the appropriate antibiotics and cultivated over night under the aforementioned conditions. Cultures were pelleted by centrifugation at 6000 x g for 15 min and plasmid DNA was isolated using the NucleoBond PC500 Maxi prep kit (for Maxi preps) or the Plasmid Giga kit (for Giga preps) according to the manufacturer's manuals. DNA was eluted in 100-200 μ l (Maxi prep) or 500 μ l (Giga prep) 10 mM TE buffer (pH 8.0) and DNA concentration was determined using a Nano Photometer.

Isolation of RNA from human cells

RNA was isolated from human cells using the RNeasy Mini Kit (Qiagen) according to the manufacturer's manual. Concentration and purity of the RNA was determined at 260 and 280 nm using a Nano Photometer.

Reverse transcription of RNA

Reverse transcription of isolated RNA was performed using the First Strand cDNA Synthesis Kit with oligo-dT18 primers according to the manufacturer's manual. In each reaction 1 μ g RNA was transcribed.

End-point RT-PCR

Polymerase chain reaction (PCR) of cDNA templates was performed according to the following protocol:

Reagent	Volume [μ l]
Buffer (+KCl, -MgCl ₂)	5
MgCl ₂	4
dNTPs	2
Taq DNA polymerase	0.5
ddH ₂ O	35.5
Fwd primer	1 [1:10]
Rev primer	1 [1:10]
cDNA	1 – 2

Reaction mixes were prepared on ice and drops were collected by brief centrifugation before starting the reaction. The reaction was performed in a Primus Thermo-cycler using the following programme:

PCR step	Temperature [°C]	Time	
Denaturation	94	1 min	1x
Melting	94	30 sec	30-35x
Annaealing	54 - 55, as indicated	30 sec	
Elongation	72	1 min	
Final elongation	72	5 min	1x
Storage	4	∞	

PCR products were analysed by gel electrophoresis on a 2 % agarose gel.

PCR for Mycoplasma detection

For *Mycoplasma* testing, cells were cultured over night in the appropriate medium without antibiotics. Aliquots of the supernatant were boiled at 100 °C for 5 min and briefly centrifuged. PCR mixes were prepared according to the following protocol:

MATERIALS AND METHODS

Reagent	Amount / Volume [μ l]
PuReTaq™ Ready-To-Go™ beads	1 bead
Myco fwd primer	0.8
Myco rev primer	0.8
Boiled supernatant (template)	1
ddH ₂ O	22.4

Reaction mixes were prepared on ice and drops were collected by brief centrifugation before starting the reaction. The reaction was performed in a Primus Thermo-cycler using the following programme:

Temperature [°C]	Time	
94	2 min	1x
57	2 min	1x
72	2 min	34x
92	30 sec	
57	1 min	
72	1 min	
72	4 min	1x
4	∞	

PCR products were analysed by gel-electrophoresis on a 2 % agarose gel.

Agarose gel electrophoresis

PCR products were analysed by gel electrophoresis on 2 % agarose gels. Agarose was dissolved in 1xTBE buffer, boiled for 1 ½ min and poured in a gel tray. After letting the gel cool down to ~50 °C, 0.5 μ l/ml Ethidiumbromide was added. Samples were diluted in DNA loading buffer and 10 μ l of the dilution was applied to the gel. Four μ l GeneRuler DNA ladder or GeneRuler DNA ladder low range were applied to the gel as standard. Samples were subjected to electrophoresis for 35 min at 80 V. PCR products were detected under UV light in a LAS4000 device.

Reagents

TBE (Tris-borate EDTA): Prepared as 10x solution. 0.89 M (108 g) Tris Base and 0.89 M (55 g) of boric acid were dissolved in 900 ml H₂O. 20 mM (40 ml 0.5 M) Na₂EDTA (pH 8.0) was added and the volume was adjusted to 1 l with ddH₂O. The solution was sterilised by autoclaving.

6xDNA loading buffer: 2 % glycerol in ddH₂O, bromophenol blue powder was added using a pipette tip.

Quantitative real-time PCR

Quantitative real-time PCR (qRT-PCR) was performed using a Bio-Rad iQ™ cyclor and the iQ™ SYBR® Green Supermix. For each reaction, 5 ng/μl cDNA in a volume of 5 μl was used. The reaction was prepared as follows:

Reagent	Volume / Conc.
iQ™ SYBR® Green Supermix	12.5 μl
Fwd primer	0.188 μl / 7.5 pmol
Rev. primer	0.188 μl / 7.5 pmol
H ₂ O	ad. 20 μl

5 μl cDNA (corresponding to 5 ng/ml) was added to each reaction. Reaction mixes were prepared on ice and drops were collected by brief centrifugation before starting the reaction. The PCR was performed in 96 well PCR plates according to the following settings:

Temperature [°C]	Time	
95	3 min	1x
95	15 sec	40x
60	1 min	
55	30 sec	81x
25	∞	1x

Reactions were performed in triplicates. Data was processed according to the $\Delta\Delta C_t$ method with GAPDH as reference gene using the Bio-Rad software package iQ5 version 2.0.

2.2.4 Biochemical methods

Measurement of protein concentrations

Protein concentrations of samples were determined using the Dc Protein Assay according to the manufacturer's manual.

SDS polyacrylamide electrophoresis

Proteins from cell lysates were separated by SDS-polyacrylamide gelelectrophoresis (SDS-PAGE) (Laemmli, 1970). A discontinuous gel system consisting of a lower separation gel (10 %) and an upper stacking gel (4 %) was used. Samples were diluted in 2xLaemmli buffer and boiled at 95 °C for 10 min. 10 µl of the samples was loaded in the gel pockets. Electrophoresis was performed in SDS-PAGE running buffer at 195 V for 45 min.

Reagents

Separating gel: 2.1 ml ddH₂O, 2.5 ml acrylamide (40 %), 5 ml 0.5 M Tris/0.4 % SDS pH 8.8, 25 µl TEMED, 50 µl APS (10 %)

Stacking gel: 4.5 ml ddH₂O, 650 µl acrylamide (40 %), 1.25 ml 0.5 M Tris/0.4 % SDS, pH 6.8, 25 µl TEMED, 50 µl APS (10 %)

6xLaemmli buffer: 7 ml 0.5 M Tris pH 6.8 containing 0.4 % SDS, 3 ml glycerol, 1 g SDS, 1.2 mg bromophenol blue. 60 µl β-mercaptoethanol was added per ml before use

SDS-PAGE running buffer: 250 mM Tris, 1.92 M glycine, 34.67 mM SDS, add up to 1 l with ddH₂O

Western Blot

Proteins were transferred to a nitrocellulose membrane by semidry Western transfer at 15 V for 30 min. Blotting efficiency was controlled by Ponceau-S staining. Membranes were blocked for 20 min at RT in PBS containing 5 % milk. Proteins were detected by over night incubation at 4 °C of the membrane in PBS containing 5 % milk and a primary antibody. Subsequently, membranes were washed three times in PBST and then incubated for 1 h at RT with the secondary antibody in PBS containing 5 % milk. After washing again three times in PBST, membranes were finally incubated with Pico substrate or Femto maximum sensitivity substrate, depending on the strength of the signal. Chemiluminescence was detected using a LAS4000 device. For detection of phospho-specific antibodies, TBS containing 5 % milk was used for blocking and incubation and TBST was used for washing.

Reagents

Transfer buffer: Prepared as 10x solution. 250 mM Tris and 1.92 M glycine were adjusted to 1 l with H₂O. Working solution was prepared by 1:10 dilution in H₂O and addition of 20 % methanol.

PBST: Prepared as a 10x solution. 80 g NaCl, 2 g KCl, 14.4 g Na₂HPO₄ x 2 H₂O and 2.4 g KH₂PO₄ in 1 l H₂O, pH adjusted to 7.4 using HCl. Working solution was prepared by 1:10 dilution in H₂O and 0.5 ml tween 20 was added per litre

TBST: Prepared as 10x solution. 50 mM TRIS, 150 mM NaCl, pH 7.5. Working solution was prepared by 1:10 dilution in H₂O and 0.5 ml tween 20 was added per litre

MATERIALS AND METHODS

Ponçeau-S solution: 0.2 % Ponçeau S, 3 % acetic acid in 100 ml ddH₂O

Protein stability assay

To determine XIAP protein stability, 2×10^5 THP1-Blue cells were seeded in 24 well plates in 500 μ l RPMI1640 (containing FCS and P/S). Cells were differentiated over night with 0.1 μ M PMA. After 24 h, the growth medium was discarded and replaced with 200 μ l RPMI1640 (containing FCS and P/S). Cells were treated with 0.5 μ g/ml cycloheximide (diluted in DMSO) and/or 0.5 μ g/ml BMP-2 (diluted in 4 mM HCl). Untreated control cells were treated with DMSO and/or 4 mM HCl to ensure equal conditions. After 3 h and 6 h, the medium was discarded and samples were lysed in 50 μ l 2xLaemmli buffer, boiled for 10 min at 95 °C and then subjected to SDS-PAGE and Western-blotting to detect XIAP and GAPDH protein levels.

Detection of p44/42 activation

To determine p44/42 MAPK activation in response to BMP-2 treatment, 2×10^5 THP1-Blue cells were seeded in 24 well plates in 500 μ l RPMI1640 (containing FCS and P/S). Cells were differentiated over night with 0.1 μ M PMA. After 24 h, the growth medium was discarded and replaced with 200 μ l RPMI1640 (containing FCS and P/S). Cells were treated with 0.5 μ g/ml BMP-2 (diluted in 4 mM HCl) for the indicated time points. Untreated control cells were treated with 4 mM HCl to ensure equal conditions. After incubation, the medium was discarded and samples were lysed in 50 μ l 2xLaemmli buffer, boiled for 10 min at 95 °C and then subjected to SDS-PAGE and Western-blotting to detect phospho-p44/42 and total p44/42 protein levels.

ELISA

Secretion of interleukin 8 (IL-8, CXCL-8) from human cells was measured using enzyme-linked immuno absorbent assays (ELISAs) purchased from BD and R&D Systems according to the manufacturer's manuals. Assays were performed in duplicates or triplicates, as indicated.

3 Results

3.1 High-throughput siRNA screen to identify factors involved in NOD1 signalling

To identify factors involved in NOD1-mediated NF- κ B activation, we conducted a high-throughput (HT) siRNA screen in human embryonic kidney (HEK293T) cells. HT reverse genetic screens, such as siRNA screens, have the advantage over other screening techniques that factors that do not necessarily physically interact with each other can be identified. Typically, the first step in a HT siRNA screen is to build a library of genes of interest that are to be targeted by siRNA. Often, the whole genome of an organism is targeted, but there are also libraries targeting sub-sets of genes that are related to certain biological processes or enzymatic functions. It should be considered that each gene is targeted by more than one siRNA, as RNAi-based methods are prone to off-target effects (reviewed in Singh *et al.*, 2011; Svoboda, 2007). Next, a suitable read-out system that allows monitoring of the phenotypic effect(s) of siRNA-mediated gene-silencing has to be established. This system has to be easy to handle, applicable to automated procedures and yield highly reproducible results. Typically, more than one biological replicate is conducted, to ensure statistical significance of the obtained results. For final hit-list generation, several methods for ranking are available that include simple mean- or median-based cutoff methods and probability-based algorithms (reviewed in Birmingham *et al.*, 2009). Ideally, hits are validated in an additional read-out or cell system (reviewed in Moffat and Sabatini, 2006). The screening procedure, statistical methods and data handling should be fixed beforehand to avoid introduction of a bias during the data generation and analysis.

First, the well accepted cell-based reportersystem for NOD1 activation in HEK293T cells (Girardin *et al.*, 2003c; Inohara *et al.*, 1999) was adapted for siRNA-mediated gene-silencing. To test if the system was suited for HTS approaches, a pilot screen with a smaller sub-library consisting of 418 apoptosis-related genes was conducted (Fig. 5A). In the next step, the human druggable genome library was screened on NOD1-mediated NF- κ B activation (“primary screen”). The druggable genome consists of 6992 genes that are regarded as potential drug targets, based on their encoded protein domain structure. A subset of this library containing hits showing effects on NOD1 signalling (“hit library”) was subsequently re-screened on NOD1-mediated NF- κ B activation to validate the hits, and in parallel used for a counter-screen on TNF- α -mediated NF- κ B activation to identify factors that are specifically involved in NOD1 signalling.

RESULTS

Finally, the hit library was screened for NOD1 activation in the myeloid cell line THP1-Blue. Data from all the screening steps was merged to generate a double validated, NOD1-specific hit-list (Fig. 5B).

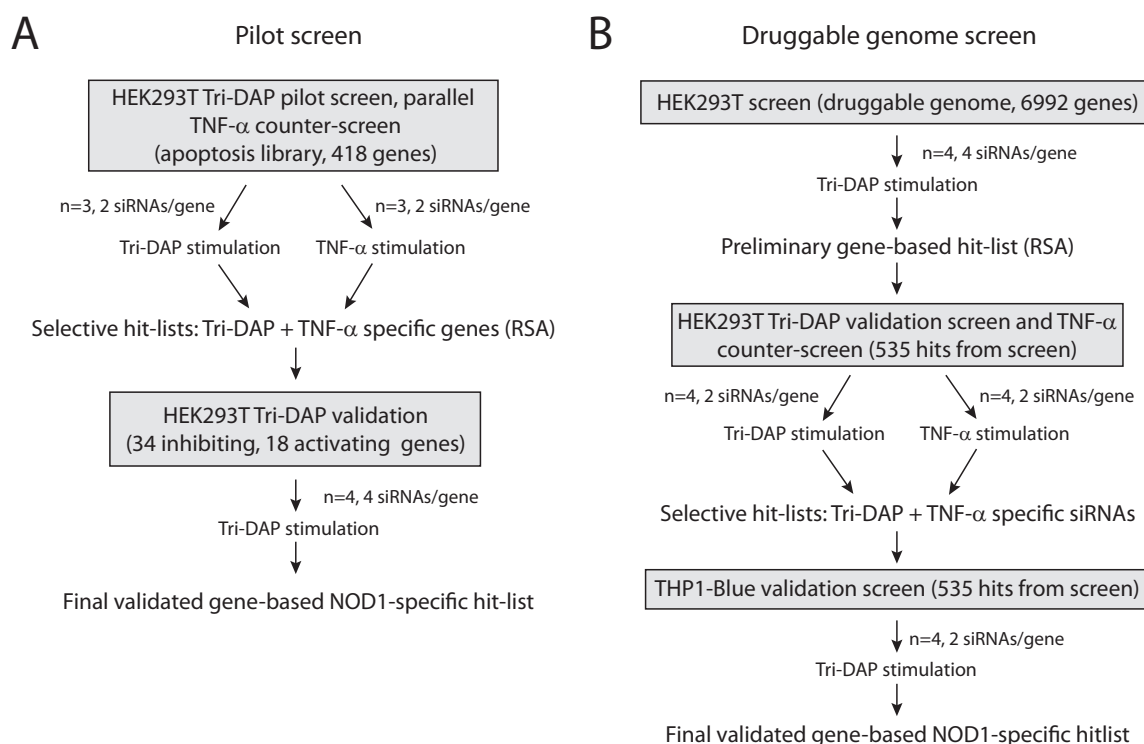


Figure 5. Schematic overview of the screening projects. **A** The pilot screen was conducted using the Apoptosis V1.0 set siRNA library, each gene was targeted by two siRNAs. The whole library was screened on Tri-DAP- and TNF- α -mediated NF- κ B activation and data was merged to generate Tri-DAP/NOD1- and TNF- α -specific hit-lists. The top 34 NOD1-specific inhibiting and top 18 activating hits were subsequently validated using 4 siRNAs per gene. **B** The druggable genome screen was conducted using the Human Druggable Genome set V2.0 siRNA library. The library was first screened on Tri-DAP-mediated NF- κ B activation and gene-based hit-lists were generated by applying the RSA algorithm. The 435 inhibiting and top 100 activating hits were subsequently validated with two siRNAs that were newly synthesised based on the siRNAs that showed the strongest effects in the primary screen. In parallel, a counter-screen on TNF- α -mediated NF- κ B activation was conducted using the same hit-library. Next, the same hit-library was validated in THP1-Blue cells stimulated with Tri-DAP. Finally, data was merged to generate a validated, NOD1-specific hit-list.

3.1.1 Establishment of the assay system in HEK293T cells

3.1.1.1 Establishment of the reporter system

In order to quantify the phenotypic effects of siRNA-mediated knock-down of a certain gene on NOD1-mediated NF- κ B activation, a reliable and easy-to-perform read-out system was needed. We decided to use a cell-based luciferase reporter gene assay specific for NF- κ B activation. This assay is a modification of the original luciferase assay (Kain and Ganguly, 2001), and

RESULTS

is widely used to decipher basic functions of the NOD1 and NOD2 signalling cascades (Girardin *et al.*, 2003c; Inohara *et al.*, 1999). We recently showed that this system can be used to elucidate the function of candidate NOD regulatory proteins and can be combined with siRNA (Bielig *et al.*, 2009; Kufer *et al.*, 2006). The human embryonic kidney cell line HEK293T was used, as these cells are quickly growing, easy to culture and can be transfected with very high efficiency. Furthermore, HEK293T cells do not have functional TLR signalling that might interfere with the read-out (Kurt-Jones *et al.*, 2004; Brightbill *et al.*, 1999). The cells were transiently transfected with the NF- κ B luciferase reporter plasmid together with a β -galactosidase plasmid containing a constitutive promoter, which served for normalisation of the assay (in the following referred to as “reporter system”). As HEK293T cells do not express high levels of NOD1, low amounts of a NOD1-expression plasmid were co-transfected with the reporter system to obtain a higher reactivity towards NOD1 elicitors. We have chosen to specifically activate NOD1 using the chemically synthesised minimal NOD1 elicitor Tri-DAP. Using this defined compound instead of living bacteria, such as *Shigella flexneri*, that naturally trigger NOD1 signalling (Girardin *et al.*, 2001) has the advantage that conditions can be better controlled, leading to a higher reproducibility of the results. Most importantly, this also prevents that pathogen-specific host factors, such as proteins involved in the invasion process of *S. flexneri*, are found as hits. To facilitate uptake of Tri-DAP into the cells, the cells were stimulated directly following transfection of the reporter system, taking advantage of the transfection reagent for delivery of Tri-DAP into the cells, as recently described (Girardin *et al.*, 2003c). In order to allow for accumulation of sufficient amounts of luciferase enzyme for detection, cells were incubated overnight (~ 16 h), as the activation ratio was higher than after shorter incubation periods (data not shown).

The original assay (Girardin *et al.*, 2003c), described for 24 well plates, was scaled down to 96 well plates and optimised for NOD1 and NOD2 activation. Activation of the NOD1 reporter system with Tri-DAP and of the NOD2 reporter system with the NOD2-specific elicitor MDP induced a strong NF- κ B activation, dependent on the amounts of the expression plasmids (Fig. 6A). The best ratio of NF- κ B activation between stimulated cells and non-stimulated cells (specific activation vs. background caused by auto-activation of the proteins) was obtained with 0.5 ng NOD1 plasmid (ratio stimulated/non-stimulated ~ 40), for the NOD2 plasmid, 0.1 ng per well were optimal (ratio stimulated/non-stimulated ~ 20). With increasing amounts of transfected plasmids, the ratio decreased due to the tendency of the NOD proteins to auto-activate. Thus, standard conditions for further experiments were defined as 0.5 ng NOD1 plasmid and 0.1 ng NOD2 plasmid per well.

RESULTS

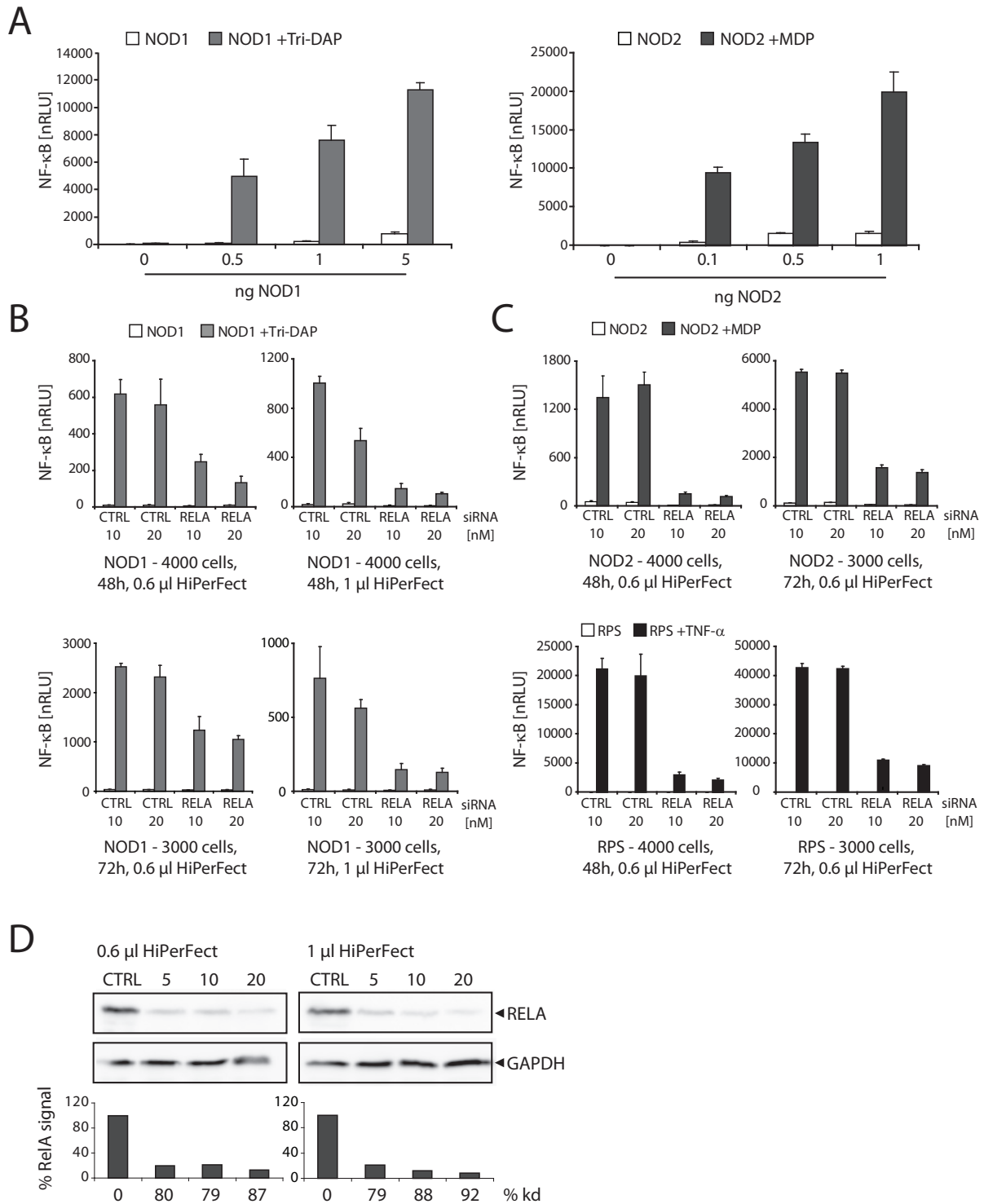


Figure 6. Establishment of the NF- κ B-luciferase reporter system as read-out for siRNA experiments in HEK293T cells. **A** Titration of the NOD1 and NOD2 expression plasmids. HEK293T cells were transiently transfected with a reporter system consisting of a NF- κ B-luciferase plasmid, a β -galactosidase plasmid and different amounts of NOD1 or NOD2 expression plasmids. Subsequently, cells were stimulated with 0.5 μ M Tri-DAP or 50 nM MDP, respectively. After 16 h, cells were lysed and luciferase activation was determined and normalised with the β -galactosidase values (nRLU). Values are mean \pm SD (n=3). **B-C** Establishment of the knock-down conditions. 4000 or 3000 HEK293T cells were transfected with 10 or 20 nM CTRL or RELA siRNA using 0.6 or 1 μ l HiPerFect and incubated for 48 – 72 h. Subsequently, cells were transfected with the NF- κ B luciferase RPS 0.5 ng NOD1 expression plasmid (**B**), the RPS containing 0.1 ng NOD2 expression plasmid (**C**, upper panel) or the RPS alone (**C**, lower panel) and stimulated with Tri-DAP (0.5 μ M), MDP (50 nM) or TNF- α (10 ng/ml), respectively. After 16 h, cells were lysed and luciferase activation was determined

RESULTS

and normalised with the β -galactosidase values (nRLU). Values are mean \pm SD (n=3). **D** Determination of knock-down conditions by Western blot. 5000 HEK293T cells were transfected with 20 nM CTRL siRNA or 5, 10 or 20 nM RELA siRNA using 0.6 or 1 μ l HiPerFect. After 72 h, cells were lysed and RELA protein levels were determined by Western blot using a RELA-specific antibody. Detection of GAPDH served as loading control. RPS: reporter system, nRLU: normalised relative light units

3.1.1.2 Establishment of the siRNA knock-down conditions

Next, the siRNA knock-down protocol was established and the parameters cell number, incubation times and concentrations of transfection reagent and siRNA were optimised. Again, optimal conditions were established for the NOD1- and for the NOD2-reporter system, as well as for stimulation with TNF- α . A siRNA targeting the essential NF- κ B subunit RELA (v-rel reticuloendotheliosis viral oncogene homolog A; also termed p65) was used as positive control, as depletion of RELA is known to abrogate canonical NF- κ B signalling regardless of the triggered pathway (reviewed in Hayden and Ghosh, 2008). HEK293T cells were transfected with different concentrations of CTRL or RELA siRNA using 0.6 or 1 μ l HiPerFect per well. 24 h after siRNA transfection, the growth medium was exchanged in order to minimise toxic effects of the transfection reagent. Cells were incubated for 48 h or 72 h prior to transfection of the reporter system, and subsequently stimulated with Tri-DAP, MDP or TNF- α over night. In assays using the NOD1 reporter system, a higher knock-down efficiency was achieved using 1 μ l HiPerFect compared to 0.6 μ l HiPerFect. The knock-down efficiency with 20 nM RELA siRNA was higher compared to 10 nM siRNA. The 48 h knock-down displayed comparable results to the 72 h knock-down (Fig. 6B). For the NOD2 and TNF assay systems, again 20 nM RELA siRNA showed a slightly stronger reduction of NF- κ B activation compared to 10 nM siRNA. In this case, the knock-down efficiency after 48h was clearly higher than after 72h (Fig. 6C).

Having demonstrated the phenotypic effect of the RELA knock-down and the functionality of the combined siRNA and NF- κ B reporter gene assay system, we next validated the effect of the RELA knock-down as well on protein level by transfecting HEK293T with different amounts of RELA siRNA using 0.6 or 1 μ l HiPerFect per well. Higher cell numbers were used to facilitate detection of RELA on protein level. After 48 or 72 h, cells were lysed and RELA protein levels were determined by Western blotting. Knock-down was visible starting at 5 nM siRNA, and 1 μ l HiPerFect per well induced to a stronger knock-down than 0.6 μ l HiPerFect (Fig. 6D and data not shown).

Taking these results into account, standard operating procedures (SOPs) for the siRNA NF- κ B luciferase reporter gene assay were defined as follows: 4000 cells per well, 20 nM siRNA, an intermediate value of 0.8 μ l HiPerFect per well and a knock-down time of 48 h.

3.1.1.3 Proof of principle for the differential read-out

We used TNF- α -stimulation as differential read-out to identify NOD1-specific genes. The TNF signalling pathway also leads to activation of the canonical NF- κ B pathway, but through a different signalling cascade than NOD1. Stimulation of cells with TNF- α activates NF- κ B through a cascade involving the TNF receptor TNFR1, the factors TRADD, RIP1 and others. This pathway converges with the NOD1 signalling cascade at the level of TAK1 (Fig. 7A) (reviewed in Hayden and Ghosh, 2008). To prove the principle of the differential read-out in our assay system, the essential NF- κ B subunit RELA and the kinase RIP2, which is specific and essential for NOD1/2-mediated NF- κ B activation (Inohara *et al.*, 2000; Bertin *et al.*, 1999; Inohara *et al.*, 1999; McCarthy *et al.*, 1998) were targeted by siRNA and cells were subsequently transfected with the NOD1 NF- κ B-luciferase reportersystem and stimulated with Tri-DAP or TNF- α . As expected, silencing of RIP2 strongly impaired NF- κ B activation in response to NOD1 stimulation (Fig. 7B, lower panel), but did not exert a significant effect on TNF- α -mediated NF- κ B activation (Fig. 7B, upper panel), whereas knock-down of RELA strongly inhibited both signalling pathways (Fig. 7B). This proved that our assay system was suited to attribute siRNA targets to the NOD1 or to the TNF- α signalling pathway.

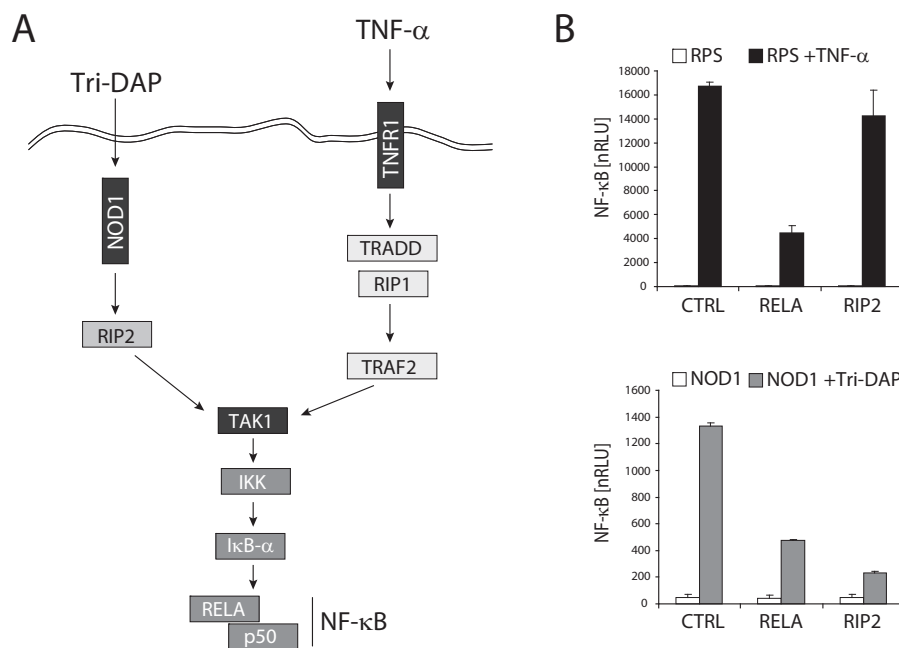


Figure 7. Proof-of-principle for the differential read-out. **A** Simplified overview of the NOD1 and TNF signaling pathways. The different cascades merge at the stage of TAK1 and induce the canonical NF- κ B pathway (for details see text). **B** HEK293T cells were transfected with 20 nM CTRL, RELA or RIP2 siRNA and incubated for 48 h. Subsequently, cells were transfected with the NF- κ B luciferase RPS alone (*upper panel*) or the RPS together with 0.5 ng NOD1 expression plasmid (*lower panel*) and stimulated with TNF- α (10 ng/ml) or Tri-DAP (0.5 μ M), respectively. After 16 h, cells were lysed and luciferase activation was determined and normalised with the β -galactosidase values (nRLU). Values are mean +SD (n=3). RPS: reporter system, nRLU: normalised relative light units

3.1.1.4 Validation of the assay principle

In order to get a statistical size that is large enough to draw conclusions on the quality of the assay system, NOD1 NF- κ B-luciferase reporter gene assays were performed with two sets of three 96 well plates containing untreated cells (n=30), mock-transfected cells (n=30), cells transfected with non-targeting control siRNA (CTRL) (n=60) and RELA siRNA transfected cells (n=30). The first set of three plates was prepared using the same master mixes (cell suspension, siRNA mixes and plasmid mixes) for each plate, for the second set each plate was prepared independently. The data of the three plates of each set was subjected to statistical analyses. First, the p-values of each sample in comparison to the values of CTRL siRNA-transfected cells were calculated using the two-sided student's T-test. Analysis of the three dependent plates revealed that the values of non-treated cells and mock-transfected cells did not significantly differ from cells treated with CTRL siRNA. In contrast, treatment of cells with RELA siRNA caused a highly significant reduction in NF- κ B activation ($p=1.69 \times 10^{-31}$) (Fig. 8A). Next, the Z'-factor was calculated. This method is widely used for quality assessment of assay systems in HTS. The Z'-factor reflects the assay signal dynamic range as well as the data variation associated with the signal measurements (Zhang *et al.*, 1999). It indicates the separation between the positive (c+; here: RELA siRNA) and negative controls (c-; here: non-targeting CTRL siRNA). The Z'-factor is calculated according to the following formula:

$$Z' = 1 - \frac{3(\sigma_{c+} + \sigma_{c-})}{|\mu_{c+} - \mu_{c-}|}$$

The Z'-factor for CTRL vs. RELA was 0.19, which indicated that the assay system was fairly stable and suited for high-throughput applications (Birmingham *et al.*, 2009).

For the set of three independent plates, the overall variations in the RELA and non-targeting CTRL containing wells were higher, but nevertheless the effect of the knock-down of RELA compared to CTRL siRNA-treated cells was still highly significant ($p=2.5 \times 10^{-28}$) (Fig. 8B). The Z'-factor for CTRL vs. RELA of -0.09 was lower than for the three dependent plates. Of note, the assay design provided that each single plate was normalised to internal controls during the screening. Thus only well-to-well variations were of crucial importance, plate-to-plate variations were aligned during the normalisation process.

Taken together, the obtained results indicated that the HEK293T NF- κ B reporter system was suited for HTS.

RESULTS

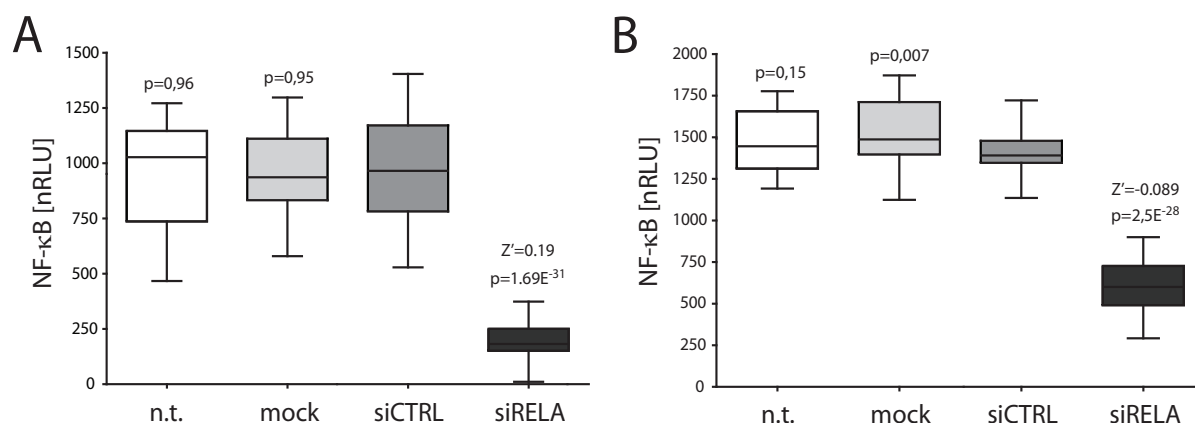


Figure 8. Validation of the NF- κ B luciferase assay as read-out for siRNA-mediated knock-down in HEK293T cells. Cells in three 96 well plates were transfected with CTRL (n=60) or RELA siRNA (n=30), mock-transfected (n=30) or left untreated (n=30) according to the SOPs using the same master mixes (**A**) or using independent master mixes (**B**). After 48 h, cells were transfected with the NOD1 RPS and stimulated with Tri-DAP (0.5 μ M). After 16 h, cells were lysed and luciferase activation was determined and normalised with the β -galactosidase values (nRLU). Data was subjected to statistical analyses. The indicated p-values were calculated using the two-sided student's T-test, assay quality was assessed by calculating the Z'-factor. n.t.: non-treated; RPS: reporter system; nRLU: normalised relative light units

3.1.1.5 Downscaling and automation of the protocol

In order to apply the established assay protocol to an automated high-throughput screen, first the assay procedure had to be scaled down to the 384 well format. The critical factors (most importantly cell number, amount of NOD1-plasmid and amount of transfection reagent) were re-optimised and some major modifications had to be done in order to match the requirements of the automated screening platform. Thorough testing (data not shown) indicated that 1×10^3 cells in 30 μ l medium, transfected with 20 nM siRNA in 8 μ l medium with 0.25 μ l HiPerFect were the optimal conditions, and thus used for the whole following screening procedures with HEK293T cells (Fig. 9). To enhance reproducibility of the results, we decided to use exclusively cells with a defined passage number of 3 (downscaling was accomplished with the help of Dr. Peter Braun and co-workers, MPIIB Berlin).

Furthermore, the protocols for the automated liquid handling and plate processing were designed and optimised (data not shown) (automation of the procedure was established by Dr. Peter Braun and co-workers, MPIIB Berlin).

RESULTS

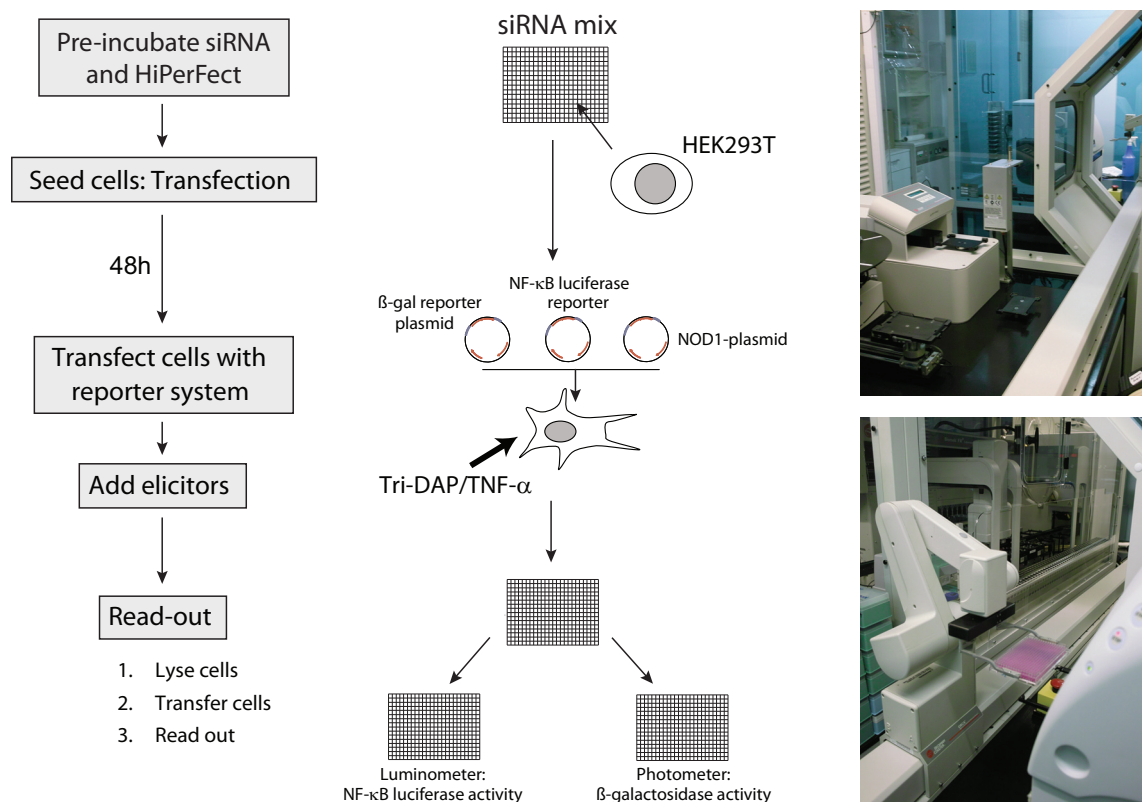


Figure 9: Schematic overview of the NF-κB luciferase assay as read-out for siRNA-mediated knock-down in HEK293T cells as used for screening. In brief, pre-spotted siRNAs were incubated with medium containing HiPerFect. Subsequently, HEK293T cells were reversely transfected by seeding onto the siRNA mixes. 48 h later, cells were transfected with the NOD1 reporter system and stimulated with Tri-DAP (0.5 μM) or TNF-α (10 ng/ml). After 16 h, cells were lysed and luciferase activation was determined in parallel to measurement of β-galactosidase activation. All steps were performed automatically.

3.1.2 Pilot screen with an apoptosis library

To test if the established and optimised automated system was suited for our aimed HTS, a pilot screen was performed. We have chosen the apoptosis siRNA set V1 (Qiagen) consisting of 418 apoptosis-related genes, as there were several recent reports indicating that factors involved in the control of apoptosis also act in inflammatory pathways (Bauler *et al.*, 2008; Bertrand *et al.*, 2008; Conte *et al.*, 2006). First, the NOD1/Tri-DAP screen was carried out in 384 well plates with pre-spotted siRNAs according to the established conditions (screening was performed by Dr. Peter Braun and co-workers, MPIIB Berlin). Each gene was covered by two different siRNAs and four independent biological replicates were performed in order to increase statistical validity of the data. Data was normalised to plate-internal controls. On each plate, RELA siRNA served as positive control and non-targeting siRNA as negative control. Furthermore, PLK (Polo-like kinase) siRNA was included as control to monitor transfection efficiency, as knock-down of PLK induces cell death in cancer cells (Liu *et al.*, 2006; Liu and Erikson, 2003),

RESULTS

which can be monitored by microscopy. Mock-transfected controls were also included. Statistical analyses confirmed robustness of the RELA and non-targeting CTRL assay controls and the reproducibility of the results.

For plates that met the quality requirements (described in the methods section), first the normalised percent inhibition (NPI) for each sample in relation to the RELA controls was calculated plate internally (RELA control siRNA: NPI=100, non-targeting CTRL siRNA: NPI=0). Then data was normalised by Z-transformation to the overall screen data and individual Z-scores were calculated for each replicate according to the following formula:

$$z = \frac{x - \mu}{\sigma}$$

Toxic samples were removed from the data pool. Definition for toxicity was <60 % β -galactosidase signal compared to the screen-average. Only genes that were covered by at least two non-toxic siRNAs were further processed (bioinformatics performed by Dr. Peter Braun, MPIIB Berlin).

In order to determine if identified siRNAs were specific to the NOD1 pathway, a counter-screen with TNF- α -stimulation of the cells was performed in parallel. The counter-screen also covered the whole apoptosis-library and was conducted analogous to the NOD1/Tri-DAP screen. Data was processed as described above. Samples differing at least 2 standard deviations (SD) of the CTRL siRNAs from the median of the CTRL siRNAs (+2 SD: “inhibiting hit siRNA”; -2 SD: “activating hit siRNA”) in the respective screen were defined as significant for the Tri-DAP/NOD1 or the TNF- α /TNFR1 pathways (Fig. 10A).

Final ranking and generation of gene-based hit-lists was performed using the RSA (redundant siRNA activity) algorithm. This method is based on an iterative hypergeometric distribution formula and assigns probability (p) values to each gene, based on the behaviour of the different corresponding siRNAs. Thus it accounts for differences in the effects of multiple siRNAs for the same gene: *i.e.* genes with multiple moderately active wells are weighed more heavily than genes with fewer, but highly active wells, minimising the contribution of off-target effects (Konig *et al.*, 2007). By applying the RSA-algorithm to the normalised data sets from the Tri-DAP/NOD1 screen and the TNF- α counter-screen, gene-based hit-lists were generated. Genes with p-values lower than 0.05, according to the RSA analysis, were considered as strong hits. Among the inhibiting hits, 24 genes from the Tri-DAP/NOD1 screen and 25 genes from the TNF- α counter-screen fulfilled these criteria. The hit-lists were merged and NOD1- and TNF- α -specific hit-lists were generated by excluding factors appearing in both lists (12 factors in total) (Fig. 10B). Furthermore, a hit-list containing genes that were found in both of the screening steps

RESULTS

was generated (NF- κ B associated hits) (Fig. 10B). In total, out of 24 hits from the Tri-DAP/NOD1 screen, 12 were also positive in the TNF- α counter-screen. Of note, we were able to identify many genes that are well established to be critically involved in the canonical NF- κ B and the NOD1 signalling cascades, such as RELA, p50, CUL1, RIP2, TAK1 or TNFR1, among the inhibiting hits (Fig. 10B).

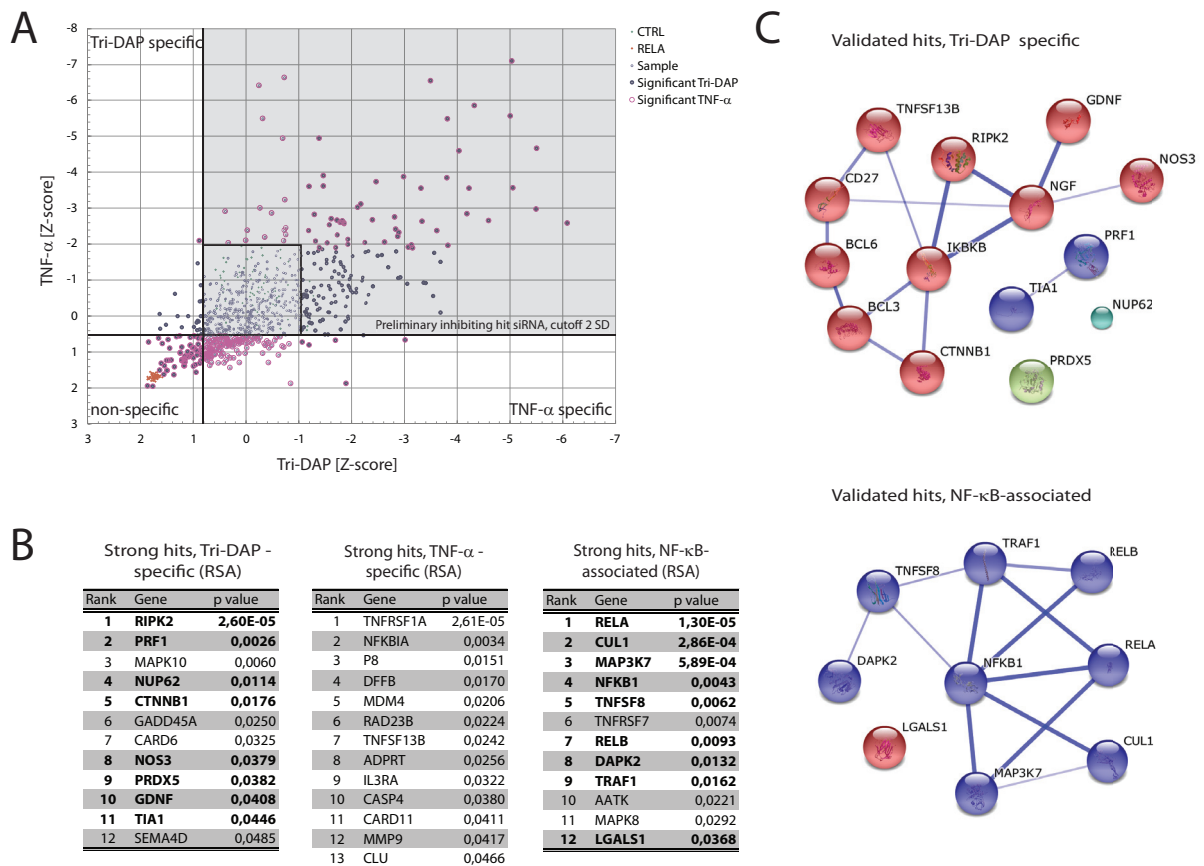


Figure 10. Results of the pilot screen. **A** Data from the Tri-DAP-screen was merged with data from the TNF- α counter-screen to identify factors that are specifically involved in NOD1-signalling. Each dot represents the median Z-scores after NPI-normalisation (Normalised Percent Inhibition) to the plate-internal RELA-controls for the single siRNAs, Tri-DAP/NOD1 activation is plotted on the x-axis, the corresponding TNF- α /TNFR1 values are plotted on the y-axis. A positive value represents an inhibitory effect of the respective siRNA on NF- κ B activation, siRNAs activating NF- κ B activation are represented by negative values. Samples differing at least 2 SD of CTRL from the median of the CTRL siRNAs of the respective screen were defined as significant for Tri-DAP or TNF- α . **B** Gene-based hit-lists displaying strong ($p < 0.05$) Tri-DAP-specific, TNF- α -specific and non-specific hits according to the RSA algorithm. Bold: Hits that could be validated **C** STRING database analysis of the validated Tri-DAP-specific and NF- κ B-associated hits. Genes, where the NPI values of at least two out of four siRNAs exceeded 2 SD of CTRL from the median of CTRL were regarded as validated. Genes were clustered according to the Marcov cluster (MCL) algorithm. Stronger associations are represented by thicker blue lines.

RESULTS

The same procedure was applied to the activating hits as well. In total, out of 34 activating hits from the Tri-DAP/NOD1 screen, 16 were also positive in the TNF- α counter-screen (data not shown).

Finally, the top NF- κ B inhibiting hits from the Tri-DAP/NOD1 screen, including the 24 genes with p-values below 0.05, and the next 10 genes with less significant RSA scores from this list were validated with a set of four different siRNAs, consisting of the two sequences already used in the screen and two new sequences, to knock down gene function individually. The assay procedure was repeated four times individually, Z-scores were calculated and genes were ranked according to the RSA algorithm. Genes, where NPI values of at least two out of the four siRNAs exceeded 2 SD of CTRL from the median of CTRL were regarded as validated. In total, 25 out of the 34 NF- κ B inhibiting genes from the Tri-DAP/NOD1 screen could be validated. Among those, 14 genes were specific for the NOD1 pathway, as compared with the TNF-specific RSA list. STRING database analysis revealed that there are several known and predicted functional and physical interactions between the identified non-specific and NOD1-specific factors (Fig. 10C).

Moreover, the top 18 NF- κ B activating hits were validated according to the same procedure. However, out of the 18 hits, only three could be validated with at least 2 siRNAs below -2 SD of CTRL from the median of CTRL (data not shown). For that reason we decided to focus on the inhibiting hits in the further screening steps.

3.1.3 Druggable genome screen

3.1.3.1 Primary druggable genome screen

In the next step, we conducted the HT screen with the druggable genome siRNA set V2.0 library (Qiagen) consisting of 6992 genes, each represented by four individual siRNAs. The library was screened for NOD1-mediated NF- κ B activation induced by Tri-DAP in four independent biological replicates (Fig. 5B). Normalisation, quality control and data processing were conducted as described for the pilot screen (screening and bioinformatics performed by Dr. Peter Braun and co-workers, MPIIB Berlin). Statistical analyses confirmed robustness of our assay controls (RELA and the non-targeting AllStars siRNA) and reproducibility of the results (average correlation of the four replicates: 0.65). siRNAs with at least 2 functional biological replicates were subjected to the RSA algorithm to generate a gene-based hit-list. In total, 435 genes where silencing inhibited NF- κ B activation were identified as hits by fulfilling two criteria:

RESULTS

(I) a minimum of 2 siRNAs per gene were identified as hits by the RSA algorithm (“preliminary hit siRNAs”) and (II) the gene-specific p-value was below 0.06. According to the same parameters, 379 genes were identified that activated NF- κ B activation upon siRNA-mediated knock-down (Fig. 11A).

Of note, the RSA-based ranking identified many factors that are known to be involved in the NOD1 pathway or canonical NF- κ B signalling, such as RIP2, RNF31, IKK α , IKK β , p50 and RELA. Furthermore, the known general negative regulators of canonical NF- κ B signalling A20 and CYLD were identified as activating hits. The gene-based hit-lists were then used to compile an siRNA library consisting of the 435 inhibiting and the top 100 activating hits from the RSA ranking for subsequent validation and TNF- α counter-screening. To create this library, the two siRNAs from the primary screen that displayed the strongest effects were re-synthesised and spotted on 384 well plates.

3.1.3.2 Validation and TNF- α counter-screen

To validate the hit-lists generated from the druggable genome screen, and to allow for identification of NOD1-specific factors, a validation- and counter-screen was performed. The hit library consisting of the 435 inhibiting and the top 100 activating hits identified in the druggable genome screen was screened according to the previously used conditions in four independent biological replicates. Cells were stimulated with Tri-DAP to validate the hits from the druggable genome screen. In parallel, the same library was screened in cells stimulated with TNF- α .

Aligning the data from the Tri-DAP-stimulated cells with the data from the TNF- α -stimulated cells allowed extraction of hits specific for either the NOD1- or the TNFR-signalling cascade, *i.e.* factors that act upstream of TAK1 in the corresponding pathway (Fig. 11B). Of note, the Tri-DAP results of the counter-screen showed a high reproducibility of the primary screen (correlation coefficient 0.77). The overall hit-list comprised 173 genes inhibiting NF- κ B activation when silenced (1-2 siRNAs >2 SD in Tri-DAP validation), among those, 66 genes were specific for Tri-DAP/NOD1 (1-2 siRNAs <2 SD in TNF- α counter-screen). All of the hit-lists contained factors with known functions in the NOD1 pathway or directly linked to NF- κ B signalling. Top NOD1-specific hits comprised RIP2, GALK2, XIAP, KLK8, MSH3 and KIF22 (2 siRNAs >2 SD in Tri-DAP validation, no TNF- α hit).

RESULTS

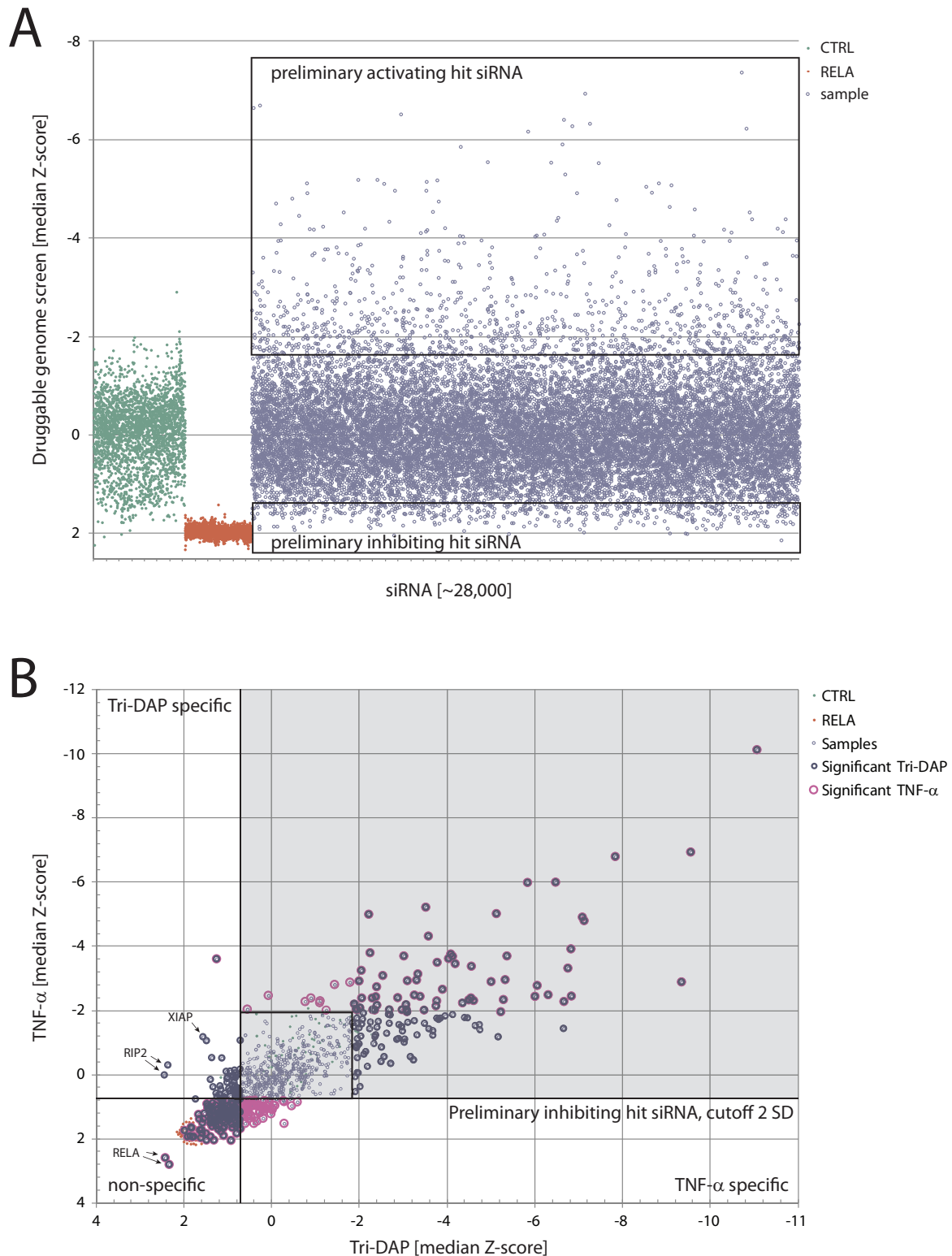


Figure 11. Results of the druggable genome screen in HEK293T cells. **A** Distribution of the siRNAs in the primary druggable genome screen. Each dot represents the median Z-score of the experimental replicates after NPI-normalisation (Normalised Percent Inhibition) to the plate-internal RELA-controls. A positive value represents an inhibitory effect of the respective siRNA on NF- κ B activation. Preliminary hit-siRNAs are defined by the RSA (redundant siRNA activity) algorithm. **B** Data from the Tri-DAP-validation screen was merged with data from the TNF- α counter-screen to identify factors that are specifically involved in NOD1-signalling. The graph displays the Z-scores for the single siRNAs, Tri-DAP/NOD1 activation is plotted on the x-axis, corresponding TNF- α values are plotted on the y-axis. Samples differing at least 2 SD of CTRL from the median of the CTRL siRNAs of the respective screen were defined as significant for Tri-DAP or TNF- α . CTRL: non-targeting control siRNAs.

3.1.4 THP1-Blue validation screen

3.1.4.1 Assay setup, downscaling and automation

In order to validate the hits in a more physiological system, we conducted a final validation screen on endogenous NOD1 activation in myeloid THP1-Blue cells. THP1-Blue cells are derivatives of the human monocytic cell line THP-1 that contain a NF- κ B-inducible secreted alkaline phosphatase (SEAP) reporter gene. In contrast to HEK293T cells, THP1 cells express functional endogenous NOD1 and are reactive towards Tri-DAP (Uehara *et al.*, 2005). THP-1 and THP1-Blue cells can be differentiated into adherent macrophage-like cells by stimulation with phorbol 12-myristate 13-acetate (PMA).

In order to apply the THP1-Blue assay for HTS using our pre-spotted siRNA plates, a suitable protocol had to be established. To this end, a previously described THP1-Blue siRNA assay (Bielig *et al.*, 2011b) was first performed in 96 well plates to test if down-scaling is possible with this system, as this assay is typically performed in 24 well plates. This required re-adjustment of the cell number and the volume of medium in which the transfection was performed. For that purpose, different cell numbers were transfected with CTRL or RELA siRNA in the presence of PMA. Growth medium was exchanged twice a day to remove excess SEAP induced by stimulation with PMA. After 72 h, cells were stimulated with LPS over night, as LPS induces a stronger SEAP-secretion than NOD1-elicitors. The best knock-down effect of the RELA siRNA was observed with 1×10^4 cells, but the measured SEAP-induction was rather low. With 2×10^4 cells, the read-out was more robust and the knock-down effect of the RELA siRNA was still very pronounced, albeit lower than with 1×10^4 cells (Fig. 12A).

Next, it was tested if reverse transfections, which were required for the automated platform, were possible in this system, and which elicitor was suited best to stimulate NOD1. To this end, cells were reversely transfected with CTRL, RELA or NOD1 siRNA. After 72 h, cells were stimulated with Tri-DAP or C12-ieDAP over night. C12-ieDAP consists of the minimal motif required for NOD1 stimulation that additionally contains a lipophilic group that facilitates entry into cells and was tested in this setting, because it induces a stronger NOD1 activation in THP1 cells (data not shown). To normalise the obtained data for cell death induced by toxic side effects of siRNAs, we decided to include cell viability assays using the XTT system as additional read-out system. The SEAP read-out indicated that stimulation with C12-ieDAP induced a stronger NF- κ B activation than stimulation with Tri-DAP, as expected (Fig. 12B, upper panel). Of note, a robust SEAP secretion was only observed with 2×10^4 cells per well, SEAP-levels measured with

RESULTS

1×10^4 cells per well were hardly above the background level (Fig. 12B, upper panel), correlating with the XTT read-out (Fig. 12B, lower panel).

Collectively, these results indicated that downscaling of the siRNA THP1-Blue assay procedure and reverse transfections were possible, the next step was to scale the assay further down based on these optimised parameters.

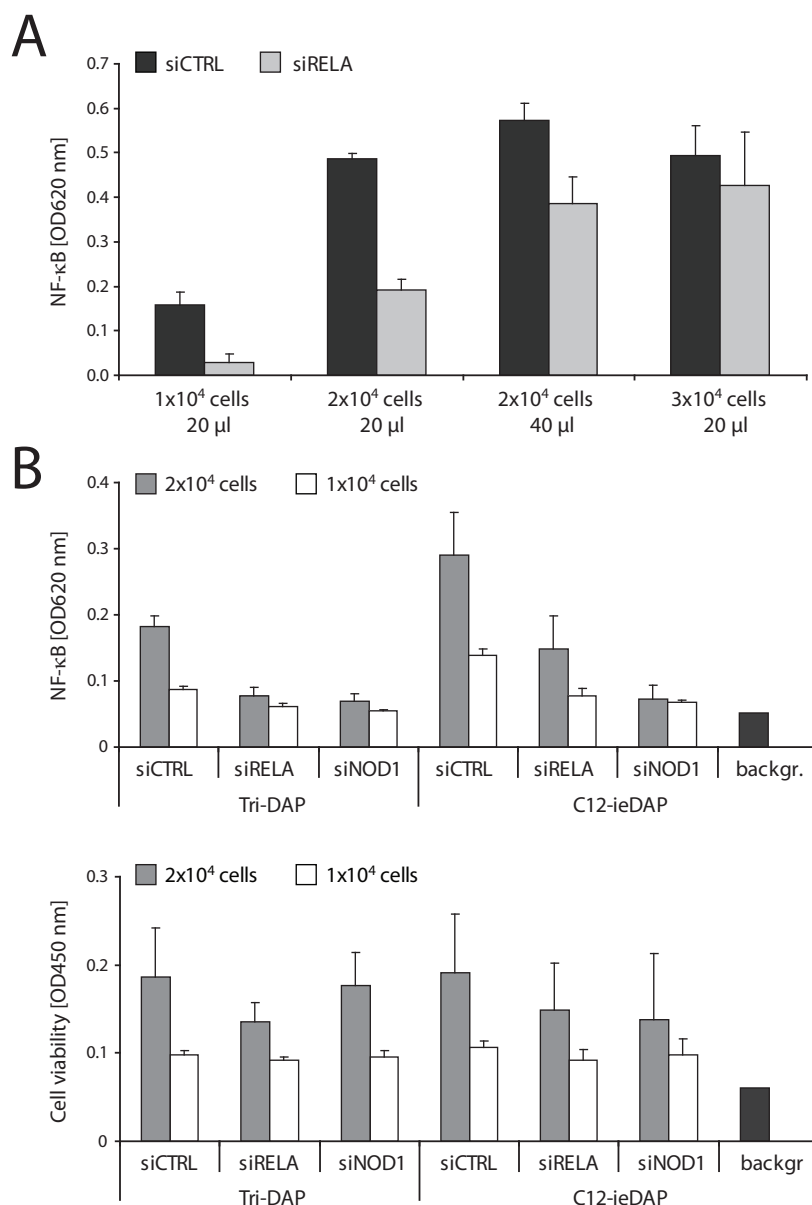


Figure 12. Downscaling to 96 well and re-optimisation of the THP1-Blue siRNA assay. **A** Titration of the cell numbers. Either 1×10^4 , 2×10^4 or 3×10^4 THP1-Blue cells were seeded in 20 μ l medium, or 2×10^4 cells were seeded in 40 μ l medium in 96 well plates and transfected with 20 nM CTRL or RELA siRNA. Cells were differentiated with 0.1 μ M PMA 10 min after transfection. After 72 h, cells were stimulated with LPS (100 ng/ml), 16 h later, NF- κ B activation was determined by measurement of SEAP activation from the supernatants at OD620. Values are OD620, mean +SD (n=3). **B** Assessment of different elicitors to stimulate NOD1-mediated NF- κ B activation. Either 1×10^4 or 2×10^4 THP1-Blue cells in 20 μ l medium containing 0.1 μ M PMA were reversely transfected with 20 nM CTRL, RELA or NOD1 siRNA in 96 well plates. After 72 h, cells were stimulated with Tri-DAP or C12-ieDAP (10 μ g/ml each), 16 h later, NF- κ B activation was determined by measurement of SEAP activity in the supernatants. (*upper panel*). Values are OD600, mean +SD (n=3). In parallel, cell viability was determined by XTT assays (*lower panel*). Values are OD450, mean +SD (n=3).

RESULTS

For downscaling to the 384 well format, the same automated workstation was used as for screening, and cell number and amount of transfection reagent were optimised. Cells were in parallel stimulated with C12-ieDAP and Tri-DAP. Additionally, cell viability was measured after 16 h using the XTT assay to normalise the data. Data was subjected to statistical analysis using the Z'-method. The results indicated that stimulation with C12-ieDAP induced a ~3 fold higher SEAP activation than stimulation with Tri-DAP. But the effect of the RELA and NOD1 knock-downs were much less pronounced with C12-ieDAP stimulation compared to stimulation with Tri-DAP. The best results were obtained using 6.5×10^3 cells per well, as lower cell numbers displayed a weak signal-to-noise ratio (data not shown).

In order to decide which stimulus to use in the screen, we performed further test assays. Also the optimal amount of HiPerFect was titrated. In all cases, C12-ieDAP induced a much stronger NF- κ B activation, but the observed knock-down effects were less pronounced compared to Tri-DAP as stimulus. Moreover, standard deviations were much higher when using C12-ieDAP compared to Tri-DAP. Thus we decided to use Tri-DAP as stimulus for further testing and for the screen (Fig. 13A).

As Tri-DAP is a weaker inducer of SEAP compared to C12-ieDAP, the cell number was re-adjusted to yield a more robust read-out. For that purpose, different cell numbers were transfected using 0.2 or 0.25 μ l HiPerFect per well and stimulated with Tri-DAP after 72 h. The results indicated that 8×10^3 cells per well, transfected using 0.25 μ l HiPerFect, were optimal among the tested conditions, showing the best knock-down effects for the RELA and NOD1 siRNAs, the highest signal-to-noise ratio, the lowest standard deviations and the best Z'-factor (CTRL/NOD1: 0.14) (Fig. 13B).

In the final pilot experiment, the read-out conditions and the cell culture volume for the Tri-DAP stimulation were optimised. Optimal results were obtained using a volume of 15 μ l, of which 10 μ l were used for the QUANTI-Blue measurement. The optimal incubation time for the QUANTI-Blue assay was 6 h, for the XTT assay 2 h proved to be optimal (data not shown).

According to these experiments, SOPs were defined as indicated in the materials and methods section (Fig. 14) (down-scaling to 384 well was accomplished with the help of Dr. Peter Braun and co-workers at the MPIIB Berlin).

RESULTS

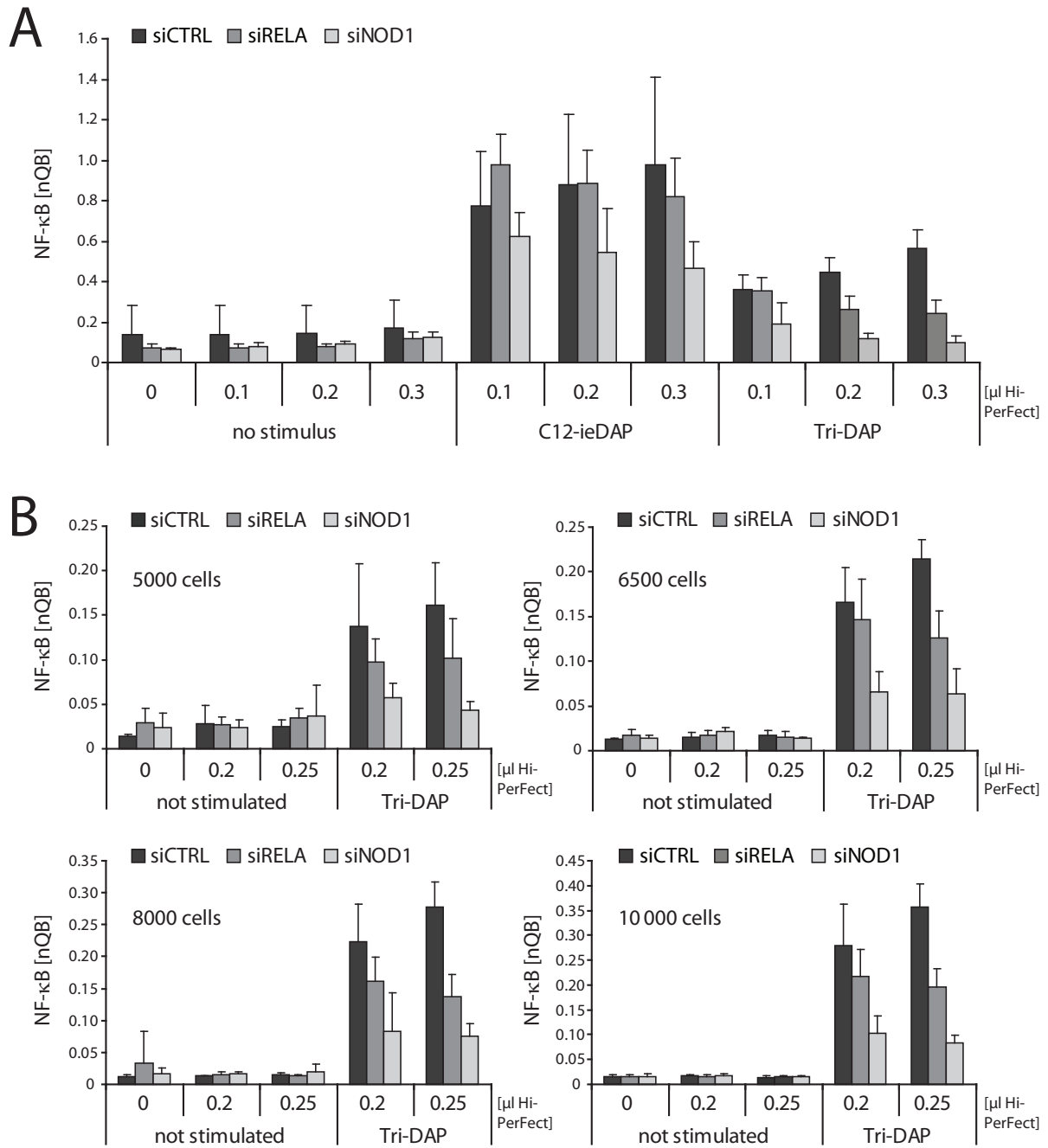


Figure 13: Downscaling to 384 well and re-establishment of the THP1-Blue siRNA assay. **A** Assessment of different elicitors to stimulate NOD1-mediated NF- κ B activation. 6500 cells were reversely transfected with 20 nM CTRL, RELA or NOD1 siRNA using 0.1, 0.2 or 0.3 μ l HiPerFect. Cells were incubated for 72 h and subsequently stimulated with C12-ieDAP or Tri-DAP (10 μ g/ml each), 16 h later, NF- κ B activation was determined by measurement of SEAP activation from the supernatants at OD600. In parallel, cell viability was assessed by XTT assays. Values are OD600 normalised with XTT values, mean +SD (n=16). **B** Titration of the cell numbers. 5000, 6500, 8000 or 10000 cells were reversely transfected with 20 nM CTRL, RELA or NOD1 siRNA using 0.2 or 0.25 μ l HiPerFect. Cells were incubated for 72 h and subsequently stimulated with Tri-DAP (10 μ g/ml), 16 h later, NF- κ B activation was determined by measurement of SEAP activity in the supernatants. In parallel, cell viability was assessed by XTT assays. Values are OD600 normalised with XTT values [nQB], mean +SD (n=16).

RESULTS

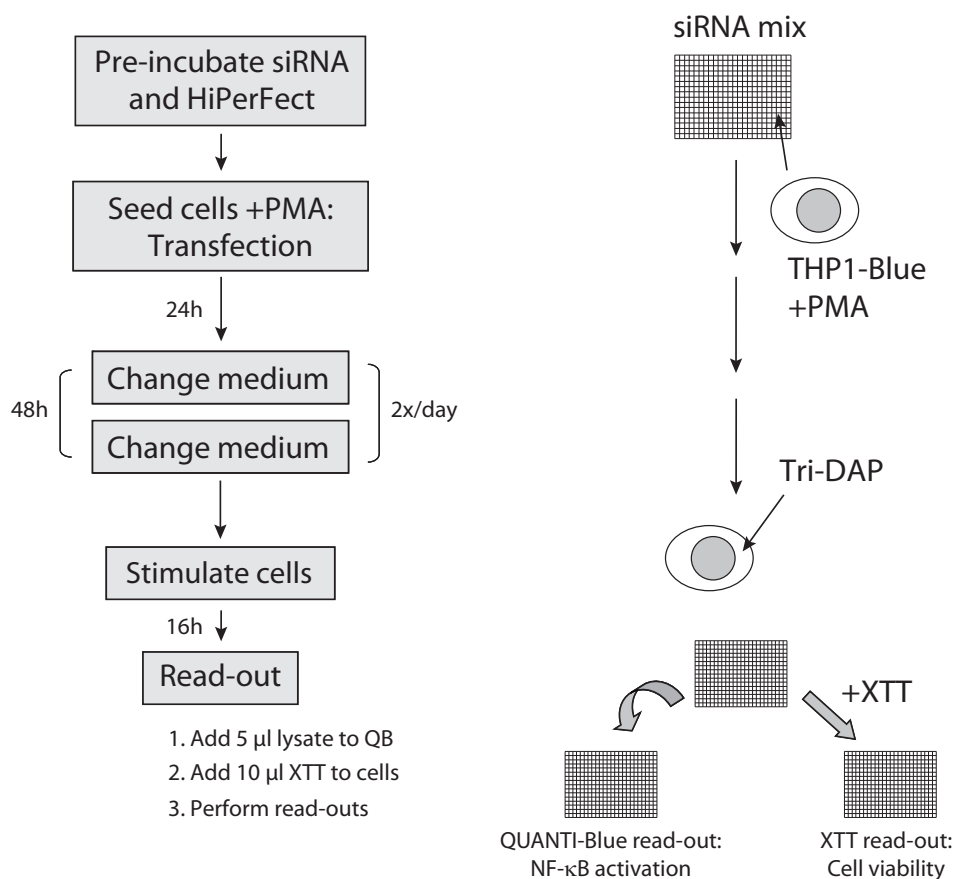


Figure 14: Schematic overview of the THP1-Blue assay as read-out for siRNA-mediated knock-down as used for the validation screen. In brief, pre-spotted siRNAs were incubated with medium containing HiPerFect. Subsequently, THP1-Blue cells were reversely transfected by seeding onto the siRNA mixes. Cells were washed twice a day for 72 h and subsequently stimulated with Tri-DAP (10 µg/ml). After 16 h, NF-κB activation was determined by measurement of SEAP activity in the supernatants. In parallel, cell viability was assessed by XTT assays.

3.1.4.2 THP1 screen and results

For the validation in THP1-Blue cells, our hit-library consisting of the 435 inhibiting and the top 100 activating hits identified in the primary screen was screened in four independent biological replicates. In brief, 8×10^3 THP1-Blue cells were seeded onto the pre-spotted siRNAs (final concentration of 20 nM) in the presence of 0.25 µl HiPerFect transfection reagent in 384-well plates and treated with PMA. Cells were washed twice a day to get rid of excess SEAP induced by stimulation of the cells with PMA. After 72 h, cells were stimulated with Tri-DAP and NF-κB activation was measured 16 h later by SEAP-detection from the supernatants. To normalise for toxic effects, XTT cell viability assays were performed in parallel (Fig. 14). In this screen we used siRNAs directed against NOD1 as positive controls (set to 100% NF-κB inhibition), as the effect of a knock-down of RELA in these cells was not as pronounced compared to the effect in HEK293T cells (Fig. 12 and 13). Data was normalised by Z-transformation to the

RESULTS

overall screen data, individual Z-scores were calculated for each replicate (Fig. 15) (screening was performed by Dr. Peter Braun and co-workers, MPIIB Berlin). In total, 28 genes with two siRNAs inhibiting Tri-DAP-induced NF- κ B activation (> 1.5 SD) could be identified (Fig. 22D). Among those, RIP2, NOD1, RELA, XIAP, DTX4, CALR, OR12D2 and RNF31 were the strongest hits (> 3 S.D).

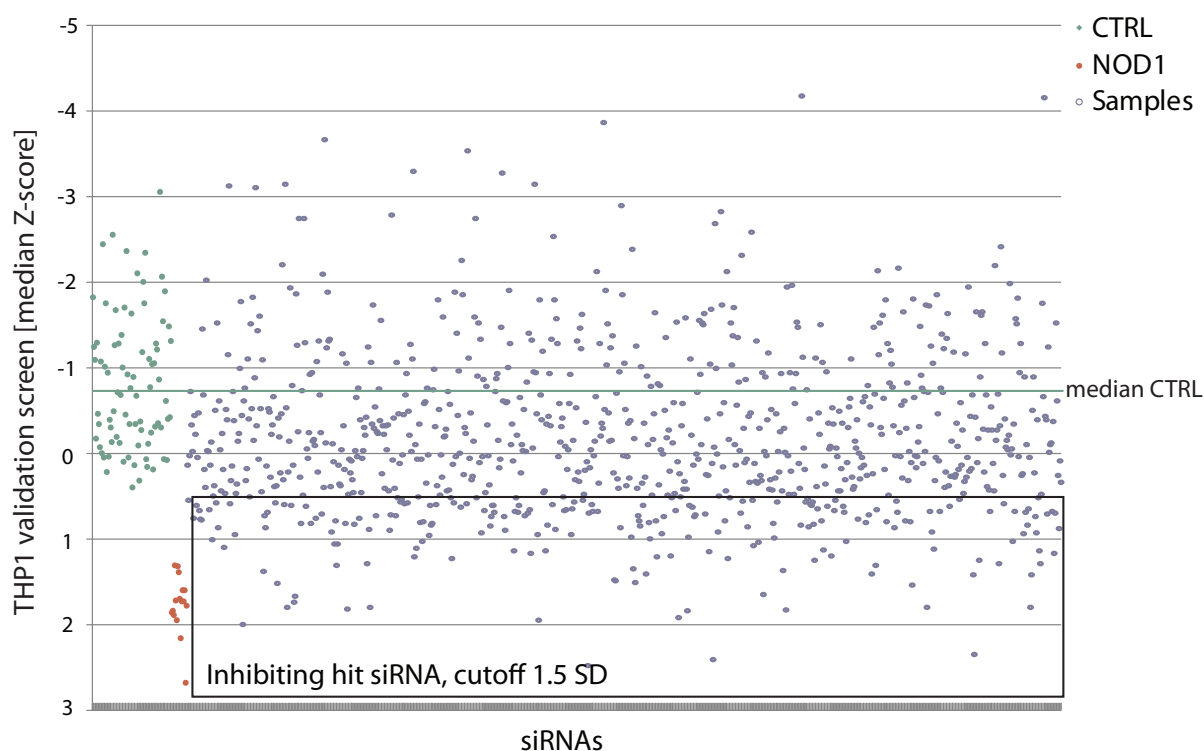


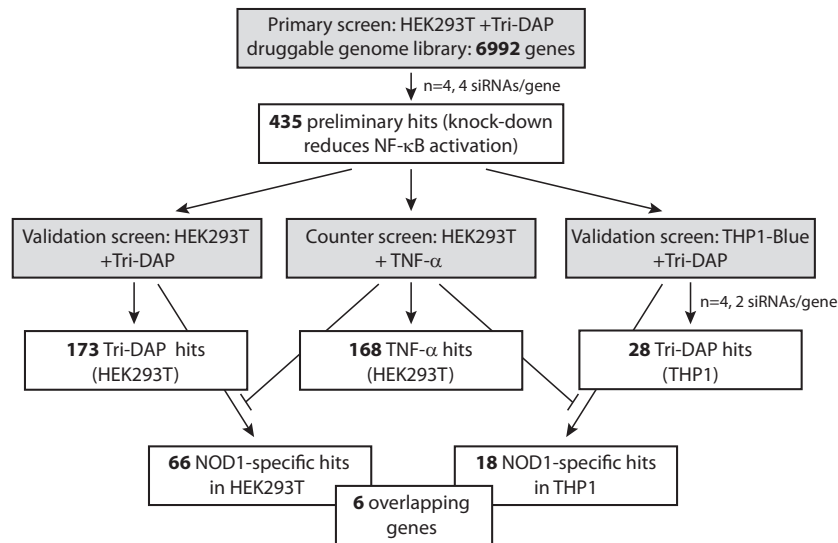
Figure 15. Distribution of the siRNAs in the THP1-Blue validation screen. Each dot represents the median Z-score of the experimental replicates after NPI-normalisation (Normalised Percent Inhibition) to the plate-internal NOD1-controls. A positive value represents an inhibitory effect of the respective siRNA on NF- κ B activation. THP1 hit-siRNAs are defined as exceeding 1.5 SD of CTRL from the median of the CTRL siRNAs. CTRL: non-targeting controls.

3.1.5 Final hitlist generation

The primary druggable genome screen yielded 435 preliminary inhibiting hits with p-values below 0.06, according to the RSA analysis. These preliminary hits were subsequently validated in HEK293T cells using two different siRNAs to target each gene. In total, 173 genes inhibiting NF- κ B activation when silenced could be validated (1-2 siRNAs per gene >2 SD), among them 66 genes were specific for Tri-DAP/NOD1 (1-2 siRNAs per gene <2 SD in TNF- α counter-screen) (Fig. 16A).

RESULTS

A



B

Rank	Gene	Druggable genome screen (Tri-DAP)		HEK validation (Tri-DAP)		Counter-screen (TNF-α)		THP1 validation (Tri-DAP)	
		Best	Mean	Best	Mean	Best	Mean	Best	Mean
	CTRL	-0.13	-0.13	-0.621	-0.621	-0.64	-0.64	-0.71	-0.71
1	RIPK2	2.11	2.11	2.44	2.40	0.02	-0.14	2.59	2.33
2	XIAP	1.67	1.65	1.56	1.56	-1.17	-1.17	2.03	1.81
3	DTX4	1.74	1.40	-0.59	-0.59	-0.35	-0.35	1.95	1.29
4	PFKFB2	1.33	1.17	0.5	-0.50	-1.06	-0.77	1.76	1.23
5	ARID1A	1.77	1.43	-0.26	-0.26	0.51	0.51	1.63	1.46
6	GPR17	1.32	1.30	1.18	1.18	0.63	0.63	1.52	1.28
7	ANAPC1	1.30	1.20	n.d.	n.d.	n.d.	n.d.	1.49	1.19
8	CUBN	1.53	1.39	0.27	0.27	0.44	0.44	1.24	1.02
9	SSH1	1.27	1.14	0.87	0.87	0.51	0.51	1.03	0.90
10	SNAI1	1.46	1.31	1.4	-0.16	-1.58	-1.58	1.01	0.82
11	GCLM	1.20	1.16	-0.57	-0.66	0.48	0.08	0.88	0.84
12	DDI2	1.43	1.26	0.37	-0.25	0.09	0.04	0.85	0.85
13	SETD1A	1.58	1.32	0.29	0.04	0.39	0.13	0.85	0.74
14	PATE1	1.37	1.23	0.47	0.41	0.24	0.19	0.83	0.83
15	EXT2	1.77	1.48	0.64	-0.80	0.44	-0.49	0.79	0.74
16	CHUK	1.20	1.11	0.83	0.71	0.36	0.19	0.78	0.70
17	OPRL1	1.54	1.47	0	0	0.58	0.58	0.78	0.74
18	FNTB	1.15	1.07	-1.07	-1.94	-1.20	-1.20	0.72	0.69

Figure 16. Final ranking of the inhibiting screen hits. **A** Schematic representation of the siRNA screening procedure including the numbers of identified hit genes for the respective screening steps. 435 preliminary hit genes from the primary druggable genome screen were re-tested in three different settings. After differential analysis of the validation screens and the counter-screen, 66 and 18 genes could be validated as NOD1-specific in HEK293T or THP1 cells, respectively. Of those, 6 were involved in NOD1-specific signaling in both cell lines. **B** Final hit-list of genes specifically involved in NOD1-dependent NF-κB activation. Ranked to the results of the THP1 screen (best score). Bold: NOD1-specific genes also validated in the HEK293T Tri-DAP validation screen.

To rule out the possibility that the obtained hits were cell-type specific regulators, the same library was subsequently used for a validation screen in THP1 cells. In this screen, 28 genes were regarded as significant hits (2 siRNAs per gene >1.5 SD), among those, 18 were specific

RESULTS

for NOD1 signalling, as compared with the results of the TNF- α screen (Fig. 16A, B). Although the hit-list achieved in THP1 cells differed from the one from HEK293T cells, the genes RIP2, XIAP, GPR17, SSH1, SNAI1, and CHUK could be confirmed as hits in all screening rounds in both cell lines and did not show an inhibiting effect in the TNF- α counter screen (Fig. 16B).

3.1.6 Hit validation: XIAP

Beside RIP2, XIAP was the top hit in the final ranking that takes into account all steps of the screening procedure (Fig. 17A). XIAP (X-linked inhibitor of apoptosis, also termed BIRC4) is a protein belonging to the BIRC family that is known to exert strong anti-apoptotic functions. Beside its important role in counter-acting apoptosis, it has also been attributed to other functions. Of note, there are recent reports linking XIAP to functions in innate immunity (Krieg *et al.*, 2009; Bauler *et al.*, 2008).

In order to validate the predicted role of XIAP in NOD1 signalling, we first performed knock-down experiments in HEK293T cells using a different siRNA than in the screen. To this end, cells were transfected with XIAP-specific siRNA or non-targeting CTRL siRNA in 96 well plates for 48 h, then the NF- κ B-luciferase reporter system containing NOD1 or NOD2 expression plasmids was transfected and cells were stimulated with Tri-DAP or MDP, respectively. In line with the data obtained in the screen, knock-down of XIAP strongly reduced NOD1-mediated NF- κ B-luciferase activation (Fig. 17B, left panel). Of note, also NOD2-mediated NF- κ B activation was strongly impaired by knock-down of XIAP, indicating a role for XIAP as well in NOD2 signalling (Fig. 17B, right panel). Importantly, this siRNA largely reduced XIAP protein levels, as judged by Western blot analysis, confirming the functionality of this siRNA (Fig. 17C).

To expand the analysis to another cell type, additional siRNA experiments were performed in human myeloid THP1-Blue cells. THP1-Blue cells differentiated with PMA were transfected with CTRL, NOD1, NOD2 or XIAP siRNA and stimulated with Tri-DAP or MDP, or left untreated. The NOD1 and NOD2 positive controls clearly reflect the functionality of the assay system: Knock-down of NOD1 selectively impaired Tri-DAP-mediated NF- κ B activation, whereas knock-down of NOD2 selectively impaired MDP-mediated NF- κ B activation. In contrast, knock-down of XIAP reduced both Tri-DAP- and MDP-induced NF- κ B activation to background levels, supporting the essential role for XIAP in both of the pathways and confirming the results from the screen (Fig. 17D). Measurement of IL-8 (CXCL-8) in the supernatants of the same cells revealed that IL-8 secretion in response to Tri-DAP and MDP stimulation was also strongly impaired by knock-down of XIAP (Fig.17E).

RESULTS

In order to validate the effect of XIAP knock-down on NOD1 signalling in a more physiological system, we performed infection experiments with epithelial HeLa cells stably expressing short hairpin RNA (shRNA) targeting XIAP. For that purpose, HeLa^{WT}, HeLa^{shSCR} cells (expressing a non-targeting control shRNA) and HeLa^{shXIAP} cells were infected with the invasive Gram-negative pathogen *Shigella flexneri* (strain M90T afaE). This strain is known to induce NOD1-specific NF- κ B and cytokine responses (Girardin *et al.*, 2001). As control, cells were infected with the non-invasive (virulence plasmid cured) *S. flexneri* strain BS176. Infection of HeLa^{WT} and HeLa^{shSCR} cells with M90T induced a strong IL-8 secretion. IL-8 secretion in response to M90T was strongly impaired in HeLa^{shXIAP} cells compared to HeLa^{WT} and HeLa^{shSCR} cells. Moreover, over-expression of Myc-XIAP in HeLa^{shXIAP} cells fully restored M90T-induced IL-8 secretion, clearly confirming an essential role for XIAP in NOD1 signalling (Fig. 17F). Infection with the non-invasive strain BS176, in contrast, did not induce IL-8 secretion in any of the cell lines (experiments with shRNA cell lines were performed by Maureen Menning, University of Cologne).

The mitochondrial protein SMAC is known to inhibit XIAP by direct binding (reviewed in Riedl and Salvesen, 2007). Of note, expression of a truncated version of SMAC that localises to the cytoplasm (SMAC Δ MTS) potently inhibited NOD1-mediated NF- κ B activation in a dose-dependent manner in the HEK293T reporter system. In this setting, also NF- κ B activation triggered by over-expression of RIP2 was inhibited by expression of SMAC Δ MTS (Fig. 17 G), providing further evidence that XIAP is essential for NOD1 signalling. In contrast, NF- κ B activation triggered by over-expression of IKK β was not inhibited by expression of SMAC Δ MTS, indicating that XIAP acts upstream of the IKK complex in the NOD1 signalling cascade (Fig. 17G).

Collectively, these findings confirmed the results obtained in the screen and revealed that XIAP is essentially involved in NOD1-mediated NF- κ B activation and IL-8 secretion in epithelial and myeloid-like cells. Furthermore, we provide evidence for an important role for XIAP also in NOD2 signalling.

RESULTS

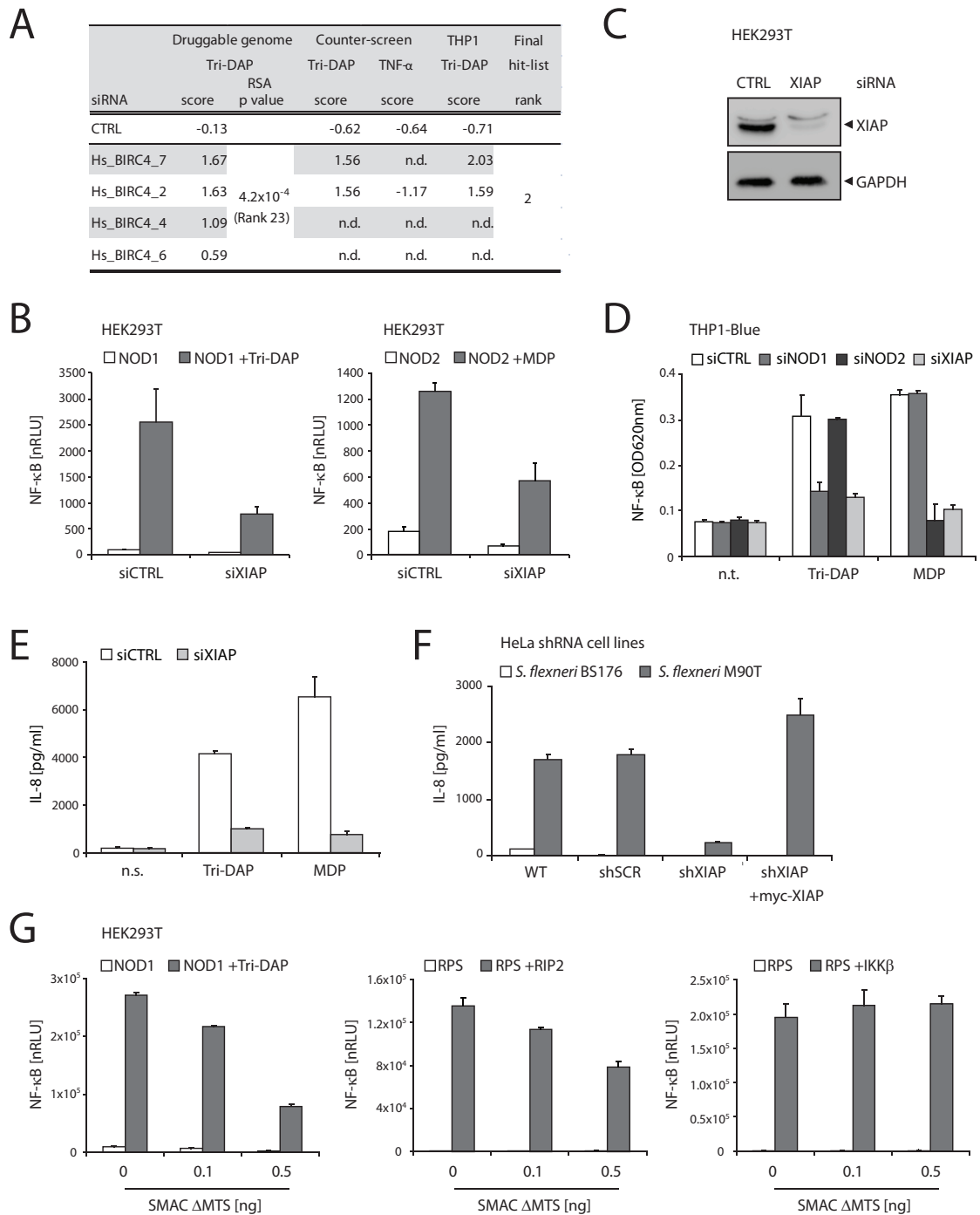


Figure 17. Validation of the role of XIAP in NOD1 signalling. **A** Screening results for XIAP in the different screening steps. **B** HEK293T cells were transfected with CTRL or XIAP siRNA and incubated for 48 h. Subsequently, cells were transfected with the NF- κ B luciferase RPS containing NOD1 (left panel) or NOD2 (right panel) expression plasmids and stimulated with Tri-DAP (0.5 μ M) or MDP (50 nM), respectively. After 16 h, cells were lysed, luciferase activation was determined and normalised with the β -galactosidase values (nRLU). Values are mean \pm SD (n=3). **C** Confirmation of the XIAP knock-down on protein level. HEK293T cells were transfected with CTRL or XIAP siRNA. After 72 h, cells were lysed and XIAP protein levels were determined by Western blot using a XIAP-specific antibody. Detection of GAPDH served as loading control. **D** Differentiated THP1-Blue cells were transfected with CTRL, NOD1, NOD2 or XIAP siRNA. Cells were incubated for 72 h and subsequently stimulated with Tri-DAP or MDP (10 μ g/ml each), 16 h later, NF- κ B activation was determined by measurement of SEAP activity in the supernatants. In parallel, IL-8 secretion was determined by ELISA (**E**). Values are NF- κ B activation [OD620] or IL-8 secretion [pg/ml], respectively, mean \pm SD (CTRL, XIAP: n=3; NOD1, NOD2: n=2). Data is representative for at least 3 independent experiments. **F** HeLa^{WT}, HeLa^{shSCR} or HeLa^{shXIAP} were incubated for 24 h and subsequently infected with *Shigella flexneri*

RESULTS

BS176 or M90T for 6 h. IL-8 secretion was determined by ELISA. Values are IL-8 secretion [pg/ml], mean +SD (n=2). **G** HEK293T were transfected with the NF- κ B luciferase RPS containing NOD1 (*left panel*), RIP2 (5 ng) (*middle panel*) or IKK β (5 ng) (*right panel*) expression plasmids. The indicated amounts of SMAC Δ MTS were co-expressed. NOD1 transfected cells were subsequently stimulated with Tri-DAP (0.5 μ M). After 16 h, cells were lysed and luciferase activation was determined and normalised with the β -galactosidase values (nRLU). Values are mean +SD (n=3). Data is representative for 3 independent experiments. nRLU: normalised relative light units

3.1.7 Hit validation: BMPR-2

The bone morphogenetic receptor 2 (BMPR-2) is a receptor for growth factors of the transforming growth factor β (TGF- β) superfamily (reviewed in Miyazono *et al.*, 2005). Intriguingly, it has been shown that BMPR-2 interacts with XIAP and stabilises XIAP protein levels under serum starvation conditions (Liu *et al.*, 2009). For that reason we decided to validate the role for BMPR-2 in NOD1 signalling clearly indicated by our screen data, even though BMPR-2 was not among the top inhibiting hits. Still, in the druggable genome screen, most siRNAs targeting BMPR-2 stably displayed clear inhibiting effects on NOD1-mediated NF- κ B-luciferase activation, and this was confirmed in the HEK293T validation screen. In contrast, depletion of BMPR-2 did not exert any effect in the TNF- α counter-screen, indicating that BMPR-2 specifically acts on the NOD1 signalling pathway. In the THP1 validation screen, again one of the siRNAs (BMPR2_6) inhibited NOD1-mediated NF- κ B activation. Surprisingly, another siRNA (BMPR2_4) induced a slight increase in NF- κ B activation in these cells (Fig. 18A). Although this was likely an off-target effect, owing to the strict parameters for ranking this led to exclusion of BMPR-2 from the final hit-list.

As it has been described that BMPR-2 might be expressed cell type specifically (Liu *et al.*, 2009), expression of BMPR-2 in several myeloid and non-myeloid cell lines was assessed by RT-PCR. This revealed that BMPR-2 is expressed in HEK293T and HeLa cells, in myeloid THP1 and Jurkat cells and also in the colon epithelial cell line TC-7/CaCo2 (Fig. 18B). Next, siRNA knock-down experiments in HeLa cells were performed to confirm the data obtained in the screen. Treatment of HeLa cells with two different siRNAs targeting BMPR-2 strongly impaired IL-8 secretion induced by infection with invasive *S. flexneri* M90T (Fig. 18C, upper panel). Infection of cells with the non-invasive *S. flexneri* strain BS176, in contrast, did not lead to secretion of detectable amounts of IL-8 (data not shown). Knock-down of the validated screen hit XIAP was used as positive control. RT-PCR using cDNA transcribed from RNA isolated from cells of the same experiment confirmed that both siRNAs targeting BMPR-2 efficiently reduced BMPR-2 mRNA levels (Fig. 18C, lower panel).

RESULTS

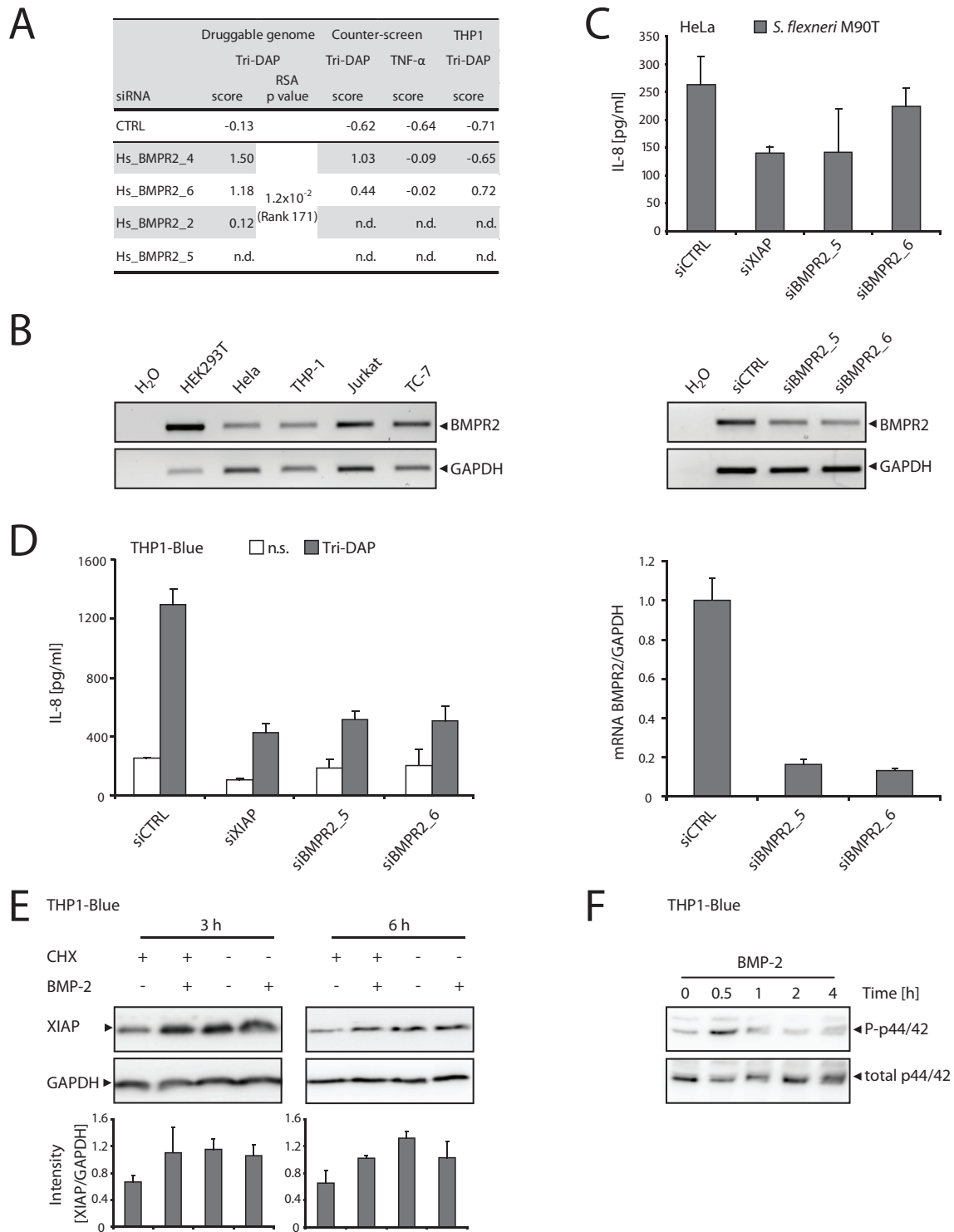


Figure 18. Validation and characterisation of the role of BMPR-2 in NOD1 signalling. **A** Screening results for BMPR-2 in the different screening steps. **B** Expression of BMPR-2 in different cell lines, determined by RT-PCR with BMPR-2-specific primers. GAPDH expression levels served as loading control. **C** Knock-down of BMPR-2 in HeLa cells. Cells were transfected with CTRL, XIAP or BMPR-2 siRNA and incubated for 72 h. Subsequently, cells were infected with *Shigella flexneri* M90T and IL-8 secretion was determined 6 h after infection by ELISA (*upper panel*). Values are mean +SD (n=2). Knock-down efficiency was determined by RT-PCR using BMPR-2-specific primers and cDNA transcribed from RNA isolated from cells of the same experiment. RT-PCR with GAPDH-specific primers served as control (*lower panel*). **D** Knock-down of BMPR-2 in THP1-Blue cells. Differentiated THP1-Blue cells were transfected with CTRL, XIAP or BMPR-2 siRNA and incubated for 72 h. Subsequently, cells were stimulated with Tri-DAP (10 μ g/ml) and IL-8 secretion was determined after 16 h incubation by ELISA (*left panel*). Values are mean +SD (n=2). Data is representative for two independent

RESULTS

experiments. Knock-down efficiency was determined by qRT-PCR using BMPR-2-specific primers and cDNA transcribed from RNA isolated from cells of the same experiment. Data was normalised to GAPDH-levels (*right panel*). Data is representative for two independent experiments. **E** Differentiated THP1-Blue cells were treated with 0.5 µg/ml cycloheximide and/or 0.5 µg/ml recombinant BMP-2 for 3 h or 6 h. Cells were lysed and XIAP protein levels were determined by Western blot using a XIAP-specific antibody. Detection of GAPDH served as loading control (*upper panels*). Densitometric quantification of two independent experiments (XIAP/GAPDH, +SD) (*lower panels*). **F** Differentiated THP1-Blue cells were treated 0.5 µg/ml recombinant BMP-2 for the indicated time points. Cells were lysed and phospho-p44/42 protein levels were determined by Western blot using a phospho-p44/42-specific antibody. Detection of total p44/42 levels served as loading control. Data is representative for 2 independent experiments.

In order to further confirm the involvement of BMPR-2 in NOD1 signalling in another setting, knock-down experiments in myeloid THP1-Blue cells were performed. Knock-down of BMPR-2 with two different siRNAs impaired Tri-DAP induced IL-8 secretion in THP1-Blue cells (Fig. 18D, left panel). Quantitative PCR using cDNA transcribed from RNA isolated from cells of the same experiment confirmed that both siRNAs highly efficiently reduced BMPR-2 mRNA levels in THP1-Blue cells (Fig. 18D, right panel). Collectively, these results strongly support a role for BMPR-2 in NOD1 signalling. Preliminary data from knock-down experiments in THP1-Blue cells indicated that BMPR-2 might also be involved in NOD2 signalling (data not shown).

Recently, it has been described that treatment of mouse embryonic fibroblasts (MEFs) with the BMPR-2 ligands BMP-2 and GDF-5 (growth differentiation factor 5) counter-acted apoptosis induced by serum starvation by stabilising XIAP protein levels and preventing its proteasomal degradation (Liu *et al.*, 2009). Strikingly, we observed that administration of recombinant BMP-2 to differentiated THP1-Blue cells, cultured in medium containing FCS, also stabilised XIAP protein levels when protein neo-synthesis was blocked with cycloheximide (CHX), as monitored by Western blot analysis using a XIAP-specific antibody. This effect was observed 3 h and still 6 h after treatment with CHX and BMP-2, whereas GAPDH protein levels remained unchanged (Fig. 18E). In order to assure the functionality of the recombinant BMP-2 used for these experiments, BMP-2 induced p42/p44 phosphorylation was monitored by Western blot analysis using an antibody that specifically detects phosphorylated p42/44. As described for MEFs (Liu *et al.*, 2009), BMP-2 induced a strong p42/44 phosphorylation as well in the differentiated THP1-Blue cells 15 min after treatment (Fig. 18F). This revealed that THP1 cells have a functional BMP-2 signalling pathway and demonstrated the functionality of the recombinant BMP-2.

Taken together, these results reveal BMPR-2 as interesting novel regulator of the NOD1 pathway, that likely acts by stabilising XIAP.

3.1.8 Analysis of the roles of BIRC proteins in NOD1 signalling

The finding that XIAP is essentially involved in NOD1 and NOD2 signalling and recent reports linking the closely related proteins BIRC2 and BIRC3 to innate immunity (Tseng *et al.*, 2010; Bertrand *et al.*, 2008; Conte *et al.*, 2006) and NOD signalling (Bertrand *et al.*, 2009), raised the question if also other members of the BIRC family might contribute to NOD1 signalling. The data obtained in our screen was not very conclusive on this point, as among the BIRC family members only XIAP was identified as a robust hit (Fig. 17A). The other BIRC family members did not achieve high ranks in the RSA-based hit-lists, mostly due to heterogeneity in the effects of different siRNAs (data not shown). As siRNA screens are prone to off-target effects (reviewed in Singh *et al.*, 2011; Svoboda, 2007), and as the raw data for some of the BIRCs, for example for BIRC5 (data not shown) indicated that there might be effects on NOD1 signalling caused by some of the siRNAs, we investigated the possible roles for the BIRC proteins in NOD1 signalling in more detail. To this end, BIRC2, BIRC3, BIRC5, BIRC7 and BIRC8 were targeted with two different siRNAs each in HeLa cells. Cells were then infected with invasive *S. flexneri* M90T or non-invasive *S. flexneri* BS176. Knock-down of the validated screen hit XIAP thereby served as positive control. Measurement of IL-8 secretion in response to *S. flexneri* infection indicated that knock-down of BIRC2, BIRC5 and BIRC8 impaired *S. flexneri* M90T induced IL-8 secretion, whereas knock-down of BIRC3 enhanced IL-8 secretion in response to *S. flexneri* M90T infection. Infection with *S. flexneri* BS176, in contrast, did not induce secretion of detectable amounts of IL-8 (Fig. 19 A, upper panel and data not shown).

The experiment was subsequently repeated with the siRNAs that showed the strongest effect on IL-8 secretion to validate the findings from the first experiment. The results were qualitatively comparable to the results from the first experiment, albeit the effects were not as pronounced. Again, knock-down of BIRC2, BIRC5 and BIRC8 impaired *S. flexneri* M90T induced IL-8 secretion, knock-down of BIRC3 enhanced IL-8 secretion (Fig. 19A, lower panel). RT-PCRs performed with cDNA generated from RNA isolated from cells in the same experiment confirmed reduction of the corresponding mRNA levels (Fig. 19B). However, we failed to detect BIRC7 mRNA using RT-PCR (data not shown).

To expand this analysis to another cell system, differentiated THP1 cells were transfected with our BIRC-specific siRNAs. Subsequently, IL-8 secretion induced by stimulation of NOD1 with Tri-DAP was measured. In line with the observations made in HeLa cells, knock-down of XIAP, BIRC2, BIRC5 and BIRC8 impaired NOD1-mediated IL-8 secretion. In contrast to the observations made in HeLa cells, knock-down of BIRC3 did not exert any effect on NOD1-mediated IL-8 secretion in THP1 cells, indicating that effects of BIRC3 on NOD1 signalling are cell-type specific (Fig. 19C).

RESULTS

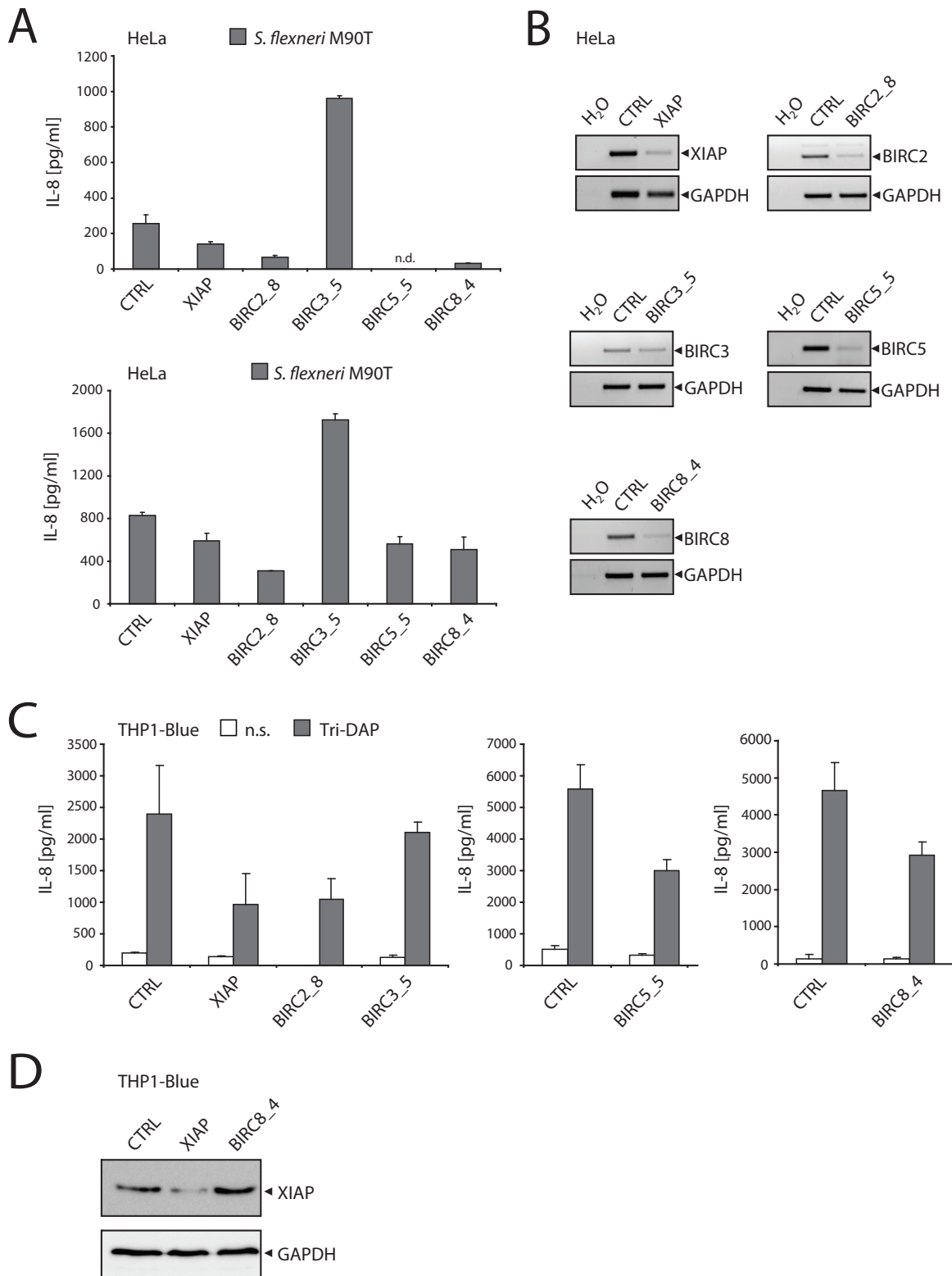


Figure 19. Analysis of the roles of BIRC proteins in NOD1 signalling. **A** Knock-down of BIRC2, 3, 5 and 8 in HeLa cells. Cells were transfected with CTRL, XIAP, BIRC2, BIRC3, BIRC5 or BIRC8 siRNA and incubated for 72 h. Subsequently, cells were infected with *Shigella flexneri* M90T and IL-8 secretion was determined 6 h after infection by ELISA. The experiment was repeated twice (*upper panel / lower panel*). Values are mean +SD (n=2). **B** Knock-down efficiency was determined by RT-PCR using primers specific for the respective BIRC gene and cDNA transcribed from RNA isolated from cells of the same experiment. RT-PCR with GAPDH-specific primers served as control. **C** Knock-down of BIRC2, 3, 5 and 8 in THP1-Blue cells. Differentiated THP1-Blue cells were transfected with CTRL, XIAP, BIRC2, BIRC3, BIRC5 or BIRC8 siRNA and incubated for 72 h. Subsequently, cells were stimulated with Tri-DAP (10 µg/ml) and IL-8 secretion was determined after 16 h

RESULTS

incubation by ELISA. Values are mean \pm SD (n=2). Data is representative for at least two independent experiments. **D** Assessment of the specificity of the BIRC8 siRNA. THP1-Blue cells were transfected with siRNA targeting CTRL, XIAP or BIRC8. After 72 h incubation, cells were lysed and XIAP protein levels were determined by Western blot analysis using a XIAP-specific antibody. Detection of GAPDH levels served as loading control.

To exclude that the effects observed for the knock-down of BIRC8 were caused by a simultaneous knock-down of XIAP induced by the BIRC8 siRNA due to the high sequence similarity of BIRC8 with XIAP (Richter *et al.*, 2001), THP1 cells were transfected with CTRL, XIAP- or BIRC8-specific siRNAs and XIAP protein levels were determined by Western blot analysis. Of note, treatment of cells with BIRC8 siRNA did not affect XIAP protein levels, whereas treatment with XIAP siRNA strongly reduced XIAP protein levels, confirming the specificity of the BIRC8 siRNA (Fig. 19D).

Collectively, these results indicate that beside XIAP (BIRC4) also BIRC2, BIRC3, BIRC5 and BIRC8 are implicated in NOD1 signalling. However, the molecular functions and physiological relevances of these findings still remain to be established.

3.2 Bacterial outer-membrane vesicles trigger NOD-mediated inflammatory responses in a quorum sensing-dependent manner

Even though it is well established that NOD1 and NOD2 detect PGN fragments derived from bacteria, it is not fully understood how PGN from extracellular bacteria is translocated to the cytoplasm of host cells. Recent publications indicate that different host cell mechanisms, such as peptide transporters (Swaan *et al.*, 2008; Ismair *et al.*, 2006; Vavricka *et al.*, 2004) and endocytic pathways (Lee *et al.*, 2009; Marina-Garcia *et al.*, 2009), but also bacterial mechanisms, such as secretion systems (Viala *et al.*, 2004) and pore-forming toxins (Ratner *et al.*, 2007), contribute to this process. In this part of the project we aimed at elucidating if outer-membrane vesicles (OMVs) derived from the Gram-negative non-invasive pathogen *Vibrio cholerae* might serve as mechanism for delivery of NOD1/2 active PGN to the cytoplasm of human cells.

3.2.1 Activation of NOD1 and NOD2 by extracellular bacteria

OMVs are spherical membrane fragments consisting of bacterial outer-membrane material that are produced during normal growth of many Gram-negative bacteria (reviewed in Kulp and Kuehn, 2010). They enclose a variety of outer-membrane and periplasmic constituents, includ-

RESULTS

ing proteins, phospholipids, DNA, bacterial toxins and LPS (Deatherage *et al.*, 2009; Lindmark *et al.*, 2009; Renelli *et al.*, 2004; Wai *et al.*, 2003; Kolling and Matthews, 1999). Consistently, it has been shown that OMVs derived from *Pseudomonas aeruginosa* induce IL-8 secretion in epithelial cells (Bauman and Kuehn, 2006).

Vibrio cholerae is an inhabitant of aquatic systems and one of the causative agents of severe dehydrating diarrhea in humans. *V. cholerae* bacteria belonging to the O1 and O139 serogroups cause cholera epidemics in many developing countries, whereas strains belonging to non-O1 non-O139 *V. cholerae* (NOVC) serogroups have been associated with endemic gastroenteritis and extraintestinal infections in humans (Faruque *et al.*, 1998; Kaper *et al.*, 1995). Unlike the case for the O1 and O139 strains of *V. cholerae*, little is known about the virulence and pathogenicity of NOVC strains.

Of note, we could show that several *V. cholerae* strains, including V:5/04, produce OMVs (data not shown) (Bielig *et al.*, 2011b). As OMVs very likely contain physiologically relevant PAMPs, we wanted to elucidate if *V. cholerae* OMVs trigger inflammatory responses in human cells.

To assess if *V. cholerae* OMVs can activate NOD1 and/or NOD2, HEK293T cells were transfected with a NF- κ B reportersystem and NOD1 or NOD2 expression plasmids and treated with OMVs isolated from the *V. cholerae* NOVC strain V:5/04 or the *V. cholerae* O1 El Tor Inaba strain P27459. OMV preparations were adjusted to equal protein concentrations. Stimulation of cells with the NOD1 or NOD2 elicitors Tri-DAP or MDP, respectively, served as positive controls. The results clearly revealed that OMVs from both strains induced a robust NOD1- and NOD2-dependent NF- κ B activation in HEK293T cells, but failed to activate the reporter in the absence of NOD1 or NOD2. Of note, OMVs isolated from *V. cholerae* V:5/04 induced a stronger NF- κ B activation compared to OMVs from *V. cholerae* P27459 (Fig. 20A). These findings were affirmed by experiments using an IL-8-luciferase reportersystem that yielded qualitatively similar results (data not shown). Importantly, the OMVs did not induce cell death in the cells at the concentrations used and during the incubation time used, as monitored by cell viability assays (XTT) in the same experiments (data not shown).

In line with the previous findings, treatment of HeLa cells with OMVs isolated from V:5/04 induced a strong IL-8 secretion (Bielig *et al.*, 2011b) (performed by Prof. Dr. Sun Nyunt Wai and co-workers, Umeå University, Sweden). Furthermore, stimulation of THP1-Blue cells with V:5/04 OMVs induced a very pronounced NF- κ B activation (Fig. 20B). The OMV preparations contained LPS (Bielig *et al.*, 2011b), which likely contributed to the observed inflammatory responses by activating TLR4 in HeLa and THP1 cells. To address whether V:5/04 OMVs also elicit TLR4-independent responses in THP1 cells, we quenched the activity of the LPS by incubation of the vesicles and cells with the LPS-sequestering drug polymyxin B. This revealed that

RESULTS

a great fraction of the inflammatory activity was induced by LPS. However, a highly significant response was still seen in the presence of polymyxin B, indicating that the inflammatory response towards OMVs in THP1 cells was partly mediated by other receptors than TLR4 (Fig.20B).

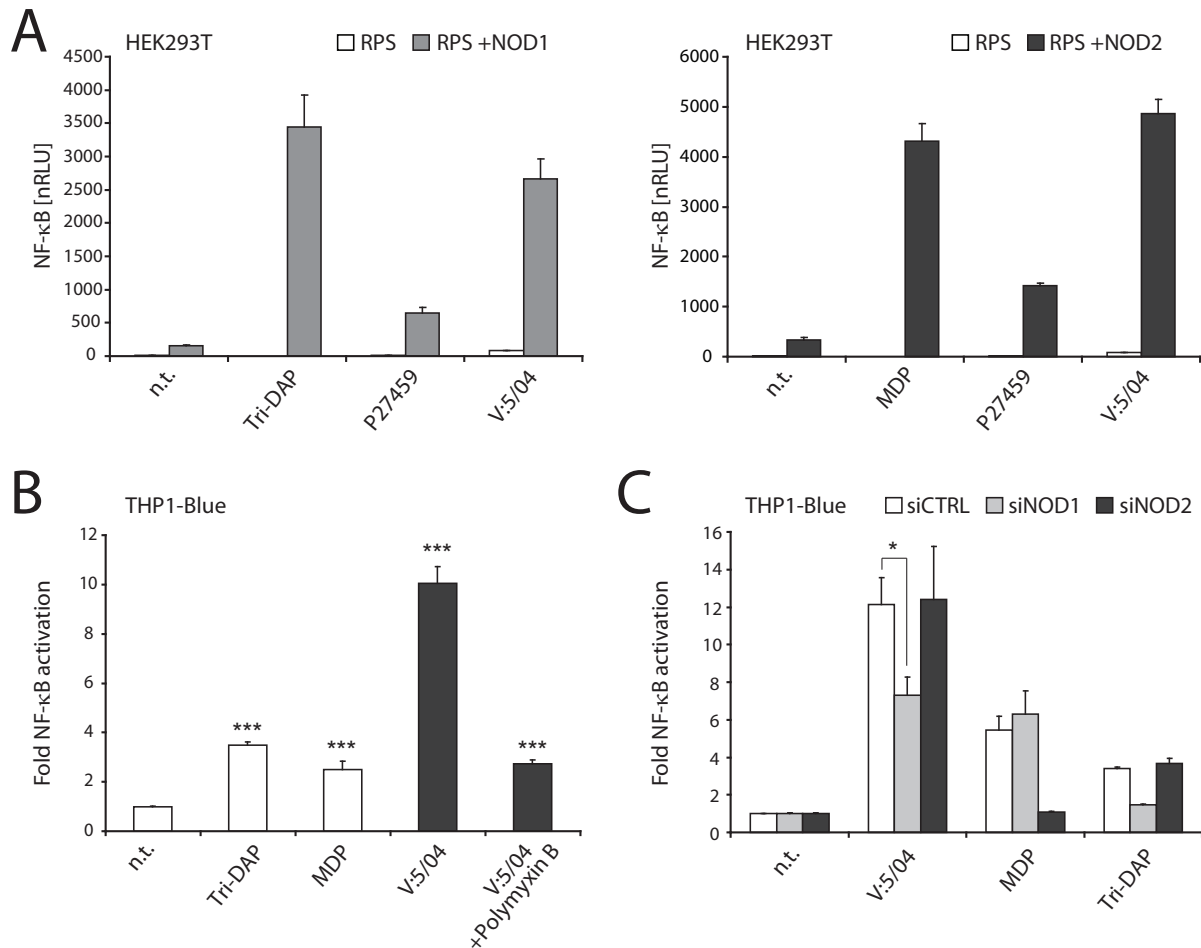


Figure 20. Activation of NOD1 and NOD2 by *V. cholerae* OMVs. **A** HEK293T cells were transfected with the NF-κB luciferase RPS containing NOD1 (left panel) or NOD2 (right panel) expression plasmids and treated with Tri-DAP (0.5 μM) or MDP (50 nM), respectively, or with P27459 or V:5/04 OMVs (0.5 μg/ml each). After 16 h, cells were lysed and luciferase activation was determined and normalised with the β-galactosidase values (nRLU). Values are mean +SD (n=3). Data is representative for at least two independent experiments. **B** Differentiated THP1-Blue cells were treated with Tri-DAP (10 μg/ml), LPS (100 ng/ml) or V:5/04 OMVs (0.5 μg/ml). OMVs were either pre-treated with Polymyxin B (25 μg/ml) or left untreated. After 16 h incubation, NF-κB activation was determined by measurement of SEAP activation from the supernatants. Activity is given as fold over background, mean +SD (n=3). **C** Knock-down of NOD1 impairs NF-κB activation in response to V:5/04 OMVs. THP1-Blue cells were transfected with CTRL, NOD1 or NOD2 siRNA and incubated for 72 h. Subsequently, cells were treated with Tri-DAP or MDP (10 μg/ml each) or with V:5/04 OMVs (1 μg/ml). After 16 h incubation, NF-κB activation was determined by measurement of SEAP activity in the supernatants. Activity is given as fold over background, mean +SD (n=4), data represents two independent experiments. n.t.: non-treated; nRLU: normalised relative light units. Differences were regarded as significant (*), when the p value was <0.05 or as highly significant (***) when the p value was <0.0005, as assessed by the two-sided Student's T-Test.

RESULTS

To gain evidence that NOD1 and NOD2 are involved in inflammatory responses towards OMVs in THP1-Blue cells, NOD1 or NOD2 expression was silenced by treatment with specific siRNAs. Silencing of NOD1 significantly reduced NF- κ B activation in response to V:5/04 OMVs compared to cells treated with non-targeting control siRNA. However, silencing of NOD2 seemed to exert no effect on NF- κ B activation in response to V:5/04 OMVs (Fig. 20C). Knock-down efficiency was assessed by qRT-PCR using cDNA generated from RNA isolated from cells from the same experiment (Bielig *et al.*, 2011b).

In order to gain insight into the mode of interaction of *V. cholerae* OMVs with mammalian cells, HeLa cells were incubated for 8 h with OMVs isolated from V:5/04. OMVs were visualised by indirect immunofluorescence analysis with an antibody specific for the outer membrane protein (Omp) U. This revealed a specific localisation pattern for the OMVs, which appeared to accumulate in the vicinity of the nucleus, whereas the antibody did not stain untreated cells (Bielig *et al.*, 2011b) (Microscopy performed by Birte Zurek, University of Cologne).

Collectively, these results provide evidence that *V. cholerae* OMVs are taken up into human epithelial cells and that NOD1 and NOD2 are at least partially involved in their detection.

3.2.2 The role of quorum sensing in subverting host-detection by NODs

Quorum sensing is well known to control the expression of virulence factors in O1 serotypes of *V. cholerae* (Raychaudhuri *et al.*, 2006; Vaitkevicius *et al.*, 2006; Vance *et al.*, 2003; Miller *et al.*, 2002; Zhu *et al.*, 2002). The protein HapR (hemagglutinin/protease regulatory protein) is thought to act as major regulator of quorum sensing, as it represses virulence gene expression under conditions where the density of bacterial cells is high (reviewed in Sanchez and Holmgren, 2008). However, the role of HapR in virulence gene regulation in NOVC is currently not well established. In order to investigate a putative function of quorum sensing in the regulation of OMV-mediated responses, a mutant of V:5/04 with an in-frame deletion of the *hapR* gene was constructed and analysed in comparison to wild-type (WT) NOVC V:5/04. OMVs from both strains were isolated and the composition and structure of the OMVs were analysed by SDS-PAGE, Western blot analysis, and electron microscopic (EM) examination. Although deletion of HapR led to slight changes in the appearance of the vesicles in EM analysis, yielding a more uniform size, the protein compositions of OMVs from V:5/04 Δ *hapR* and the parent WT strain were highly similar. The amounts of vesicles released from these two strains also were comparable as shown by Western blot analysis detecting a major outer membrane protein, OmpU, as a marker protein for *Vibrio* OMVs. Silverstained SDS-PAGE of preparations of these OMVs also revealed similar amounts and patterns of lipopolysaccharide (LPS) in both samples (Bielig *et al.*,

RESULTS

2011b) (bacterial genetics, OMV purification, biochemistry and EM microscopy were performed by Prof. Dr. Sun Nyunt Wai and co-workers, Umeå University, Sweden). In conclusion, both NOVC V:5/04 strains produced OMVs, whereas the amounts of OMVs and the overall protein and LPS compositions in V:5/04 WT cells and V:5/04 $\Delta hapR$ mutant cells, which are locked in a “virulence-like” state, were similar.

To assess whether there were differences in the immunogenicity of OMVs isolated from WT and $\Delta hapR$ bacteria, HeLa cells were treated with OMV preparations of either of the two strains. As observed before, treatment of cells with WT OMVs induced a robust IL-8 secretion. Strikingly, OMVs isolated from the $\Delta hapR$ strain induced significantly less IL-8 secretion compared to WT OMVs (Fig. 21A). In line with that, OMVs isolated from the $\Delta hapR$ strain also induced significantly less IL-8 secretion than WT OMVs in THP1 cells (Fig. 21B). Qualitatively similar results were observed in HEK293T cells, where OMVs isolated from either the WT or $\Delta hapR$ strain induced NOD1- and NOD2-dependent NF- κ B activation. However, again $\Delta hapR$ OMVs were significantly less active than WT OMVs (Fig. 21C). The same was observed when using an IL-8 reporter plasmid (Bielig *et al.*, 2011b). Taken together, these findings indicated that OMVs derived from V:5/04 $\Delta hapR$ were less immunogenic compared to OMVs derived from WT V:5/04 bacteria. As NOD1 and NOD2 specifically detect PGN fragments, we concluded that this effect might be caused by PGN contained in the OMVs and that $\Delta hapR$ OMVs might contain less PGN than WT OMVs. Indeed, X-ray photoelectron spectroscopy (XPS) confirmed that V:5/04 OMVs contained PGN and that $\Delta hapR$ OMVs contained lower amounts of PGN than WT OMVs (Bielig *et al.*, 2011b) (XPS was performed by Dr. M. Ramstedt, Umeå University, Sweden).

Next, we tested whether the inflammatory activity of whole bacterial lysates, generated by boiling of the bacteria, might also be differently affected by HapR compared to OMVs. That is, does *Vibrio* change the overall PGN/PAMP composition or selectively omit PGN or PAMPs from OMVs during infection? To this end, the inflammatory potentials of equal amounts of lysates from WT V:5/04 and V:5/04 $\Delta hapR$ bacteria were tested. Cell lysates induced a NF- κ B response in THP1-Blue cells (Fig. 21D), as well as NOD2 activation in HEK293T cells (Bielig *et al.*, 2011b). Strikingly, in contrast to the observations obtained with the OMVs, lysates from V:5/04 bacteria lacking HapR did not show a diminished potential to activate NF- κ B (Fig. 21D) (Bielig *et al.*, 2011b). In contrast, lysates from V:5/04 $\Delta hapR$ bacteria induced even slightly stronger responses (Fig. 21D) (Bielig *et al.*, 2011b). Similar results were obtained when measuring IL-8 release from HeLa cells by ELISA (Bielig *et al.*, 2011b).

RESULTS

Taken together, these results displayed that PGN can be delivered by bacterial OMV to host cells where it is sensed by intracellular NOD1 and in some cases NOD2. Furthermore, we revealed a novel mechanism of how bacteria can escape NOD1 detection by actively influencing NOD1/2 immunogenicity of shed OMVs by a pathway involving the quorum-sensing system.

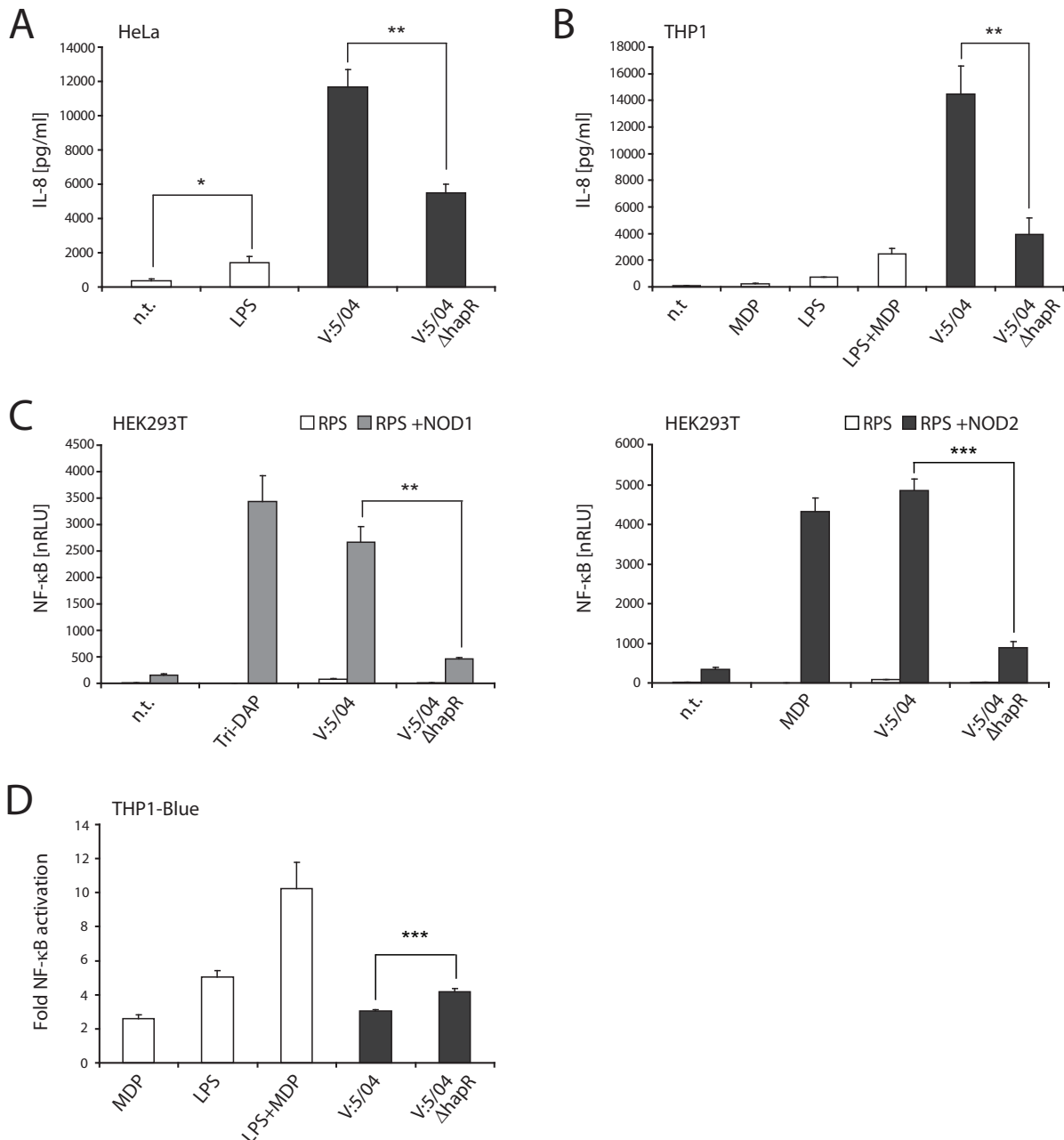


Figure 21. Differential NOD1/2 responses to OMVs and bacterial cell lysates. **A** HeLa cells were treated for 8 h with V:5/04 or V:5/04 Δ hapR OMVs (1 μ g/ml). Stimulation with LPS (0.1 μ g/ml) served as control for the reactivity of the cells. Subsequently, IL-8 secretion was determined by ELISA. Values are mean +SD (n=3). **B** THP1 cells were treated for 16 h with V:5/04 or V:5/04 Δ hapR OMVs (0.05 μ g/ml). Stimulation with MDP (10 μ M) or LPS (0.1 μ g/ml) served as controls. Subsequently, IL-8 secretion was determined by ELISA. Values are mean +SD (n=3). **C** HEK293T cells were transfected with the NF- κ B luciferase RPS containing NOD1 (left panel) or NOD2 (right panel) expression plasmids and treated with V:5/04 or V:5/04 Δ hapR OMVs (0.5 μ g/ml). Stimulation with Tri-DAP (0.5 μ M) or MDP (50 nM) served as controls. After 16 h, cells were lysed and luciferase activation was determined and normalised with the β -galactosidase values (nRLU). Values are

RESULTS

mean +SD (n=3). **D** THP1-Blue cells were treated for 16 h with bacterial lysates from V:5/04 or V:5/04 $\Delta hapR$ OMVs (0.5 $\mu\text{g/ml}$ each). Stimulation with MDP (10 $\mu\text{g/ml}$) or LPS (0.1 $\mu\text{g/ml}$) served as controls. NF- κ B activity was determined by measuring SEAP activity in the supernatant. Activity is given as fold over background, mean +SD (n=3). n.t.: non-treated; nRLU: normalised relative light units; RPS: reporter system. Differences were regarded as highly significant (**) when the p value was <0.005. A p value <0.0005 is indicated by ***, as assessed by the two-sided Student's T-Test.

4 Discussion

4.1 Screen results

In this project we aimed to further elucidate the regulation of the NOD1 innate immune signalling cascade by conducting a high-throughput siRNA screen based on NF- κ B activation in HEK293T cells. In the first step, a pilot screen using a smaller sub-library consisting of apoptosis-related genes was performed. After analysis and validation of the obtained data, we used the established protocols to conduct a high-throughput screen using the human druggable genome library. Subsequent validation and counter-screening, in combination with validation in an additional cell system, yielded a list of NOD1-specific candidates. The quality of this procedure was reflected by the fact that many factors that are known to be involved in the regulation of NOD1 signalling were identified. Detailed characterisation confirmed XIAP (BIRC4) and BMPR-2 as novel components of the NOD1-mediated NF- κ B cascade. Additional analyses indicated that also other BIRC family members are implicated in the regulation of NOD1-mediated inflammatory responses.

4.1.1 Pilot screen

To evaluate and optimise the automated assay protocols and data pipelines, we first screened a sub-library consisting of apoptosis-related genes in 384 well plates. The whole library was screened both for Tri-DAP- and for TNF- α -mediated NF- κ B activation. In the subsequent validation, we were able to validate 73.5 % of the identified inhibiting hits with four different siRNAs targeting each gene, underscoring the reproducibility of the results and the robustness of the assay system. In contrast, only 16.7 % of the activating hits could be validated. This is in line with observations made in other siRNA screens conducted at the same platform, suggesting that false-positives appear to be overrepresented over false negative results (Dr. Peter Braun, personal communication). Therefore we focused our efforts on the inhibiting hits in the following druggable genome screen.

Of note, we were able to identify many factors that are known to be involved in NF- κ B pathways among the inhibiting hits of the pilot screen. Strikingly, the strongest hit in the Tri-DAP/NOD1-specific hit-list was RIP2, a kinase that is well established to be essentially and specifically involved in NOD1-mediated NF- κ B activation (reviewed in Kufer, 2008). Another factor contained in the NOD1-specific hit-list that is known to be involved in NOD1-mediated NF- κ B activation was CARD6. CARD6 has been shown to positively modulate NOD-mediated

DISCUSSION

NF- κ B activation by interaction with RIP2 (Dufner *et al.*, 2006). Beside these established factors, the screen also identified a number of factors that have so far not been linked to NOD1 signalling, such as PRF1 (perforin 1), CTNNB1 (β -catenin) or NOS3 (nitric oxide synthase 3) (Fig. 10B, left panel). Follow-up work is required to validate these and other candidates in other cell systems and to characterise their putative functions in the NOD1 cascade.

The strongest TNF- α -specific hit was the TNF-receptor itself, TNFR1 (TNFRSF1A). TNFR1 is a transmembrane receptor of the TNFR-superfamily crucially involved in NF- κ B activation following TNF- α stimulation (reviewed in Chen and Goeddel, 2002) (Fig. 10B, middle panel).

Notably, we were also able to identify factors that are generally involved in the regulation of canonical NF- κ B signalling, *i.e.* which inhibited both NOD1- and TNF- α -mediated NF- κ B activation. The strongest NF- κ B-associated hit was the NF- κ B subunit RELA. RELA forms heterodimers with other Rel-family members. The canonical NF- κ B heterodimer consists of RELA and p50 (NFKB1, nuclear factor of kappa light polypeptide gene enhancer in B-cells 1) (reviewed in Hayden and Ghosh, 2008). Strikingly, also p50 was found in the screen as a strong NF- κ B-associated hit. Moreover, cullin1 (CUL1), a subunit of the SCF (Skp, Cullin, F-box containing) E3 ubiquitin ligase complex, was contained in this hit-list. The SCF complex is essential for the canonical NF- κ B pathway, as it mediates the phosphorylation-dependent degradation of I κ B- α (reviewed in Maniatis, 1999). Furthermore, the NF- κ B-associated hit-list contained TAK1 (MAP3K7), a kinase that is essential both the NOD1 and the TNFR1 signalling cascades (reviewed in Hayden and Ghosh, 2008) (Fig. 10B, right panel).

Taken together, these results clearly demonstrated that the HEK293T NF- κ B reporter assay system and the established conditions were well suited to identify novel components of the NOD1 signalling pathway.

4.1.2 Druggable genome screen

In the subsequent primary druggable genome screen, again a number of factors that are established to be involved in canonical NF- κ B and/or NOD1 signalling could be identified. Most importantly, however, the hit list contained several factors that have not been associated with NOD1 signalling. Ingenuity pathway analysis revealed that 56 out of the 435 preliminary screen hits (12.9 %) are known components of NF- κ B signalling. Among these 56 preliminary hits, 28 could be validated in the HEK validation screen, of which 14 were not influencing TNF- α -

DISCUSSION

induced NF- κ B activation (Ingenuity pathway analysis was performed by Dr. Peter Braun, MPIIB Berlin) (Fig. 22A).

Same as in the pilot screen, RIP2, p50 and RELA were identified as preliminary inhibiting hits. Furthermore, also IKK α and IKK β were identified as significant hits. IKK β mediates the phosphorylation and subsequent targeting for degradation of I κ B- α in the canonical NF- κ B pathway (reviewed in Hayden and Ghosh, 2008). Of note, IKK α has recently been linked to NOD1 signalling in response to *S. flexneri* infection (Kim *et al.*, 2010). Furthermore, the TAB/TAK complex component TAB2 was identified in the screen. TAB2 mediates activation of the IKK complex through TAK1 by binding to K63-linked ubiquitin chains on upstream proteins and is indispensable for canonical NF- κ B activation (reviewed in Chiu *et al.*, 2009). This process is also critical for NOD1 signalling (Hasegawa *et al.*, 2008; Abbott *et al.*, 2007). Another gene identified with high confidence was RNF31 (ring finger protein 31). RNF31 is part of the LUBAC E3 ligase complex that mediates M1-linked linear ubiquitination of IKK γ and is required for canonical NF- κ B signalling (reviewed in Bianchi and Meier, 2009). Of note, also the activating hit list obtained in the druggable genome screen identified known NF- κ B regulatory factors. The de-ubiquitinating enzymes A20 and CYLD, which are known to negatively regulate canonical NF- κ B signalling, as well as the NOD1 pathway (reviewed in Liu and Chen, 2011), were identified with strong probability values (Fig. 22B). Collectively, these findings prove that the primary druggable genome screen effectively identified anticipated factors involved in the regulation of canonical NF- κ B activation and NOD1 signalling.

To gain insight in which biological processes the identified 435 candidates are involved, gene ontology (GO) enrichment was performed using the GOrilla (Gene Ontology enRIchment anaLysis and visualizAtion) tool. Clustering of the primary hits according to their GO terms revealed that genes linked to immunity and in particular to immune receptors, among others, were significantly enriched in comparison to the druggable genome library used as background. Moreover, genes involved in the regulation of NLR signalling were also significantly over-represented among the preliminary hits (Fig.22C).

As we aimed to identify general regulators of NOD1 signalling, we next validated the 535 preliminary hits (the 435 inhibiting and the top 100 activating) in another cell system, to exclude cell-type specific regulators. For that purpose, we used the monocytic cell line THP1. THP1 cells are accessible with siRNA and have the advantage that they are competent for endogenous NOD and TLR signalling and thus provide a more physiological system than the previously used HEK293T cells (Uehara *et al.*, 2005).

DISCUSSION

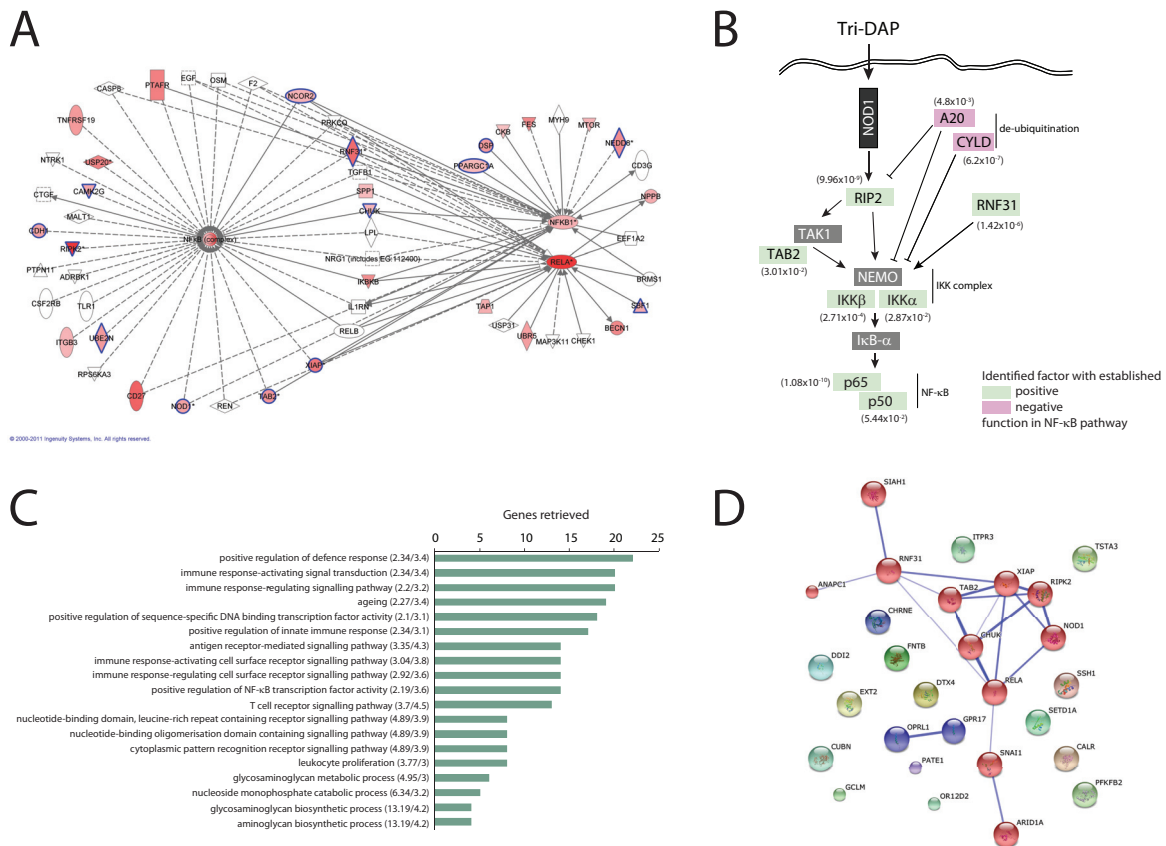


Figure 22. In-depth analyses of the screen results. **A** Known regulators of NF- κ B retrieved by the screens. Shown are 56 (out of 435) preliminary inhibiting screen hits already known to be involved in NF- κ B regulation (Ingenuity Pathway Analysis). Among them, 28 could be validated in the HEK validation screen (dark red: strong hit; light red: weaker hit; white: not validated). A sub group of 14 were not influencing TNF- α -induced NF- κ B activation (blue borders). **B** Schematic representation of the NOD signalling cascade. Known positive regulators retrieved by the primary screen are highlighted in green, known negative regulators in red. The corresponding p-values (RSA-based) are indicated. **C** Gene ontology (GO) enrichment of the 435 preliminary hit genes retrieved by the primary screen compared to the druggable genome library (background). Number of hit genes associated with enriched terms according to the GO of biological processes. Enrichment factors and negative log(P-values) are indicated in brackets. **D** STRING database analysis of the 28 hits from the THP1 screen. Genes, where the NPI values of both siRNAs exceeded 1.5 SD of CTRL from the median of CTRL were regarded as validated. Stronger associations are represented by thicker blue lines. Genes were clustered according to the Marcov cluster (MCL) algorithm.

Although the hit-list obtained in THP1 cells differed markedly from the one obtained in HEK293T cells, a number of factors known to be involved in NF- κ B signalling, such as RELA and RNF31, and factors known to be involved in NOD1 signalling, such as NOD1, RIP2 and IKK α , were identified in these cells as well (Fig. 22D). Of note, again XIAP was found in this hit-list in a very prominent position. Among the hits identified in THP1 cells, the genes RIP2, XIAP, GPR17, SSH1, SNAI1, and CHUK could be confirmed as hits in all screening rounds in both cell lines and did not show inhibiting effects in the TNF- α counter-screen (Fig. 16B). RIP2 is well known to be critically involved in the NOD1 signalling cascade (discussed above); CHUK/

DISCUSSION

IKK α was recently also linked to NOD1 signalling (discussed above). SSH1 (slingshot homolog 1 (*Drosophila*)) was also contained in the hit-list of a recently published NOD1 screen (discussed below). GPR17 (G protein-coupled receptor 17) and SNAI1 (snail homolog 1 (*Drosophila*)) were so far not linked to any events in innate immunity; follow-up work is required to validate the observed effects and to characterise their putative roles in NOD1 signalling. The top NOD1-specific hit XIAP was subsequently extensively characterised in this study (Fig. 17).

4.1.3 Comparison with published screens

During our screening project, two other siRNA screening projects aiming at identifying NOD1 regulatory factors were published. Kim *et al.* screened a small siRNA library targeting 132 genes of the signalling proteome in HeLa cells by monitoring p65 translocation to the nucleus following *Shigella flexneri* infection. In this process, CHUK (conserved helix-loop-helix ubiquitous kinase, also termed IKK α) was identified as primary hit and subsequently validated. Consistently, the authors could demonstrate that IKK α was required for *S. flexneri* and PGN-induced NOD1-mediated NF- κ B activation and IL-8 secretion in HeLa cells (Kim *et al.*, 2010). Strikingly, we also identified IKK α as NOD1-specific hit, albeit at a lower position in the final ranking (Fig. 16B). This prompted us to compare our screening results with the published results to find out if there were more common factors. Out of the 132 genes screened by Kim *et al.*, 105 were also contained in our druggable genome library (Fig. 23A, left panel). Among those, 10 genes were classified as preliminary hits in our primary druggable genome screen. In total, Kim *et al.* identified 13 genes from their library as significant hits; three of those (NOD1, RIP2 and IKK α) were likewise identified as hits in our primary druggable genome screen. Of note, exactly these three genes could also be validated in the THP1 screen, whereas the remaining 7 genes displayed results differing from the druggable genome screen and were not regarded as validated (Fig. 23A, right panel). Taken together, the identification of IKK α in our screen supports the findings of Kim *et al.*, as it has previously been presumed that only IKK β is required for NOD1-mediated NF- κ B activation. We further add to this by showing that IKK α acts NOD1-specific, as we did not observe effects on TNF- α -mediated NF- κ B activation. Moreover, the identification of IKK α provides further evidence that our screening project effectively identified NOD1-specific regulators.

During the finalisation of this project, another siRNA screen on NOD1 activation was published. The authors screened the same druggable genome library in human HT29 colonocytes,

DISCUSSION

making this screen in principle comparable to our data. Measurement of IL-8 secretion in response to stimulation with Tri-DAP served as read-out for the primary screen. In total they identified 227 inhibiting and 198 activating hits. Among those, they could validate a total number of 200 genes by measuring IL-8 expression by qRT-PCR. In a secondary screen, cells were stimulated with TNF. Altogether, they could identify 114 genes as non-specific common regulators of both pathways; among those, 60 were found to be specifically involved in NOD1 signalling. Surprisingly, the authors then characterised the non-specific hit BID (BH3 interacting domain death agonist), despite the rather low position in their hit-list (position 74 in the primary screen, position 5 in the secondary TNF screen). They revealed that BID interacts with NOD1, NOD2 and the IKK complex and that human and murine cells deficient for BID are defective in inflammatory responses to NOD agonists. (Yeretssian *et al.*, 2011).

However, we could not identify BID in our screening approach and none of the siRNAs targeting BID displayed any significant effect on NF- κ B activation induced by Tri-DAP in our primary screen (data not shown). The overlap of the hits identified by Yeretssian *et al.* and the hits identified in our screen was rather small, even though the same druggable genome library and a similar screen set-up was used. In total, there was an overlap of 10 inhibiting hits between the published primary screen and our primary screen. The established factors RELA and RIP2 were identified in both of the screens, however, most other factors were either not validated, or not NOD1-specific in at least one of the screens (Fig. 23B). Interestingly, the only validated and NOD1-specific factors found in both of the screening projects are RIP2 and SSH1 (Fig. 23B). This strongly suggests that SSH1 might play a pivotal role in the NOD1 signalling pathway. Indeed, preliminary data obtained by knock-down of SSH1 in THP1 cells and subsequent measurements of Tri-DAP-induced IL-8 secretion indicated that SSH1 is necessary for NOD1 signalling (data not shown). SSH1 belongs to the SSH family of phosphatases, which is crucially implicated in the regulation of actin filament dynamics (reviewed in Huang *et al.*, 2006). Intriguingly, there are reports linking actin dynamics to NOD signalling. It has been shown that NOD2 is present at the plasma membrane (Kufer *et al.*, 2006; Barnich *et al.*, 2005a; McDonald *et al.*, 2005) and that disruption of the actin cytoskeleton increases NOD2-mediated NF- κ B activation (Legrand-Poels *et al.*, 2007). Furthermore, there is evidence that NOD1 activation in response to *S. flexneri* infection is dependent on a membrane-localisation of NOD1, which in turn is dependent on an intact actin cytoskeleton (Kufer *et al.*, 2008). However, so far it is not understood how NOD1 and NOD2 are recruited to the plasma membrane. The small RhoGTPase RAC1 (ras-related C3 botulinum toxin substrate 1), a factor that is involved in the regulation of the actin cytoskeleton, has been shown to interact with NOD2 at the plasma membrane (Eitel *et al.*, 2008; Legrand-Poels *et al.*, 2007). The regulation of this process remains to be elucidated,

DISCUSSION

but there is evidence that RAC1 is also essential for the membrane localisation of NOD1 (Regueiro *et al.*, 2011). In addition, the cytoskeleton-associated factor GEF-H1 (guanine nucleotide exchange factor H1) has been shown to be required for NOD1-activation in response to *S. flexneri* infection (Fukazawa *et al.*, 2008). It might well be that also SSH1 is somehow involved in the regulation of the membrane recruitment of NOD1. Further experiments are required to validate the observed effect of SSH1 knock-down on NOD1-mediated IL-8 secretion and to characterise the putative role of SSH1 in NOD signalling.

Taken together, the comparison with the published screen and preliminary validation data revealed SSH1 as promising candidate for further characterisation.

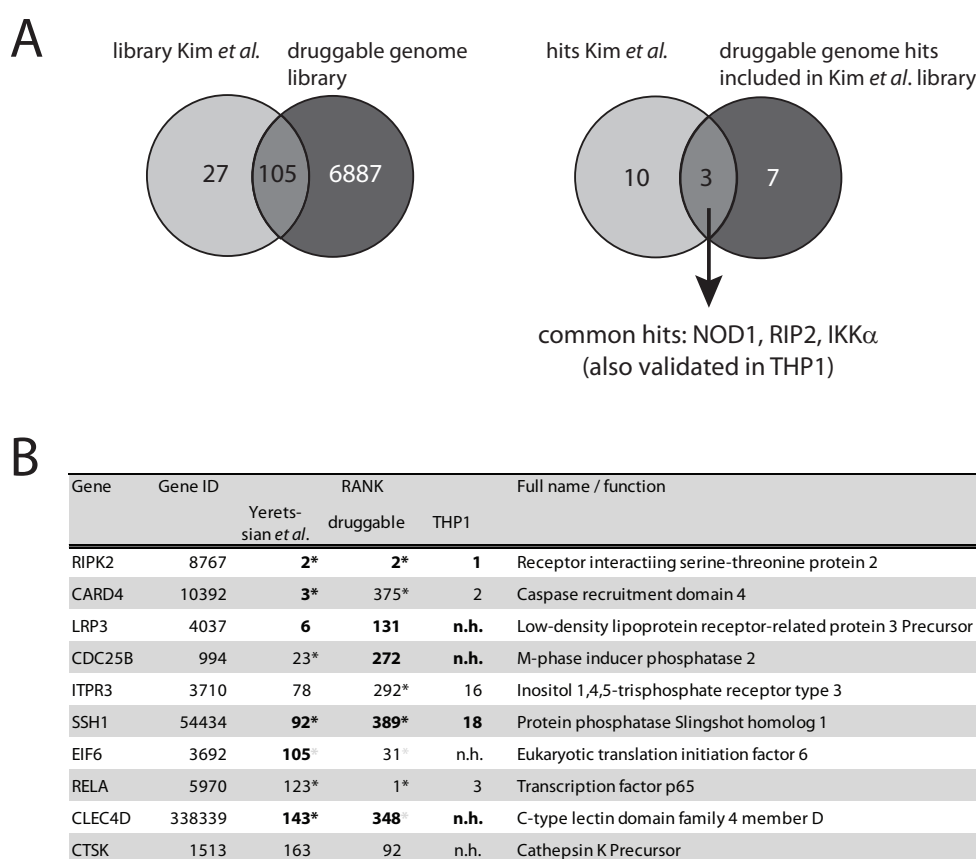


Figure 23. Meta-analysis comparing the screening results with published NOD1 siRNA screens. **A** Comparison with the screen from Kim *et al.*. In this approach, 132 genes were screened in HeLa cells by monitoring p65 translocation to the nucleus following *Shigella flexneri* infection. Out of the 132 genes targeted in this screen, 105 were also contained in the druggable genome library (*left panel*). Among those, 10 genes were classified as preliminary hits in the primary druggable genome screen and three (NOD1, RIP2, IKK α) were also classified as hits by Kim *et al.* (*right panel*). **B** Comparison with the screen from Yeretssian *et al.*. In this approach, the human druggable genome library was screened in HT29 cells. IL-8 secretion following Tri-DAP stimulation served as read-out. Hits were subsequently validated using qRT-PCR to monitor IL-8 gene expression. NOD1-specific hits were obtained by using a secondary screen with TNF stimulation. The table shows the primary screen data obtained by Yeretssian *et al.* that overlap with our preliminary hit-list in comparison to the HEK293T druggable genome screen and the THP1 validation screen. Note that THP1 ranks do not necessarily correspond to THP1 ranks in Fig. 16B, as Fig. 16B uniquely represents NOD1-specific hits. Bold: NOD1-specific in the respective screen; * validated in the respective screen; n.h.: no hit in THP1 validation screen

4.1.4 XIAP and BMPR-2 are involved in NOD1 signalling

XIAP (X-linked inhibitor of apoptosis, also termed BIRC4) was found as top inhibiting hit throughout the whole screening steps, indicating that XIAP is of crucial importance in the NOD1 pathway.

XIAP belongs to the BIRC (baculoviral IAP repeat-containing) family, which is known to play important roles in counter-acting apoptosis. It has been shown that XIAP counter-acts apoptosis by direct inhibition of caspases (Eckelman and Salvesen, 2006; Eckelman *et al.*, 2006). However, the physiological role of XIAP in the regulation of apoptosis is still not clear, as mice deficient for XIAP did not display obvious defects in induction of apoptosis (Harlin *et al.*, 2001).

There is increasing evidence that XIAP is implicated in a variety of other important regulatory cascades, such as TGF- β signalling, MAPK and NF- κ B activation and ubiquitin pathways (Gyrd-Hansen and Meier, 2010; Kashkar, 2010; Srinivasula and Ashwell, 2008; Birkey Reffey *et al.*, 2001). Importantly, there is also evidence for crucial functions of XIAP in innate immune responses. For instance, mutations in XIAP caused a primary immunodeficiency in patients with X-linked lymphoproliferative syndrome (XLP) (Rigaud *et al.*, 2006). Strikingly, it has been shown that macrophages from mice deficient for XIAP displayed reduced NF- κ B activation and cytokine secretion in response to a combined treatment with TLR2 and NOD2 ligands and in response to the invasive pathogen *Listeria monocytogenes*. Accordingly, XIAP showed to be crucial for protection of mice against *L. monocytogenes* infection (Bauler *et al.*, 2008). This is in line with our observations from the screen and with subsequent siRNA experiments indicating that XIAP is of crucial importance for inflammatory responses to NOD1 and NOD2 elicitors as well as to the invasive pathogen *S. flexneri* in human cells. Of note, during the time when we discovered XIAP as NOD1-specific hit in the druggable genome screen, a publication revealed that XIAP mediates NOD signalling via interaction with RIP2. The authors demonstrated that cells deficient for XIAP display a strong reduction in NF- κ B activation induced by NOD-elicitors as well as by over-expression of NOD1 or NOD2, strongly supporting our observations. Furthermore, this study revealed that the interaction of RIP2 with XIAP is dependent on the BIR2 domain of XIAP. Consistently, expression of the XIAP inhibitor SMAC disrupts the interaction of RIP2 and XIAP, indicating that RIP2 interacts with the SMAC-binding site of the BIR2 domain (Krieg *et al.*, 2009). This is in line with our observation that over-expression of cytosolic SMAC strongly inhibited NOD1- and RIP2-mediated NF- κ B activation. In contrast, NF- κ B activation triggered by over-expression of IKK β was not inhibited by expression of SMAC, indicating that XIAP acts upstream of the IKK complex in NOD signalling. This is also underlined by the observations from the TNF- α counter-screen that indicated that silencing of XIAP does not

DISCUSSION

inhibit the TNF signalling pathway. Taken together, our observations and the literature provide strong evidence that XIAP is critically involved in NOD signalling. However, the molecular mechanisms still remain to be elucidated.

There are reports linking XIAP to TGF- β and BMP signalling (Liu *et al.*, 2009; Birkey Reffey *et al.*, 2001; Yamaguchi *et al.*, 1999). Strikingly, the bone morphogenetic protein receptor II (BMPR-2) was found as inhibiting hit throughout the screening steps, displaying moderate effects on NOD1-mediated NF- κ B activation in the druggable genome screen and the subsequent validation screen, whereas there was no effect on TNF- α signalling observed. However, BMPR-2 was not included in the final hit-list, as one out of the two used siRNAs activated NF- κ B signalling in THP1-Blue cells. It is likely that this was caused by an off-target effect, as the other siRNA targeting BMPR-2 inhibited NF- κ B signalling in THP1-Blue cells, and as knock-down of BMPR-2 clearly exerted robust inhibiting effects in the other screening steps.

Of note, the involvement of BMPR-2 in NOD1 signalling was validated in siRNA knock-down experiments in HeLa cells as well as in THP1 cells. In both cases, silencing of BMPR-2 with two different siRNAs significantly reduced the BMPR-2 message and impaired NOD1-mediated responses triggered by infection with *S. flexneri* or stimulation with Tri-DAP.

BMPR-2 belongs to the bone morphogenetic protein (BMP) receptor family. The ligands for these receptors are BMPs, which belong to the transforming growth factor β (TGF- β) superfamily. BMPs are multi-functional growth factors with a wide range of biological functions, including the regulation of cell growth, differentiation and apoptosis. BMP signalling occurs via transmembrane serine/threonine receptors. There are two subtypes of BMP receptors, type I and type II receptors. The type I receptors BMPR-1A and BMPR-1B form heterotetrameric complexes with the type II receptor BMPR-2, consisting of two pairs of type I and type II receptors (reviewed in Miyazono *et al.*, 2005). BMP signalling can only occur when receptors of both types are present. Binding of dimeric BMPs activates PRE-FORMED COMPLEXES (PFCs), (Gilboa *et al.*, 2000) or induces the formation and activation of BMP-INDUCED SIGNALLING COMPLEXES (BISCs) (Nohe *et al.*, 2002). The kinase of BMPR-2 is constitutively active and trans-phosphorylates the type I receptor, which in turn transmits intracellular signals to downstream targets. Complexes consisting of BMPR-2 and the type I receptors BMPR-1A or BMPR-1B have high affinities for BMP-2 and BMP-4, however, both type I receptors have higher affinities for BMP-2/4 than BMPR-2 (Knaus and Sebald, 2001; Koenig *et al.*, 1994). Interestingly, stimulation of PFCs induces different signalling cascades than BISCs. Activation of PFCs triggers Smad signalling, whereas BISCs activate MAPK pathways (Nohe *et al.*, 2002).

DISCUSSION

Strikingly, it has been shown that BMP triggers TAK1 activation in early *Xenopus* embryos *in vivo* by recruitment of the TAB1/TAK1 complex to BMPR-1 and that XIAP is essentially involved in this process. The same study revealed that XIAP interacts with TAB1 via its BIR domain and with the cytoplasmic region of BMPR-1A via its RING domain in mammalian cells. The authors propose that XIAP serves as an adaptor molecule to link BMP signalling to the TAB1/TAK1 complex (Yamaguchi *et al.*, 1999). Moreover, a role for XIAP as co-factor in TGF- β signalling has been described. It has been shown that XIAP co-localises and interacts with the TGF- β type I receptor (T β RI), potentiates TGF- β signalling and activates JNK and NF- κ B (Birkey Reffey *et al.*, 2001).

The implications of XIAP in BMP signalling have been further investigated by Liu *et al.* The authors revealed that anti-apoptotic effects exerted by BMP-2 and GDF-5 are mediated by an interaction between BMPR-2 and XIAP. This interaction enhanced protein stability of XIAP by reducing its ubiquitination and proteasomal degradation. The enhanced concentration of XIAP in turn counter-acts apoptosis caused by serum starvation. Of note, stabilisation of XIAP by BMPR-2 seemed to be independent of BMP downstream signalling, as inhibition of Smads and MAPKs did not affect XIAP protein levels. This effect, however, is likely cell-type specific, as BMP-induced stabilisation of XIAP was observed in MEFs, but not in human umbilical vein smooth muscle cells (HUVSMCs) (Liu *et al.*, 2009).

To investigate if BMPR-2 also stabilises XIAP in our assay system, we stimulated cycloheximide-treated THP1 cells with recombinant BMP-2. Blocking of protein neo-synthesis with cycloheximide markedly reduced XIAP protein levels. Strikingly, this effect was reversed by stimulation of the cells with BMP-2, indicating that stabilisation of XIAP by BMPR-2 does not only occur under apoptotic conditions. Thus, it is plausible that the positive effect of BMPR-2 in NOD1 signalling is caused indirectly by stabilisation of XIAP, as we and others found that XIAP is essentially involved in NOD1-mediated responses (Krieg *et al.*, 2009).

Liu *et al.* observed that siRNA-mediated knock-down of BMPR-2 inhibited the anti-apoptotic effects of BMP-2 and prevented stabilisation of XIAP. As knock-down of BMPR-2 promoted apoptosis, the authors concluded that BMPR-2 might have a basic activity that stabilised XIAP even without exogenously added ligands (Liu *et al.*, 2009). This is in line with our findings that siRNA-mediated knock-down of BMPR-2 inhibits NOD1-mediated signalling. The basic activity of BMPR-2 without exogenously added ligands might be sufficient to contribute to NOD1-mediated signalling through stabilisation of XIAP. Consistently, it has been shown that BMP receptor complexes consisting of homo- and heterotetramers of BMPR-1A, BMPR-1B and BMPR-2 also exist in the absence of ligands (Gilboa *et al.*, 2000).

DISCUSSION

Interactions of the NOD1/RIP2/XIAP signalling complex with BMPR-2 would possibly require recruitment of the complex to the plasma membrane, as BMPR-2 is a transmembrane receptor. Of note, it has been shown that active NOD1 is recruited to the plasma membrane (Zurek *et al.*, 2012; Kufer *et al.*, 2008), suggesting that a mechanism involving recruitment of NOD1 and XIAP to BMPR-2 at the plasma membrane is possible.

As functional BMP signalling requires complexes consisting of type I and type II receptors, and as it has been shown that BMPR-1B also interacted with XIAP (Liu *et al.*, 2009), it is likely that BMPR-1B might also be implicated in NOD1 signalling. Interestingly, two out of three siRNAs with sufficient replicates targeting the type I receptor BMPR-1B also exerted moderate inhibiting effects (~ 1 SD of CTRL from median CTRL) on NOD1-mediated NF- κ B activation in the druggable genome screen (data not shown). However, as the effects were not very strong, and as one siRNA targeting BMPR-1B caused enhanced NF- κ B activation (data not shown), BMPR-1B was not further subjected to the validation screens.

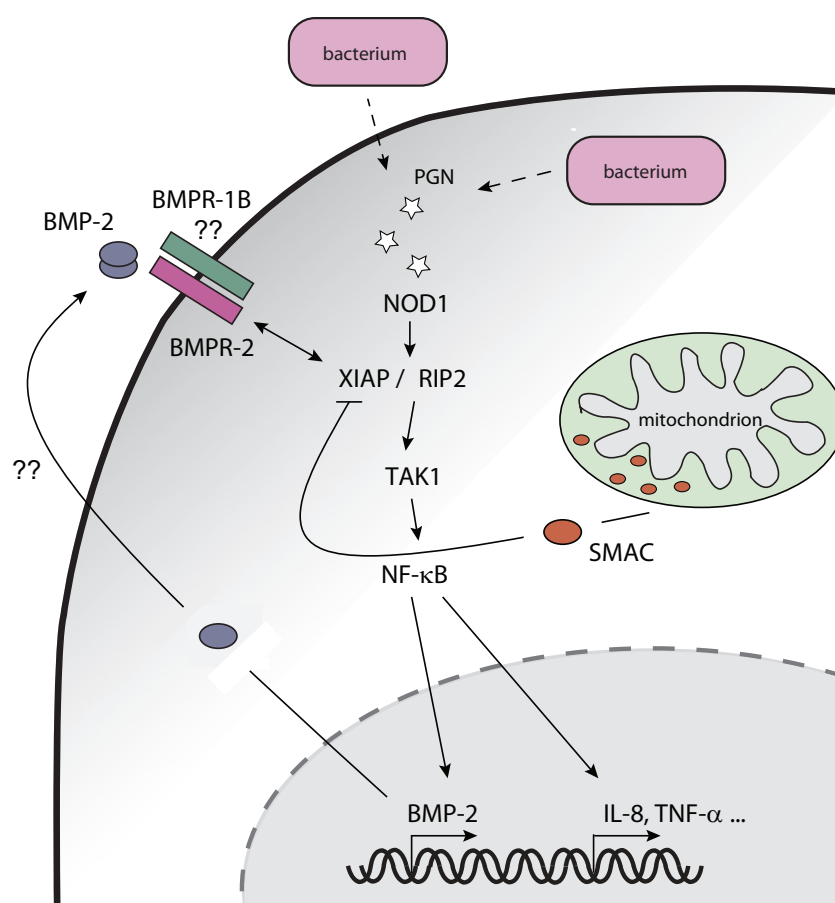


Figure 24. Working model for the positive effects of BMPR-2 on NOD1 signalling. BMPR-2 possibly contributes to NOD1 signalling by stabilising XIAP, a factor that is essential for NOD1 signalling. XIAP, in turn, is antagonised by mitochondrial pro-apoptotic factors, such as SMAC. Increased BMP-2 expression mediated by NOD1-dependent NF- κ B activation might constitute a positive feedback loop to sustain NOD1 signalling through BMPR-2. For further details please refer to the main text.

DISCUSSION

Taken together, our data indicate that BMPR-2 contributes to NOD1 signalling, likely by stabilising XIAP. Even though BMPR-2 likely contributes to NOD1 signalling also in the absence of exogenously added ligands, it is possible that ligands can sustain this effect. Further research will address this question in detail. Of note, it has been shown that inflammatory stimuli, such as TNF- α , positively regulate BMP-2 expression through NF- κ B in bone cells (Huang *et al.*, 2010; Feng *et al.*, 2003; Fukui *et al.*, 2003) and endothelial cells (Csiszar *et al.*, 2005). This might also apply to other cell types, indicating that BMP-2 might promote NOD1 signalling through BMPR-2 in a positive feedback loop (Fig. 24). Expression of TNF- α is also controlled by NOD signalling (reviewed in Fritz *et al.*, 2006), this might further increase BMP-2 expression. However, this remains to be proven, and the exact mechanisms and also the role of type I receptors in this process remain to be elucidated.

4.2 Roles for BIRC proteins in NOD1 signalling

It is well established that members of the BIRC-family (baculovirus IAP repeat containing; also termed IAPs, for inhibitors of apoptosis) are anti-apoptotic factors that counter-act apoptosis by direct or indirect inhibition of caspases that mediate the proteolytic cascades leading to cell death (reviewed in Salvesen and Duckett, 2002). However, there is increasing evidence that BIRC proteins also play important roles in other cellular processes. BIRC2 (cIAP-1) and BIRC3 (cIAP-2) have been linked to events that lead to activation of NF- κ B (Tseng *et al.*, 2010; Bertrand *et al.*, 2009; Bertrand *et al.*, 2008).

Intrigued by these findings, we analysed if also other BIRC family members, except for XIAP that we identified in the screen, are involved in NOD1-mediated innate immunity. Due to heterogeneity in the effects of the different siRNAs, our screening data was not conclusive on this point. Therefore we performed siRNA-mediated knock-down of all members of the BIRC-family, with exception of BIRC1 and BIRC6, in HeLa and THP1 cells. This revealed that silencing of BIRC2, BIRC5 and BIRC8 reproducibly impaired Tri-DAP-mediated IL-8 secretion in HeLa and THP1 cells. Silencing of BIRC3, in contrast, strongly enhanced Tri-DAP-mediated IL-8 secretion in HeLa cells, whereas there was only a weak and not reproducible enhancement observed in THP1 cells. This indicated that BIRC3 might act cell-type specifically.

This idea is underlined by a recent publication, where the authors observed that siRNA-mediated knock-down of BIRC2 in HT29 colon cells displayed no effect on DAP-mediated IL-8 secretion, whereas secretion of the cytokines TNF- α and MCP-1 (CCL2) was strongly impaired. Furthermore, depletion of BIRC2 was shown to reduce DAP-mediated NF- κ B and JNK activation in HT29 cells. Silencing of BIRC3 in HT29 cells, in contrast, was shown to im-

DISCUSSION

pair DAP-mediated IL-8 secretion, as well as secretion of TNF- α and MCP-1; in addition, DAP-mediated NF- κ B activation as well as JNK and p38 phosphorylation was inhibited. Furthermore, the authors demonstrated that murine macrophages deficient for BIRC2 or BIRC3 were defective in MDP-induced production of the cytokines IL-6, IL-1 β , IL-10 and TNF- α . Moreover, the authors showed that BIRC2 and BIRC3 co-precipitate with RIP2 and that their E3 ligase activity is required for ubiquitination of RIP2. Consistently, DAP-mediated release of the chemokines KC and MCP-1 was shown to be impaired in BIRC2^{-/-} and BIRC3^{-/-} mice (Bertrand *et al.*, 2009).

Collectively, these findings and our results strongly indicate that BIRC2 and BIRC3 are crucially implicated in NOD1 signalling. However, the exact regulatory mechanisms remain elusive. It is likely that there are cell type-specific differences in their contributions to NOD signalling, reflected by the different effects of knock-down of BIRC2 and BIRC3 on cytokine secretion in different cell types. It is also possible that the strong increase in Tri-DAP-induced IL-8 secretion that we observed in HeLa cells treated with BIRC3 siRNA was caused by excessive activation of BIRC2 caused by the knock-down of BIRC3, as it has been shown that these proteins can cross-control each other. For example, elevated levels of BIRC3 have been observed in BIRC2 null cells (Conze *et al.*, 2005). To address this question, further experiments with simultaneous silencing of BIRC2 and BIRC3 have to be conducted and protein levels should be monitored.

Furthermore, BIRC2 and BIRC3 also seem to contribute to TLR signalling, as they have been shown to positively regulate MyD88-dependent TLR signalling by mediating K48-linked ubiquitination of TRAF3 in RAW264.7 mouse macrophages and bone marrow-derived macrophages (BMDMs) (Tseng *et al.*, 2010). However, conflicting data has been reported by Bertrand *et al.*, where BMDMs from BIRC3 deficient mice displayed no defects in TLR4 signalling (Bertrand *et al.*, 2009).

Of note, also knock-down of BIRC5 and BIRC8 impaired Tri-DAP-mediated IL-8 secretion in HeLa as well as in THP1 cells. To the best of our knowledge, neither BIRC5, nor BIRC8 have been implicated in the regulation of events linked to innate immunity so far.

BIRC5 (Survivin) is the smallest of the BIRC family members and is characterised by the presence of a single BIR-domain (reviewed in Sah *et al.*, 2006) (Fig. 3). Like most other BIRC family members, BIRC5 has been shown to counter-act apoptosis (Song *et al.*, 2003; Tamm *et al.*, 1998), but also other functions have been reported, in particular in cell division (Skoufias *et al.*, 2000; Uren *et al.*, 2000). BIRC2 and BIRC3 likely act in the NOD1 signalling pathway through their E3 ligase activities, which is mediated by their RING domains. BIRC5, however, does not contain a RING domain (reviewed in Sah *et al.*, 2006) (Fig. 3), making it difficult to propose a working model for the implications of BIRC5 in NOD1 signalling. Further experiments are required to validate the putative role of BIRC5 in NOD1 signalling in other cell systems.

DISCUSSION

In contrast to the other BIRCs that are evolutionary conserved, BIRC8 (ILP-2) is only conserved in primates. BIRC8 shares 81 % sequence identity with XIAP on protein level and there is evidence that it is a processed gene derived by retrotransposition from *ILP-1*, the gene coding for XIAP. However, BIRC8 lacks the first two BIR domains that are present in XIAP (Richter *et al.*, 2001) (Fig. 3). This renders the protein conformationally unstable. In spite of its putative caspase-9 interaction domain, it is only a weak caspase-9 inhibitor on its own (Shin *et al.*, 2005). However, it has been shown that over-expression of BIRC8 potently inhibits apoptosis induced by over-expression of BAX and by co-expression of caspase-9 and APAF-1 *in vitro* (Lagace *et al.*, 2001; Richter *et al.*, 2001). Thus, it seems possible that BIRC8 needs co-factors to inhibit apoptosis *in vivo*. Thus far, expression of BIRC8 had only been detected in testis and in lymphoblastoid cells (Lagace *et al.*, 2001; Richter *et al.*, 2001), however, we clearly detected BIRC8 mRNA-expression in HeLa cells. Furthermore, we could exclude that the reduced IL-8 secretion in response to Tri-DAP-stimulation in cells treated with siRNA against BIRC8 was caused by unspecific knock-down of XIAP. This indicates that BIRC8 is implicated in the regulation of NOD1 signalling. Further experiments are required to confirm this novel finding in other cell systems and to characterise the underlying molecular mechanisms.

Collectively, these results further add to the notion that BIRC2 and BIRC3 are implicated in NOD1 signalling and indicate novel roles for BIRC5 and BIRC8 in NOD1 signalling. Furthermore, these results reveal exiting new insights into the apparent tissue-specificity of BIRC proteins in innate immunity.

4.3 *V. cholerae* OMVs trigger NOD signalling in a quorum sensing-dependent manner

In the first part of this project we identified novel factors involved in the regulation of the NOD1 signalling cascade. Sensing of PGN by NOD1 and NOD2, however, requires its translocation to the cytoplasmic compartment (Girardin *et al.*, 2003c; Girardin *et al.*, 2003b). In our screen this was artificially induced by transfection of Tri-DAP with liposomes. However, how PGN uptake is achieved under physiological conditions remains somewhat fragmentary. It has been shown for *H. pylori* that PGN can be introduced into the host cell by its type IV secretion system (Viala *et al.*, 2004), whereas macrophages and some epithelial cell lines can directly take up MDP in a dynamin-dependent process (Marina-Garcia *et al.*, 2009; Marina-Garcia *et al.*, 2008). Additionally, other bacterial factors, such as pore-forming toxins, can mediate PGN uptake and subsequent NOD1 and NOD2 activation (Ratner *et al.*, 2007). Here, we analysed the possible role of bacterial outer-membrane vesicles (OMVs) as carriers of NOD1 and NOD2 active PGN.

DISCUSSION

We revealed that OMVs derived from *V. cholerae* induce NF- κ B-mediated innate immune responses in different human cell lines. Indeed, we observed that OMV production is a common feature in different *V. cholerae* strains. We showed that OMVs from the NOVC strain V:5/04 induce a significant inflammatory response in the host cell that is partly dependent on NOD1 and NOD2. Activation of NOD1 and NOD2 in selective assays by V:5/04 OMVs indirectly revealed that PGN is associated with OMVs, which was confirmed by physicochemical characterisation of the *V. cholerae* OMV preparations. Our data suggests that OMVs represent an alternative route to deliver bacterial PGN to the host cell (Fig. 25). Indeed, delivery of bacterial PGN was also reported for *H. pylori* OMVs (Ismail *et al.*, 2003). A recent study revealed that also OMVs derived from *Pseudomonas aeruginosa*- and *Neisseria gonorrhoeae* contain PGN and activate NOD1 upon contact with host cells (Kaparakis *et al.*, 2009). Collectively, this indicates that PGN delivery by OMVs is a conserved and common bacterial strategy to modulate host immune responses. Further studies are needed to understand which mechanism is relevant under different physiological conditions.

Intriguingly, we revealed that NOD1 and NOD2 activity of *Vibrio cholerae* OMVs was dependent on the quorum-sensing master regulator HapR, a known control switch for virulence gene expression in *V. cholerae* O1 strains (Miller *et al.*, 2002; Zhu *et al.*, 2002) (Fig. 25). Deletion of HapR significantly attenuated the NOD1/2 activation potential of the V:5/04 OMVs, but at the same time did not reduce the immunogenicity of whole bacterial lysates. However, HapR did not influence the amount of OMVs produced, arguing that a natural HapR mutant might not show different OMV production. This indicates that genes under the control of HapR either change the composition of the PGN delivered by OMVs, or lead to the exclusion of PGN from the OMVs (Fig. 25). One possible candidate gene involved in the peptidoglycan biosynthesis process is VCA0981, which encodes a protein with homology to the peptidoglycan-specific endopeptidase M23, a member of the family of periplasmic binding proteins (PBPs), which binds substrate and interacts with a membrane-bound complex. We found that the expression of VCA0981 was decreased in the *hapR* mutant in comparison with the wild-type strain V:5/04 (data not shown), suggesting that this gene product is involved in the observed difference between WT- and $\Delta hapR$ -derived vesicles in activation of NOD1 and NOD2. However, overexpression of the protein in HapR-deficient bacteria did not yield complementation of this phenotype, suggesting either that overexpression is not suitable for complementation, or that additional factors under the control of HapR are involved in this process.

Evasion of NOD-mediated innate immunity likely is a common scheme for pathogens, as also *L. monocytogenes* and *H. pylori* employ strategies to modulate NOD1 and NOD2 responses when colonising the host. *L. monocytogenes* uses N-deacetylation of PGN by the N-deacetylase PgdA

DISCUSSION

(Boneca *et al.*, 2007), whereas the coccoid form of *H. pylori* escapes NOD1 detection by the AmiA PGN hydrolase (Chaput *et al.*, 2006). This suggests that PGN modelling and subsequent coupled activation of NOD1 and NOD2 constitute a more general theme for bacterial manipulation of the host innate immune response. However, to the best of our knowledge, our work is the first to provide a role for the quorum sensing machinery in OMV-mediated activation of host PRRs.

Recently, *V. cholerae* OMVs were shown to be promising candidates for vaccines, as they induce strong immunity in mice (Schild *et al.*, 2008). Furthermore, NOD1 and NOD2 activation has been linked to the onset of adaptive immune responses (Magalhaes *et al.*, 2008; Fritz *et al.*, 2007). Thus, it is likely that PGN is one of the active adjuvant components accounting for the high immunogenicity of OMVs.

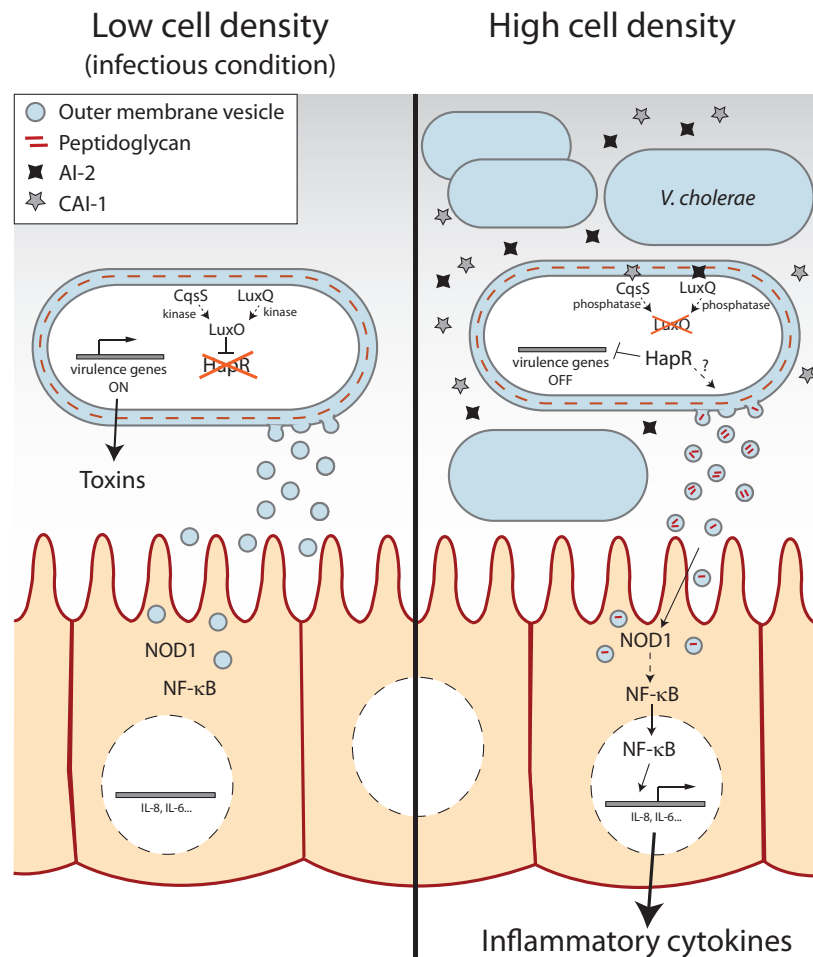


Figure 25. Schematic representation of the quorum sensing machinery in *V. cholerae* and its OMV-mediated interplay with epithelial cells. At low cell densities, the virulence gene-repressor HapR gets degraded in a process mainly dependent on the repressor protein LuxO and the autoinducer/sensor pairs AI-2/LuxQ and CAI-1/CqsS. When HapR is not present, virulence genes are expressed, OMVs contain low amounts of peptidoglycan and do not induce a strong inflammatory response. At high cell densities, the repressor HapR is active and represses virulence gene expression. At this state, OMVs contain higher amounts of peptidoglycan and induce strong inflammatory responses that are partially mediated by NOD1. For further details please refer to the main text. (From Bielig *et al.*, 2011a).

5 References

- Abbott, D.W., Wilkins, A., Asara, J.M. and Cantley, L.C. (2004) The Crohn's disease protein, NOD2, requires RIP2 in order to induce ubiquitylation of a novel site on NEMO. *Curr Biol.* **14**: 2217-2227.
- Abbott, D.W., Yang, Y., Hutti, J.E., Madhavarapu, S., Kelliher, M.A. and Cantley, L.C. (2007) Coordinated regulation of Toll-like receptor and NOD2 signaling by K63-linked polyubiquitin chains. *Mol Cell Biol.* **27**: 6012-6025.
- Abreu, M.T., Vora, P., Faure, E., Thomas, L.S., Arnold, E.T. and Arditi, M. (2001) Decreased expression of Toll-like receptor-4 and MD-2 correlates with intestinal epithelial cell protection against dysregulated proinflammatory gene expression in response to bacterial lipopolysaccharide. *J Immunol.* **167**: 1609-1616.
- Aderem, A. and Ulevitch, R.J. (2000) Toll-like receptors in the induction of the innate immune response. *Nature.* **406**: 782-787.
- Akira, S. and Takeda, K. (2004) Toll-like receptor signalling. *Nat Rev Immunol.* **4**: 499-511.
- Akira, S., Uematsu, S. and Takeuchi, O. (2006) Pathogen recognition and innate immunity. *Cell.* **124**: 783-801.
- Alnemri, E.S., Livingston, D.J., Nicholson, D.W., Salvesen, G., Thornberry, N.A., Wong, W.W. and Yuan, J. (1996) Human ICE/CED-3 protease nomenclature. *Cell.* **87**: 171.
- Auvynet, C. and Rosenstein, Y. (2009) Multifunctional host defense peptides: antimicrobial peptides, the small yet big players in innate and adaptive immunity. *Febs J.* **276**: 6497-6508.
- Barnich, N., Aguirre, J.E., Reinecker, H.C., Xavier, R. and Podolsky, D.K. (2005a) Membrane recruitment of NOD2 in intestinal epithelial cells is essential for nuclear factor- κ B activation in muramyl dipeptide recognition. *J Cell Biol.* **170**: 21-26.
- Barnich, N., Hisamatsu, T., Aguirre, J.E., Xavier, R., Reinecker, H.C. and Podolsky, D.K. (2005b) GRIM-19 interacts with nucleotide oligomerization domain 2 and serves as downstream effector of anti-bacterial function in intestinal epithelial cells. *J Biol Chem.* **280**: 19021-19026.
- Bauler, L.D., Duckett, C.S. and O'Riordan, M.X. (2008) XIAP regulates cytosol-specific innate immunity to Listeria infection. *PLoS Pathog.* **4**: e1000142.
- Bauman, S.J. and Kuehn, M.J. (2006) Purification of outer membrane vesicles from *Pseudomonas aeruginosa* and their activation of an IL-8 response. *Microbes Infect.* **8**: 2400-2408.
- Berrington, W.R., Iyer, R., Wells, R.D., Smith, K.D., Skerrett, S.J. and Hawn, T.R. (2010) NOD1 and NOD2 regulation of pulmonary innate immunity to *Legionella pneumophila*. *Eur J Immunol.* **40**: 3519-3527.
- Bertin, J., Nir, W.J., Fischer, C.M., Tayber, O.V., Errada, P.R., Grant, J.R., *et al* (1999) Human CARD4 protein is a novel CED-4/Apaf-1 cell death family member that activates NF- κ B. *J Biol Chem.* **274**: 12955-12958.
- Bertrand, M.J., Doiron, K., Labbe, K., Korneluk, R.G., Barker, P.A. and Saleh, M. (2009) Cellular inhibitors of apoptosis cIAP1 and cIAP2 are required for innate immunity signaling by the pattern recognition receptors NOD1 and NOD2. *Immunity.* **30**: 789-801.
- Bertrand, M.J., Milutinovic, S., Dickson, K.M., Ho, W.C., Boudreault, A., Durkin, J., *et al* (2008) cIAP1 and cIAP2 facilitate cancer cell survival by functioning as E3 ligases that promote RIP1 ubiquitination. *Mol Cell.* **30**: 689-700.
- Bianchi, K. and Meier, P. (2009) A tangled web of ubiquitin chains: breaking news in TNF-R1 signaling. *Mol Cell.* **36**: 736-742.

REFERENCES

- Bielig, H., Dongre, M., Zurek, B., Wai, S.N. and Kufer, T.A. (2011a) A role for quorum sensing in regulating innate immune responses mediated by *Vibrio cholerae* outer membrane vesicles (OMVs). *Gut Microbes*. **2**.
- Bielig, H., Zurek, B., Kutsch, A., Menning, M., Philpott, D.J., Sansonetti, P.J. and Kufer, T.A. (2009) A function for AAMP in Nod2-mediated NF-kappaB activation. *Mol Immunol*. **46**: 2647-2654.
- Bielig, H., Rompikuntal, P.K., Mitesh, D., Zurek, B., Lindmark, B., Ramstedt, M., *et al* (2011b) NOD-like receptor activation by outer-membrane vesicles (OMVs) from non-O1 non-O139 *Vibrio cholerae* is modulated by the quorum sensing regulator HapR. *Infect Immun*.
- Birkey Reffey, S., Wurthner, J.U., Parks, W.T., Roberts, A.B. and Duckett, C.S. (2001) X-linked inhibitor of apoptosis protein functions as a cofactor in transforming growth factor-beta signaling. *J Biol Chem*. **276**: 26542-26549.
- Birmingham, A., Selfors, L.M., Forster, T., Wrobel, D., Kennedy, C.J., Shanks, E., *et al* (2009) Statistical methods for analysis of high-throughput RNA interference screens. *Nat Methods*. **6**: 569-575.
- Boneca, I.G. (2005) The role of peptidoglycan in pathogenesis. *Curr Opin Microbiol*. **8**: 46-53.
- Boneca, I.G., Dussurget, O., Cabanes, D., Nahori, M.A., Sousa, S., Lecuit, M., *et al* (2007) A critical role for peptidoglycan N-deacetylation in *Listeria* evasion from the host innate immune system. *Proc Natl Acad Sci U S A*. **104**: 997-1002.
- Boone, D.L., Turer, E.E., Lee, E.G., Ahmad, R.C., Wheeler, M.T., Tsui, C., *et al* (2004) The ubiquitin-modifying enzyme A20 is required for termination of Toll-like receptor responses. *Nat Immunol*. **5**: 1052-1060.
- Boughan, P.K., Argent, R.H., Body-Malapel, M., Park, J.H., Ewings, K.E., Bowie, A.G., *et al* (2006) Nucleotide-binding oligomerization domain-1 and epidermal growth factor receptor: critical regulators of beta-defensins during *Helicobacter pylori* infection. *J Biol Chem*. **281**: 11637-11648.
- Bouskra, D., Brezillon, C., Berard, M., Werts, C., Varona, R., Boneca, I.G. and Eberl, G. (2008) Lymphoid tissue genesis induced by commensals through NOD1 regulates intestinal homeostasis. *Nature*. **456**: 507-510.
- Boutros, M., Bras, L.P. and Huber, W. (2006) Analysis of cell-based RNAi screens. *Genome Biol*. **7**: R66.
- Bowie, A., Kiss-Toth, E., Symons, J.A., Smith, G.L., Dower, S.K. and O'Neill, L.A. (2000) A46R and A52R from vaccinia virus are antagonists of host IL-1 and toll-like receptor signaling. *Proc Natl Acad Sci U S A*. **97**: 10162-10167.
- Brightbill, H.D., Libraty, D.H., Krutzik, S.R., Yang, R.B., Belisle, J.T., Bleharski, J.R., *et al* (1999) Host defense mechanisms triggered by microbial lipoproteins through toll-like receptors. *Science*. **285**: 732-736.
- Brooks, M.N., Rajaram, M.V., Azad, A.K., Amer, A.O., Valdivia-Arenas, M.A., Park, J.H., *et al* (2011) NOD2 controls the nature of the inflammatory response and subsequent fate of *Mycobacterium tuberculosis* and *M. bovis* BCG in human macrophages. *Cell Microbiol*. **13**: 402-418.
- Burckstummer, T., Baumann, C., Bluml, S., Dixit, E., Durnberger, G., Jahn, H., *et al* (2009) An orthogonal proteomic-genomic screen identifies AIM2 as a cytoplasmic DNA sensor for the inflammasome. *Nat Immunol*. **10**: 266-272.
- Chamaillard, M., Hashimoto, M., Horie, Y., Masumoto, J., Qiu, S., Saab, L., *et al* (2003) An essential role for NOD1 in host recognition of bacterial peptidoglycan containing diaminopimelic acid. *Nat Immunol*. **4**: 702-707.
- Chaput, C., Ecobichon, C., Cayet, N., Girardin, S.E., Werts, C., Guadagnini, S., *et al* (2006) Role of AmiA in the morphological transition of *Helicobacter pylori* and in immune escape. *PLoS Pathog*. **2**: e97.
- Chen, G. and Goeddel, D.V. (2002) TNF-R1 signaling: a beautiful pathway. *Science*. **296**: 1634-1635.

REFERENCES

- Chen, Z.J. (2005) Ubiquitin signalling in the NF-kappaB pathway. *Nat Cell Biol.* **7**: 758-765.
- Chiu, Y.H., Zhao, M. and Chen, Z.J. (2009) Ubiquitin in NF-kappaB signaling. *Chem Rev.* **109**: 1549-1560.
- Clark, N.M., Marinis, J.M., Cobb, B.A. and Abbott, D.W. (2008) MEKK4 sequesters RIP2 to dictate NOD2 signal specificity. *Curr Biol.* **18**: 1402-1408.
- Clarke, T.B., Davis, K.M., Lysenko, E.S., Zhou, A.Y., Yu, Y. and Weiser, J.N. (2010) Recognition of peptidoglycan from the microbiota by Nod1 enhances systemic innate immunity. *Nat Med.* **16**: 228-231.
- Clerc, P. and Sansonetti, P.J. (1987) Entry of *Shigella flexneri* into HeLa cells: evidence for directed phagocytosis involving actin polymerization and myosin accumulation. *Infect Immun.* **55**: 2681-2688.
- Conte, D., Holcik, M., Lefebvre, C.A., Lacasse, E., Picketts, D.J., Wright, K.E. and Korneluk, R.G. (2006) Inhibitor of apoptosis protein cIAP2 is essential for lipopolysaccharide-induced macrophage survival. *Mol Cell Biol.* **26**: 699-708.
- Conze, D.B., Albert, L., Ferrick, D.A., Goeddel, D.V., Yeh, W.C., Mak, T. and Ashwell, J.D. (2005) Posttranscriptional downregulation of c-IAP2 by the ubiquitin protein ligase c-IAP1 in vivo. *Mol Cell Biol.* **25**: 3348-3356.
- Cory, S. and Adams, J.M. (2002) The Bcl2 family: regulators of the cellular life-or-death switch. *Nat Rev Cancer.* **2**: 647-656.
- Csiszar, A., Smith, K.E., Koller, A., Kaley, G., Edwards, J.G. and Ungvari, Z. (2005) Regulation of bone morphogenetic protein-2 expression in endothelial cells: role of nuclear factor-kappaB activation by tumor necrosis factor-alpha, H2O2, and high intravascular pressure. *Circulation.* **111**: 2364-2372.
- da Silva Correia, J., Miranda, Y., Leonard, N., Hsu, J. and Ulevitch, R.J. (2007) Regulation of Nod1-mediated signaling pathways. *Cell Death Differ.* **14**: 830-839.
- da Silva Correia, J., Miranda, Y., Austin-Brown, N., Hsu, J., Mathison, J., Xiang, R., *et al* (2006) Nod1-dependent control of tumor growth. *Proc Natl Acad Sci U S A.* **103**: 1840-1845.
- Dabbagh, K. and Lewis, D.B. (2003) Toll-like receptors and T-helper-1/T-helper-2 responses. *Curr Opin Infect Dis.* **16**: 199-204.
- Deatherage, B.L., Lara, J.C., Bergsbaken, T., Rassouljian Barrett, S.L., Lara, S. and Cookson, B.T. (2009) Biogenesis of bacterial membrane vesicles. *Mol Microbiol.* **72**: 1395-1407.
- Deveraux, Q.L., Takahashi, R., Salvesen, G.S. and Reed, J.C. (1997) X-linked IAP is a direct inhibitor of cell-death proteases. *Nature.* **388**: 300-304.
- Dufner, A., Pownall, S. and Mak, T.W. (2006) Caspase recruitment domain protein 6 is a microtubule-interacting protein that positively modulates NF-kappaB activation. *Proc Natl Acad Sci U S A.* **103**: 988-993.
- Dykxhoorn, D.M. and Lieberman, J. (2005) The silent revolution: RNA interference as basic biology, research tool, and therapeutic. *Annu Rev Med.* **56**: 401-423.
- Eckelman, B.P. and Salvesen, G.S. (2006) The human anti-apoptotic proteins cIAP1 and cIAP2 bind but do not inhibit caspases. *J Biol Chem.* **281**: 3254-3260.
- Eckelman, B.P., Salvesen, G.S. and Scott, F.L. (2006) Human inhibitor of apoptosis proteins: why XIAP is the black sheep of the family. *EMBO Rep.* **7**: 988-994.
- Eden, E., Lipson, D., Yogev, S. and Yakhini, Z. (2007) Discovering motifs in ranked lists of DNA sequences. *PLoS Comput Biol.* **3**: e39.

REFERENCES

- Eden, E., Navon, R., Steinfeld, I., Lipson, D. and Yakhini, Z. (2009) GOzilla: a tool for discovery and visualization of enriched GO terms in ranked gene lists. *BMC Bioinformatics*. **10**: 48.
- Eder, W., Klimecki, W., Yu, L., von Mutius, E., Riedler, J., Braun-Fahrlander, C., *et al* (2006) Association between exposure to farming, allergies and genetic variation in CARD4/NOD1. *Allergy*. **61**: 1117-1124.
- Eitel, J., Krull, M., Hocke, A.C., N'Guessan, P.D., Zahlten, J., Schmeck, B., *et al* (2008) Beta-PIX and Rac1 GTPase mediate trafficking and negative regulation of NOD2. *J Immunol*. **181**: 2664-2671.
- Elbashir, S.M., Harborth, J., Lendeckel, W., Yalcin, A., Weber, K. and Tuschl, T. (2001) Duplexes of 21-nucleotide RNAs mediate RNA interference in cultured mammalian cells. *Nature*. **411**: 494-498.
- Elmore, S. (2007) Apoptosis: a review of programmed cell death. *Toxicol Pathol*. **35**: 495-516.
- Ender, C. and Meister, G. (2010) Argonaute proteins at a glance. *J Cell Sci*. **123**: 1819-1823.
- Faruque, S.M., Albert, M.J. and Mekalanos, J.J. (1998) Epidemiology, genetics, and ecology of toxigenic *Vibrio cholerae*. *Microbiol Mol Biol Rev*. **62**: 1301-1314.
- Feng, J.Q., Xing, L., Zhang, J.H., Zhao, M., Horn, D., Chan, J., *et al* (2003) NF-kappaB specifically activates BMP-2 gene expression in growth plate chondrocytes in vivo and in a chondrocyte cell line in vitro. *J Biol Chem*. **278**: 29130-29135.
- Ferwerda, G., Girardin, S.E., Kullberg, B.J., Le Bourhis, L., de Jong, D.J., Langenberg, D.M., *et al* (2005) NOD2 and toll-like receptors are nonredundant recognition systems of *Mycobacterium tuberculosis*. *PLoS Pathog*. **1**: 279-285.
- Fire, A., Xu, S., Montgomery, M.K., Kostas, S.A., Driver, S.E. and Mello, C.C. (1998) Potent and specific genetic interference by double-stranded RNA in *Caenorhabditis elegans*. *Nature*. **391**: 806-811.
- Fritz, J.H., Ferrero, R.L., Philpott, D.J. and Girardin, S.E. (2006) Nod-like proteins in immunity, inflammation and disease. *Nat Immunol*. **7**: 1250-1257.
- Fritz, J.H., Girardin, S.E., Fitting, C., Werts, C., Mengin-Lecreulx, D., Caroff, M., *et al* (2005) Synergistic stimulation of human monocytes and dendritic cells by Toll-like receptor 4 and NOD1- and NOD2-activating agonists. *Eur J Immunol*. **35**: 2459-2470.
- Fritz, J.H., Le Bourhis, L., Sellge, G., Magalhaes, J.G., Fsihi, H., Kufer, T.A., *et al* (2007) Nod1-mediated innate immune recognition of peptidoglycan contributes to the onset of adaptive immunity. *Immunity*. **26**: 445-459.
- Fruytoso, M.S., Hori, J.I., Pereira, M.S., Junior, D.S., Sonogo, F., Kobayashi, K.S., *et al* (2010) The pattern recognition receptors Nod1 and Nod2 account for neutrophil recruitment to the lungs of mice infected with *Legionella pneumophila*. *Microbes Infect*. **12**: 819-827.
- Fukazawa, A., Alonso, C., Kurachi, K., Gupta, S., Lesser, C.F., McCormick, B.A. and Reinecker, H.C. (2008) GEF-H1 mediated control of NOD1 dependent NF-kappaB activation by *Shigella* effectors. *PLoS Pathog*. **4**: e1000228.
- Fukui, N., Zhu, Y., Maloney, W.J., Clohisy, J. and Sandell, L.J. (2003) Stimulation of BMP-2 expression by pro-inflammatory cytokines IL-1 and TNF-alpha in normal and osteoarthritic chondrocytes. *J Bone Joint Surg Am*. **85-A Suppl 3**: 59-66.
- Geijtenbeek, T.B. and Gringhuis, S.I. (2009) Signalling through C-type lectin receptors: shaping immune responses. *Nat Rev Immunol*. **9**: 465-479.

REFERENCES

- Gilboa, L., Nohe, A., Geissendorfer, T., Sebald, W., Henis, Y.I. and Knaus, P. (2000) Bone morphogenetic protein receptor complexes on the surface of live cells: a new oligomerization mode for serine/threonine kinase receptors. *Mol Biol Cell*. **11**: 1023-1035.
- Girardin, S.E., Jehanno, M., Mengin-Lecreulx, D., Sansonetti, P.J., Alzari, P.M. and Philpott, D.J. (2005) Identification of the critical residues involved in peptidoglycan detection by Nod1. *J Biol Chem*. **280**: 38648-38656.
- Girardin, S.E., Travassos, L.H., Herve, M., Blanot, D., Boneca, I.G., Philpott, D.J., *et al* (2003a) Peptidoglycan molecular requirements allowing detection by Nod1 and Nod2. *J Biol Chem*. **278**: 41702-41708.
- Girardin, S.E., Boneca, I.G., Viala, J., Chamaillard, M., Labigne, A., Thomas, G., *et al* (2003b) Nod2 is a general sensor of peptidoglycan through muramyl dipeptide (MDP) detection. *J Biol Chem*. **278**: 8869-8872.
- Girardin, S.E., Tournebise, R., Mavris, M., Page, A.L., Li, X., Stark, G.R., *et al* (2001) CARD4/Nod1 mediates NF-kappaB and JNK activation by invasive *Shigella flexneri*. *EMBO Rep*. **2**: 736-742.
- Girardin, S.E., Boneca, I.G., Carneiro, L.A., Antignac, A., Jehanno, M., Viala, J., *et al* (2003c) Nod1 detects a unique muropeptide from gram-negative bacterial peptidoglycan. *Science*. **300**: 1584-1587.
- Graham, F.L., Smiley, J., Russell, W.C. and Nairn, R. (1977) Characteristics of a human cell line transformed by DNA from human adenovirus type 5. *J Gen Virol*. **36**: 59-74.
- Gyrd-Hansen, M. and Meier, P. (2010) IAPs: from caspase inhibitors to modulators of NF-kappaB, inflammation and cancer. *Nat Rev Cancer*. **10**: 561-574.
- Hamanaka, Y., Nakashima, M., Wada, A., Ito, M., Kurazono, H., Hojo, H., *et al* (2001) Expression of human beta-defensin 2 (hBD-2) in *Helicobacter pylori* induced gastritis: antibacterial effect of hBD-2 against *Helicobacter pylori*. *Gut*. **49**: 481-487.
- Hao, Y., Sekine, K., Kawabata, A., Nakamura, H., Ishioka, T., Ohata, H., *et al* (2004) Apollon ubiquitinates SMAC and caspase-9, and has an essential cytoprotection function. *Nat Cell Biol*. **6**: 849-860.
- Harlin, H., Reffey, S.B., Duckett, C.S., Lindsten, T. and Thompson, C.B. (2001) Characterization of XIAP-deficient mice. *Mol Cell Biol*. **21**: 3604-3608.
- Hasegawa, M., Fujimoto, Y., Lucas, P.C., Nakano, H., Fukase, K., Nunez, G. and Inohara, N. (2008) A critical role of RICK/RIP2 polyubiquitination in Nod-induced NF-kappaB activation. *Embo J*. **27**: 373-383.
- Hasegawa, M., Yang, K., Hashimoto, M., Park, J.H., Kim, Y.G., Fujimoto, Y., *et al* (2006) Differential release and distribution of Nod1 and Nod2 immunostimulatory molecules among bacterial species and environments. *J Biol Chem*. **281**: 29054-29063.
- Hayden, M.S. and Ghosh, S. (2008) Shared principles in NF-kappaB signaling. *Cell*. **132**: 344-362.
- Hegde, R., Srinivasula, S.M., Zhang, Z., Wassell, R., Mukattash, R., Cilenti, L., *et al* (2002) Identification of Omi/HtrA2 as a mitochondrial apoptotic serine protease that disrupts inhibitor of apoptosis protein-caspase interaction. *J Biol Chem*. **277**: 432-438.
- Hisamatsu, T., Suzuki, M., Reinecker, H.C., Nadeau, W.J., McCormick, B.A. and Podolsky, D.K. (2003) CARD15/NOD2 functions as an antibacterial factor in human intestinal epithelial cells. *Gastroenterology*. **124**: 993-1000.
- Hitotsumatsu, O., Ahmad, R.C., Tavares, R., Wang, M., Philpott, D., Turer, E.E., *et al* (2008) The ubiquitin-editing enzyme A20 restricts nucleotide-binding oligomerization domain containing 2-triggered signals. *Immunity*. **28**: 381-390.
- Horvath, P. and Barrangou, R. (2010) CRISPR/Cas, the immune system of bacteria and archaea. *Science*. **327**: 167-170.

REFERENCES

- Hruz, P. and Eckmann, L. (2010) Innate immune defence: NOD2 and autophagy in the pathogenesis of Crohn's disease. *Swiss Med Wkly.* **140**: w13135.
- Hsu, Y.M., Zhang, Y., You, Y., Wang, D., Li, H., Duramad, O., *et al* (2007) The adaptor protein CARD9 is required for innate immune responses to intracellular pathogens. *Nat Immunol.* **8**: 198-205.
- Hu, S. and Yang, X. (2003) Cellular inhibitor of apoptosis 1 and 2 are ubiquitin ligases for the apoptosis inducer Smac/DIABLO. *J Biol Chem.* **278**: 10055-10060.
- Huang, C.Y., Lee, C.Y., Chen, M.Y., Tsai, H.C., Hsu, H.C. and Tang, C.H. (2010) Adiponectin increases BMP-2 expression in osteoblasts via AdipoR receptor signaling pathway. *J Cell Physiol.* **224**: 475-483.
- Huang, H., Joazeiro, C.A., Bonfoco, E., Kamada, S., Leverson, J.D. and Hunter, T. (2000) The inhibitor of apoptosis, cIAP2, functions as a ubiquitin-protein ligase and promotes in vitro monoubiquitination of caspases 3 and 7. *J Biol Chem.* **275**: 26661-26664.
- Huang, T.Y., DerMardirossian, C. and Bokoch, G.M. (2006) Cofilin phosphatases and regulation of actin dynamics. *Curr Opin Cell Biol.* **18**: 26-31.
- Hysi, P., Kabesch, M., Moffatt, M.F., Schedel, M., Carr, D., Zhang, Y., *et al* (2005) NOD1 variation, immunoglobulin E and asthma. *Hum Mol Genet.* **14**: 935-941.
- Inohara, N., Koseki, T., Lin, J., del Peso, L., Lucas, P.C., Chen, F.F., *et al* (2000) An induced proximity model for NF-kappa B activation in the Nod1/RICK and RIP signaling pathways. *J Biol Chem.* **275**: 27823-27831.
- Inohara, N., Koseki, T., del Peso, L., Hu, Y., Yee, C., Chen, S., *et al* (1999) Nod1, an Apaf-1-like activator of caspase-9 and nuclear factor-kappaB. *J Biol Chem.* **274**: 14560-14567.
- Inohara, N., Ogura, Y., Fontalba, A., Gutierrez, O., Pons, F., Crespo, J., *et al* (2003) Host recognition of bacterial muramyl dipeptide mediated through NOD2. Implications for Crohn's disease. *J Biol Chem.* **278**: 5509-5512.
- Ismail, S., Hampton, M.B. and Keenan, J.I. (2003) Helicobacter pylori outer membrane vesicles modulate proliferation and interleukin-8 production by gastric epithelial cells. *Infect Immun.* **71**: 5670-5675.
- Ismair, M.G., Vavricka, S.R., Kullak-Ublick, G.A., Fried, M., Mengin-Lecreulx, D. and Girardin, S.E. (2006) hPepT1 selectively transports muramyl dipeptide but not Nod1-activating muramyl peptides. *Can J Physiol Pharmacol.* **84**: 1313-1319.
- Jorgensen, R. (1990) Altered gene expression in plants due to trans interactions between homologous genes. *Trends Biotechnol.* **8**: 340-344.
- Kain, S.R. and Ganguly, S. (2001) Overview of genetic reporter systems. *Curr Protoc Mol Biol.* **Chapter 9**: Unit9 6.
- Kaparakis, M., Turnbull, L., Carneiro, L., Firth, S., Coleman, H.A., Parkington, H.C., *et al* (2009) Bacterial membrane vesicles deliver peptidoglycan to NOD1 in epithelial cells. *Cell Microbiol.*
- Kaper, J.B., Morris, J.G., Jr. and Levine, M.M. (1995) Cholera. *Clin Microbiol Rev.* **8**: 48-86.
- Karlas, A., Machuy, N., Shin, Y., Pleissner, K.P., Artarini, A., Heuer, D., *et al* (2010) Genome-wide RNAi screen identifies human host factors crucial for influenza virus replication. *Nature.* **463**: 818-822.
- Kashkar, H. (2010) X-linked inhibitor of apoptosis: a chemoresistance factor or a hollow promise. *Clin Cancer Res.* **16**: 4496-4502.
- Kashkar, H., Deggerich, A., Seeger, J.M., Yazdanpanah, B., Wiegmann, K., Haubert, D., *et al* (2007) NF-kappaB-independent down-regulation of XIAP by bortezomib sensitizes HL B cells against cytotoxic drugs. *Blood.* **109**: 3982-3988.

REFERENCES

- Kashkar, H., Seeger, J.M., Hombach, A., Deggerich, A., Yazdanpanah, B., Utermohlen, O., *et al* (2006) XIAP targeting sensitizes Hodgkin lymphoma cells for cytolytic T-cell attack. *Blood*. **108**: 3434-3440.
- Kim, J.G., Lee, S.J. and Kagnoff, M.F. (2004) Nod1 is an essential signal transducer in intestinal epithelial cells infected with bacteria that avoid recognition by toll-like receptors. *Infect Immun*. **72**: 1487-1495.
- Kim, M.L., Jeong, H.G., Kasper, C.A. and Arrieumerlou, C. (2010) IKK α contributes to canonical NF- κ B activation downstream of Nod1-mediated peptidoglycan recognition. *PLoS One*. **5**: e15371.
- Kim, Y.G., Park, J.H., Shaw, M.H., Franchi, L., Inohara, N. and Nunez, G. (2008) The cytosolic sensors Nod1 and Nod2 are critical for bacterial recognition and host defense after exposure to Toll-like receptor ligands. *Immunity*. **28**: 246-257.
- Kischkel, F.C., Hellbardt, S., Behrmann, I., Germer, M., Pawlita, M., Krammer, P.H. and Peter, M.E. (1995) Cytotoxicity-dependent APO-1 (Fas/CD95)-associated proteins form a death-inducing signaling complex (DISC) with the receptor. *Embo J*. **14**: 5579-5588.
- Knaus, P. and Sebald, W. (2001) Cooperativity of binding epitopes and receptor chains in the BMP/TGF β superfamily. *Biol Chem*. **382**: 1189-1195.
- Kobayashi, K.S., Chamaillard, M., Ogura, Y., Henegariu, O., Inohara, N., Nunez, G. and Flavell, R.A. (2005) Nod2-dependent regulation of innate and adaptive immunity in the intestinal tract. *Science*. **307**: 731-734.
- Koenig, B.B., Cook, J.S., Wolsing, D.H., Ting, J., Tiesman, J.P., Correa, P.E., *et al* (1994) Characterization and cloning of a receptor for BMP-2 and BMP-4 from NIH 3T3 cells. *Mol Cell Biol*. **14**: 5961-5974.
- Kofoed, E.M. and Vance, R.E. (2011) Innate immune recognition of bacterial ligands by NAIPs determines inflammasome specificity. *Nature*. **477**: 592-595.
- Kolling, G.L. and Matthews, K.R. (1999) Export of virulence genes and Shiga toxin by membrane vesicles of *Escherichia coli* O157:H7. *Appl Environ Microbiol*. **65**: 1843-1848.
- Konig, R., Chiang, C.Y., Tu, B.P., Yan, S.F., DeJesus, P.D., Romero, A., *et al* (2007) A probability-based approach for the analysis of large-scale RNAi screens. *Nat Methods*. **4**: 847-849.
- Krieg, A., Correa, R.G., Garrison, J.B., Le Negrate, G., Welsh, K., Huang, Z., *et al* (2009) XIAP mediates NOD signaling via interaction with RIP2. *Proc Natl Acad Sci U S A*. **106**: 14524-14529.
- Kufer, T.A. (2008) Signal transduction pathways used by NLR-type innate immune receptors. *Mol Biosyst*. **4**: 380-386.
- Kufer, T.A., Kremmer, E., Banks, D.J. and Philpott, D.J. (2006) Role for erbin in bacterial activation of Nod2. *Infect Immun*. **74**: 3115-3124.
- Kufer, T.A., Kremmer, E., Adam, A.C., Philpott, D.J. and Sansonetti, P.J. (2008) The pattern-recognition molecule Nod1 is localized at the plasma membrane at sites of bacterial interaction. *Cell Microbiol*. **10**: 477-486.
- Kulp, A. and Kuehn, M.J. (2010) Biological functions and biogenesis of secreted bacterial outer membrane vesicles. *Annu Rev Microbiol*. **64**: 163-184.
- Kurt-Jones, E.A., Sandor, F., Ortiz, Y., Bowen, G.N., Counter, S.L., Wang, T.C. and Finberg, R.W. (2004) Use of murine embryonic fibroblasts to define Toll-like receptor activation and specificity. *J Endotoxin Res*. **10**: 419-424.
- Laemmli, U.K. (1970) Cleavage of structural proteins during the assembly of the head of bacteriophage T4. *Nature*. **227**: 680-685.

REFERENCES

- Lagace, M., Xuan, J.Y., Young, S.S., McRoberts, C., Maier, J., Rajcan-Separovic, E. and Korneluk, R.G. (2001) Genomic organization of the X-linked inhibitor of apoptosis and identification of a novel testis-specific transcript. *Genomics*. **77**: 181-188.
- Le Bourhis, L., Benko, S. and Girardin, S.E. (2007) Nod1 and Nod2 in innate immunity and human inflammatory disorders. *Biochem Soc Trans*. **35**: 1479-1484.
- Le Bourhis, L., Magalhaes, J.G., Selvanantham, T., Travassos, L.H., Geddes, K., Fritz, J.H., *et al* (2009) Role of Nod1 in mucosal dendritic cells during Salmonella pathogenicity island 1-independent Salmonella enterica serovar Typhimurium infection. *Infect Immun*. **77**: 4480-4486.
- LeBlanc, P.M., Yeretssian, G., Rutherford, N., Doiron, K., Nadiri, A., Zhu, L., *et al* (2008) Caspase-12 modulates NOD signaling and regulates antimicrobial peptide production and mucosal immunity. *Cell Host Microbe*. **3**: 146-157.
- Lee, J., Tattoli, I., Wojtal, K.A., Vavricka, S.R., Philpott, D.J. and Girardin, S.E. (2009) pH-dependent internalization of muramyl peptides from early endosomes enables Nod1 and Nod2 signaling. *J Biol Chem*. **284**: 23818-23829.
- Legrand-Poels, S., Kustermans, G., Bex, F., Kremmer, E., Kufer, T.A. and Piette, J. (2007) Modulation of Nod2-dependent NF-kappaB signaling by the actin cytoskeleton. *J Cell Sci*. **120**: 1299-1310.
- Lenz, L.L., Mohammadi, S., Geissler, A. and Portnoy, D.A. (2003) SecA2-dependent secretion of autolytic enzymes promotes *Listeria monocytogenes* pathogenesis. *Proc Natl Acad Sci U S A*. **100**: 12432-12437.
- Leuschner, P.J., Ameres, S.L., Kueng, S. and Martinez, J. (2006) Cleavage of the siRNA passenger strand during RISC assembly in human cells. *EMBO Rep*. **7**: 314-320.
- Lindmark, B., Rompikuntal, P.K., Vaitkevicius, K., Song, T., Mizunoe, Y., Uhlin, B.E., *et al* (2009) Outer membrane vesicle-mediated release of cytolethal distending toxin (CDT) from *Campylobacter jejuni*. *BMC Microbiol*. **9**: 220.
- Litvack, M.L. and Palaniyar, N. (2010) Review: Soluble innate immune pattern-recognition proteins for clearing dying cells and cellular components: implications on exacerbating or resolving inflammation. *Innate Immun*. **16**: 191-200.
- Liu, J., Carmell, M.A., Rivas, F.V., Marsden, C.G., Thomson, J.M., Song, J.J., *et al* (2004) Argonaute2 is the catalytic engine of mammalian RNAi. *Science*. **305**: 1437-1441.
- Liu, S. and Chen, Z.J. (2011) Expanding role of ubiquitination in NF-kappaB signaling. *Cell Res*. **21**: 6-21.
- Liu, X. and Erikson, R.L. (2003) Polo-like kinase (Plk)1 depletion induces apoptosis in cancer cells. *Proc Natl Acad Sci U S A*. **100**: 5789-5794.
- Liu, X., Lei, M. and Erikson, R.L. (2006) Normal cells, but not cancer cells, survive severe Plk1 depletion. *Mol Cell Biol*. **26**: 2093-2108.
- Liu, Z., Shen, J., Pu, K., Katus, H.A., Ploger, F., Tiefenbacher, C.P., *et al* (2009) GDF5 and BMP2 inhibit apoptosis via activation of BMPR2 and subsequent stabilization of XIAP. *Biochim Biophys Acta*. **1793**: 1819-1827.
- Liu, Z., Sun, C., Olejniczak, E.T., Meadows, R.P., Betz, S.F., Oost, T., *et al* (2000) Structural basis for binding of Smac/DIABLO to the XIAP BIR3 domain. *Nature*. **408**: 1004-1008.
- Lu, M., Lin, S.C., Huang, Y., Kang, Y.J., Rich, R., Lo, Y.C., *et al* (2007) XIAP induces NF-kappaB activation via the BIR1/TAB1 interaction and BIR1 dimerization. *Mol Cell*. **26**: 689-702.
- Ma, L., Huang, Y., Song, Z., Feng, S., Tian, X., Du, W., *et al* (2006) Livin promotes Smac/DIABLO degradation by ubiquitin-proteasome pathway. *Cell Death Differ*. **13**: 2079-2088.

REFERENCES

- MacFarlane, M., Merrison, W., Bratton, S.B. and Cohen, G.M. (2002) Proteasome-mediated degradation of Smac during apoptosis: XIAP promotes Smac ubiquitination in vitro. *J Biol Chem.* **277**: 36611-36616.
- Maekawa, T., Kufer, T.A. and Schulze-Lefert, P. (2011) NLR functions in plant and animal immune systems: so far and yet so close. *Nat Immunol.* **12**: 817-826.
- Magalhaes, J.G., Fritz, J.H., Le Bourhis, L., Sellge, G., Travassos, L.H., Selvanantham, T., *et al* (2008) Nod2-dependent Th2 polarization of antigen-specific immunity. *J Immunol.* **181**: 7925-7935.
- Maniatis, T. (1999) A ubiquitin ligase complex essential for the NF-kappaB, Wnt/Wingless, and Hedgehog signaling pathways. *Genes Dev.* **13**: 505-510.
- Marina-Garcia, N., Franchi, L., Kim, Y.G., Miller, D., McDonald, C., Boons, G.J. and Nunez, G. (2008) Pannexin-1-mediated intracellular delivery of muramyl dipeptide induces caspase-1 activation via cryopyrin/NLRP3 independently of Nod2. *J Immunol.* **180**: 4050-4057.
- Marina-Garcia, N., Franchi, L., Kim, Y.G., Hu, Y., Smith, D.E., Boons, G.J. and Nunez, G. (2009) Clathrin- and dynamin-dependent endocytic pathway regulates muramyl dipeptide internalization and NOD2 activation. *J Immunol.* **182**: 4321-4327.
- Martins, L.M., Iaccarino, I., Tenev, T., Gschmeissner, S., Totty, N.F., Lemoine, N.R., *et al* (2002) The serine protease Omi/HtrA2 regulates apoptosis by binding XIAP through a reaper-like motif. *J Biol Chem.* **277**: 439-444.
- Matranga, C., Tomari, Y., Shin, C., Bartel, D.P. and Zamore, P.D. (2005) Passenger-strand cleavage facilitates assembly of siRNA into Ago2-containing RNAi enzyme complexes. *Cell.* **123**: 607-620.
- McCarthy, J.V., Ni, J. and Dixit, V.M. (1998) RIP2 is a novel NF-kappaB-activating and cell death-inducing kinase. *J Biol Chem.* **273**: 16968-16975.
- McDonald, C., Chen, F.F., Ollendorff, V., Ogura, Y., Marchetto, S., Lecine, P., *et al* (2005) A role for Erbin in the regulation of Nod2-dependent NF-kappaB signaling. *J Biol Chem.* **280**: 40301-40309.
- McGovern, D.P., Hysi, P., Ahmad, T., van Heel, D.A., Moffatt, M.F., Carey, A., *et al* (2005) Association between a complex insertion/deletion polymorphism in NOD1 (CARD4) and susceptibility to inflammatory bowel disease. *Hum Mol Genet.* **14**: 1245-1250.
- Medzhitov, R. (2007) Recognition of microorganisms and activation of the immune response. *Nature.* **449**: 819-826.
- Medzhitov, R. and Janeway, C.A., Jr. (1997) Innate immunity: the virtues of a nonclonal system of recognition. *Cell.* **91**: 295-298.
- Meylan, E., Tschopp, J. and Karin, M. (2006) Intracellular pattern recognition receptors in the host response. *Nature.* **442**: 39-44.
- Miller, M.B., Skorupski, K., Lenz, D.H., Taylor, R.K. and Bassler, B.L. (2002) Parallel quorum sensing systems converge to regulate virulence in *Vibrio cholerae*. *Cell.* **110**: 303-314.
- Miyazono, K., Maeda, S. and Imamura, T. (2005) BMP receptor signaling: transcriptional targets, regulation of signals, and signaling cross-talk. *Cytokine Growth Factor Rev.* **16**: 251-263.
- Moffat, J. and Sabatini, D.M. (2006) Building mammalian signalling pathways with RNAi screens. *Nat Rev Mol Cell Biol.* **7**: 177-187.
- Morizane, Y., Honda, R., Fukami, K. and Yasuda, H. (2005) X-linked inhibitor of apoptosis functions as ubiquitin ligase toward mature caspase-9 and cytosolic Smac/DIABLO. *J Biochem.* **137**: 125-132.

REFERENCES

- Muller, P., Kuttenkeuler, D., Gesellchen, V., Zeidler, M.P. and Boutros, M. (2005) Identification of JAK/STAT signalling components by genome-wide RNA interference. *Nature*. **436**: 871-875.
- Munoz, E., Courtois, G., Veschambre, P., Jalinot, P. and Israel, A. (1994) Tax induces nuclear translocation of NF-kappa B through dissociation of cytoplasmic complexes containing p105 or p100 but does not induce degradation of I kappa B alpha/MAD3. *J Virol*. **68**: 8035-8044.
- Muzio, M., Stockwell, B.R., Stennicke, H.R., Salvesen, G.S. and Dixit, V.M. (1998) An induced proximity model for caspase-8 activation. *J Biol Chem*. **273**: 2926-2930.
- Myers, J.W., Jones, J.T., Meyer, T. and Ferrell, J.E., Jr. (2003) Recombinant Dicer efficiently converts large dsRNAs into siRNAs suitable for gene silencing. *Nat Biotechnol*. **21**: 324-328.
- Nicholson, D.W. (1999) Caspase structure, proteolytic substrates, and function during apoptotic cell death. *Cell Death Differ*. **6**: 1028-1042.
- Nigro, G., Fazio, L.L., Martino, M.C., Rossi, G., Tattoli, I., Liparoti, V., et al (2008) Muramylpeptide shedding modulates cell sensing of Shigella flexneri. *Cell Microbiol*. **10**: 682-695.
- Nohe, A., Hassel, S., Ehrlich, M., Neubauer, F., Sebald, W., Henis, Y.I. and Knaus, P. (2002) The mode of bone morphogenetic protein (BMP) receptor oligomerization determines different BMP-2 signaling pathways. *J Biol Chem*. **277**: 5330-5338.
- Ogura, Y., Inohara, N., Benito, A., Chen, F.F., Yamaoka, S. and Nunez, G. (2001) Nod2, a Nod1/Apaf-1 family member that is restricted to monocytes and activates NF-kappaB. *J Biol Chem*. **276**: 4812-4818.
- Ogura, Y., Lala, S., Xin, W., Smith, E., Dowds, T.A., Chen, F.F., et al (2003) Expression of NOD2 in Paneth cells: a possible link to Crohn's ileitis. *Gut*. **52**: 1591-1597.
- Opitz, B., Forster, S., Hocke, A.C., Maass, M., Schmeck, B., Hippenstiel, S., et al (2005) Nod1-mediated endothelial cell activation by Chlamydomphila pneumoniae. *Circ Res*. **96**: 319-326.
- Opitz, B., Puschel, A., Schmeck, B., Hocke, A.C., Rosseau, S., Hammerschmidt, S., et al (2004) Nucleotide-binding oligomerization domain proteins are innate immune receptors for internalized Streptococcus pneumoniae. *J Biol Chem*. **279**: 36426-36432.
- Opitz, B., Puschel, A., Beermann, W., Hocke, A.C., Forster, S., Schmeck, B., et al (2006) Listeria monocytogenes activated p38 MAPK and induced IL-8 secretion in a nucleotide-binding oligomerization domain 1-dependent manner in endothelial cells. *J Immunol*. **176**: 484-490.
- Pan, Q., Kravchenko, V., Katz, A., Huang, S., Li, M., Mathison, J.C., et al (2006) NF-kappa B-inducing kinase regulates selected gene expression in the Nod2 signaling pathway. *Infect Immun*. **74**: 2121-2127.
- Pan, Q., Mathison, J., Fearn, C., Kravchenko, V.V., Da Silva Correia, J., Hoffman, H.M., et al (2007) MDP-induced interleukin-1beta processing requires Nod2 and CIAS1/NALP3. *J Leukoc Biol*. **82**: 177-183.
- Pandey, A.K., Yang, Y., Jiang, Z., Fortune, S.M., Coulombe, F., Behr, M.A., et al (2009) NOD2, RIP2 and IRF5 play a critical role in the type I interferon response to Mycobacterium tuberculosis. *PLoS Pathog*. **5**: e1000500.
- Park, J.T. and Uehara, T. (2008) How bacteria consume their own exoskeletons (turnover and recycling of cell wall peptidoglycan). *Microbiol Mol Biol Rev*. **72**: 211-227, table of contents.
- Petnicki-Ocwieja, T., Hrcir, T., Liu, Y.J., Biswas, A., Hudcovic, T., Tlaskalova-Hogenova, H. and Kobayashi, K.S. (2009) Nod2 is required for the regulation of commensal microbiota in the intestine. *Proc Natl Acad Sci U S A*. **106**: 15813-15818.
- Pohl, C. and Jentsch, S. (2008) Final stages of cytokinesis and midbody ring formation are controlled by BRUCE. *Cell*. **132**: 832-845.

REFERENCES

- Ramjeet, M., Hussey, S., Philpott, D.J. and Travassos, L.H. (2010) 'Nodophagy': New crossroads in Crohn disease pathogenesis. *Gut Microbes*. **1**: 307-315.
- Ratner, A.J., Aguilar, J.L., Shchepetov, M., Lysenko, E.S. and Weiser, J.N. (2007) Nod1 mediates cytoplasmic sensing of combinations of extracellular bacteria. *Cell Microbiol*. **9**: 1343-1351.
- Raupach, B. and Kaufmann, S.H. (2001) Immune responses to intracellular bacteria. *Curr Opin Immunol*. **13**: 417-428.
- Raychaudhuri, S., Jain, V. and Dongre, M. (2006) Identification of a constitutively active variant of LuxO that affects production of HA/protease and biofilm development in a non-O1, non-O139 *Vibrio cholerae* O110. *Gene*. **369**: 126-133.
- Regueiro, V., Moranta, D., Frank, C.G., Larrarte, E., Margareto, J., March, C., *et al* (2011) *Klebsiella pneumoniae* subverts the activation of inflammatory responses in a NOD1-dependent manner. *Cell Microbiol*. **13**: 135-153.
- Renelli, M., Matias, V., Lo, R.Y. and Beveridge, T.J. (2004) DNA-containing membrane vesicles of *Pseudomonas aeruginosa* PAO1 and their genetic transformation potential. *Microbiology*. **150**: 2161-2169.
- Richter, B.W., Mir, S.S., Eiben, L.J., Lewis, J., Reffey, S.B., Frattini, A., *et al* (2001) Molecular cloning of ILP-2, a novel member of the inhibitor of apoptosis protein family. *Mol Cell Biol*. **21**: 4292-4301.
- Riedl, S.J. and Salvesen, G.S. (2007) The apoptosome: signalling platform of cell death. *Nat Rev Mol Cell Biol*. **8**: 405-413.
- Riedl, S.J., Renatus, M., Schwarzenbacher, R., Zhou, Q., Sun, C., Fesik, S.W., *et al* (2001) Structural basis for the inhibition of caspase-3 by XIAP. *Cell*. **104**: 791-800.
- Rigaud, S., Fondaneche, M.C., Lambert, N., Pasquier, B., Mateo, V., Soulas, P., *et al* (2006) XIAP deficiency in humans causes an X-linked lymphoproliferative syndrome. *Nature*. **444**: 110-114.
- Romano, N. and Macino, G. (1992) Quelling: transient inactivation of gene expression in *Neurospora crassa* by transformation with homologous sequences. *Mol Microbiol*. **6**: 3343-3353.
- Rosenstiel, P., Till, A. and Schreiber, S. (2007) NOD-like receptors and human diseases. *Microbes Infect*. **9**: 648-657.
- Rothe, M., Pan, M.G., Henzel, W.J., Ayres, T.M. and Goeddel, D.V. (1995) The TNFR2-TRAF signaling complex contains two novel proteins related to baculoviral inhibitor of apoptosis proteins. *Cell*. **83**: 1243-1252.
- Roy, N., Deveraux, Q.L., Takahashi, R., Salvesen, G.S. and Reed, J.C. (1997) The c-IAP-1 and c-IAP-2 proteins are direct inhibitors of specific caspases. *Embo J*. **16**: 6914-6925.
- Sah, N.K., Khan, Z., Khan, G.J. and Bisen, P.S. (2006) Structural, functional and therapeutic biology of survivin. *Cancer Lett*. **244**: 164-171.
- Salvesen, G.S. and Duckett, C.S. (2002) IAP proteins: blocking the road to death's door. *Nat Rev Mol Cell Biol*. **3**: 401-410.
- Sanchez, J. and Holmgren, J. (2008) Cholera toxin structure, gene regulation and pathophysiological and immunological aspects. *Cell Mol Life Sci*. **65**: 1347-1360.
- Sanna, M.G., Duckett, C.S., Richter, B.W., Thompson, C.B. and Ulevitch, R.J. (1998) Selective activation of JNK1 is necessary for the anti-apoptotic activity of hILP. *Proc Natl Acad Sci U S A*. **95**: 6015-6020.

REFERENCES

- Sanna, M.G., da Silva Correia, J., Ducrey, O., Lee, J., Nomoto, K., Schrantz, N., *et al* (2002) IAP suppression of apoptosis involves distinct mechanisms: the TAK1/JNK1 signaling cascade and caspase inhibition. *Mol Cell Biol.* **22**: 1754-1766.
- Schild, S., Nelson, E.J. and Camilli, A. (2008) Immunization with *Vibrio cholerae* outer membrane vesicles induces protective immunity in mice. *Infect Immun.* **76**: 4554-4563.
- Schroder, K. and Tschopp, J. (2010) The inflammasomes. *Cell.* **140**: 821-832.
- Seeger, J.M., Brinkmann, K., Yazdanpanah, B., Haubert, D., Pongratz, C., Coutelle, O., *et al* (2010) Elevated XIAP expression alone does not confer chemoresistance. *Br J Cancer.* **102**: 1717-1723.
- Selsted, M.E. and Ouellette, A.J. (2005) Mammalian defensins in the antimicrobial immune response. *Nat Immunol.* **6**: 551-557.
- Shahin, R.D., Engberg, I., Hagberg, L. and Svanborg Eden, C. (1987) Neutrophil recruitment and bacterial clearance correlated with LPS responsiveness in local gram-negative infection. *J Immunol.* **138**: 3475-3480.
- Sharma, M., Machuy, N., Bohme, L., Karunakaran, K., Maurer, A.P., Meyer, T.F. and Rudel, T. (2011) HIF-1alpha is involved in mediating apoptosis resistance to *Chlamydia trachomatis*-infected cells. *Cell Microbiol.* **13**: 1573-1585.
- Shin, H., Renatus, M., Eckelman, B.P., Nunes, V.A., Sampaio, C.A. and Salvesen, G.S. (2005) The BIR domain of IAP-like protein 2 is conformationally unstable: implications for caspase inhibition. *Biochem J.* **385**: 1-10.
- Singh, S., Narang, A.S. and Mahato, R.I. (2011) Subcellular fate and off-target effects of siRNA, shRNA, and miRNA. *Pharm Res.* **28**: 2996-3015.
- Skoufias, D.A., Mollinari, C., Lacroix, F.B. and Margolis, R.L. (2000) Human survivin is a kinetochore-associated passenger protein. *J Cell Biol.* **151**: 1575-1582.
- Song, Z., Yao, X. and Wu, M. (2003) Direct interaction between survivin and Smac/DIABLO is essential for the anti-apoptotic activity of survivin during taxol-induced apoptosis. *J Biol Chem.* **278**: 23130-23140.
- Srinivasula, S.M. and Ashwell, J.D. (2008) IAPs: what's in a name? *Mol Cell.* **30**: 123-135.
- Srinivasula, S.M., Gupta, S., Datta, P., Zhang, Z., Hegde, R., Cheong, N., *et al* (2003) Inhibitor of apoptosis proteins are substrates for the mitochondrial serine protease Omi/HtrA2. *J Biol Chem.* **278**: 31469-31472.
- Suzuki, Y., Nakabayashi, Y. and Takahashi, R. (2001) Ubiquitin-protein ligase activity of X-linked inhibitor of apoptosis protein promotes proteasomal degradation of caspase-3 and enhances its anti-apoptotic effect in Fas-induced cell death. *Proc Natl Acad Sci U S A.* **98**: 8662-8667.
- Svoboda, P. (2007) Off-targeting and other non-specific effects of RNAi experiments in mammalian cells. *Curr Opin Mol Ther.* **9**: 248-257.
- Swaan, P.W., Bensman, T., Bahadduri, P.M., Hall, M.W., Sarkar, A., Bao, S., *et al* (2008) Bacterial peptide recognition and immune activation facilitated by human peptide transporter PEPT2. *Am J Respir Cell Mol Biol.* **39**: 536-542.
- Tada, H., Aiba, S., Shibata, K., Ohteki, T. and Takada, H. (2005) Synergistic effect of Nod1 and Nod2 agonists with toll-like receptor agonists on human dendritic cells to generate interleukin-12 and T helper type 1 cells. *Infect Immun.* **73**: 7967-7976.
- Takeuchi, O. and Akira, S. (2010) Pattern Recognition Receptors and Inflammation *Cell* **140**: 805-820.

REFERENCES

- Tamm, I., Wang, Y., Sausville, E., Scudiero, D.A., Vigna, N., Oltersdorf, T. and Reed, J.C. (1998) IAP-family protein survivin inhibits caspase activity and apoptosis induced by Fas (CD95), Bax, caspases, and anticancer drugs. *Cancer Res.* **58**: 5315-5320.
- Tanabe, T., Chamaillard, M., Ogura, Y., Zhu, L., Qiu, S., Masumoto, J., *et al* (2004) Regulatory regions and critical residues of NOD2 involved in muramyl dipeptide recognition. *Embo J.* **23**: 1587-1597.
- Tao, M., Scacheri, P.C., Marinis, J.M., Harhaj, E.W., Matesic, L.E. and Abbott, D.W. (2009) ITC63 ubiquitinates the NOD2 binding protein, RIP2, to influence inflammatory signaling pathways. *Curr Biol.* **19**: 1255-1263.
- Traub, S., Kubasch, N., Morath, S., Kresse, M., Hartung, T., Schmidt, R.R. and Hermann, C. (2004) Structural requirements of synthetic muropeptides to synergize with lipopolysaccharide in cytokine induction. *J Biol Chem.* **279**: 8694-8700.
- Travassos, L.H., Carneiro, L.A., Ramjeet, M., Hussey, S., Kim, Y.G., Magalhaes, J.G., *et al* (2010) Nod1 and Nod2 direct autophagy by recruiting ATG16L1 to the plasma membrane at the site of bacterial entry. *Nat Immunol.* **11**: 55-62.
- Tseng, P.H., Matsuzawa, A., Zhang, W., Mino, T., Vignali, D.A. and Karin, M. (2010) Different modes of ubiquitination of the adaptor TRAF3 selectively activate the expression of type I interferons and proinflammatory cytokines. *Nat Immunol.* **11**: 70-75.
- Tsuchiya, S., Yamabe, M., Yamaguchi, Y., Kobayashi, Y., Konno, T. and Tada, K. (1980) Establishment and characterization of a human acute monocytic leukemia cell line (THP-1). *Int J Cancer.* **26**: 171-176.
- Uehara, A., Fujimoto, Y., Fukase, K. and Takada, H. (2007) Various human epithelial cells express functional Toll-like receptors, NOD1 and NOD2 to produce anti-microbial peptides, but not proinflammatory cytokines. *Mol Immunol.* **44**: 3100-3111.
- Uehara, A., Yang, S., Fujimoto, Y., Fukase, K., Kusumoto, S., Shibata, K., *et al* (2005) Muramyl dipeptide and diamino pimelic acid-containing desmuramyl peptides in combination with chemically synthesized Toll-like receptor agonists synergistically induced production of interleukin-8 in a NOD2- and NOD1-dependent manner, respectively, in human monocytic cells in culture. *Cell Microbiol.* **7**: 53-61.
- Unterholzner, L., Keating, S.E., Baran, M., Horan, K.A., Jensen, S.B., Sharma, S., *et al* (2010) IFI16 is an innate immune sensor for intracellular DNA. *Nat Immunol.* **11**: 997-1004.
- Uren, A.G., Coulson, E.J. and Vaux, D.L. (1998) Conservation of baculovirus inhibitor of apoptosis repeat proteins (BIRPs) in viruses, nematodes, vertebrates and yeasts. *Trends Biochem Sci.* **23**: 159-162.
- Uren, A.G., Wong, L., Pakusch, M., Fowler, K.J., Burrows, F.J., Vaux, D.L. and Choo, K.H. (2000) Survivin and the inner centromere protein INCENP show similar cell-cycle localization and gene knockout phenotype. *Curr Biol.* **10**: 1319-1328.
- Vaitkevicius, K., Lindmark, B., Ou, G., Song, T., Toma, C., Iwanaga, M., *et al* (2006) A *Vibrio cholerae* protease needed for killing of *Caenorhabditis elegans* has a role in protection from natural predator grazing. *Proc Natl Acad Sci U S A.* **103**: 9280-9285.
- Valanne, S., Wang, J.H. and Ramet, M. (2011) The *Drosophila* Toll signaling pathway. *J Immunol.* **186**: 649-656.
- van Heel, D.A., Ghosh, S., Butler, M., Hunt, K., Foxwell, B.M., Mengin-Lecreulx, D. and Playford, R.J. (2005) Synergistic enhancement of Toll-like receptor responses by NOD1 activation. *Eur J Immunol.* **35**: 2471-2476.
- Vance, R.E., Zhu, J. and Mekalanos, J.J. (2003) A constitutively active variant of the quorum-sensing regulator LuxO affects protease production and biofilm formation in *Vibrio cholerae*. *Infect Immun.* **71**: 2571-2576.

REFERENCES

- Vaux, D.L. and Silke, J. (2005) IAPs--the ubiquitin connection. *Cell Death Differ.* **12**: 1205-1207.
- Vavricka, S.R., Musch, M.W., Chang, J.E., Nakagawa, Y., Phanvijhitsiri, K., Waypa, T.S., *et al* (2004) hPepT1 transports muramyl dipeptide, activating NF-kappaB and stimulating IL-8 secretion in human colonic Caco2/bbe cells. *Gastroenterology.* **127**: 1401-1409.
- Verhagen, A.M., Coulson, E.J. and Vaux, D.L. (2001) Inhibitor of apoptosis proteins and their relatives: IAPs and other BIRPs. *Genome Biol.* **2**: REVIEWS3009.
- Verhagen, A.M., Silke, J., Ekert, P.G., Pakusch, M., Kaufmann, H., Connolly, L.M., *et al* (2002) HtrA2 promotes cell death through its serine protease activity and its ability to antagonize inhibitor of apoptosis proteins. *J Biol Chem.* **277**: 445-454.
- Viala, J., Chaput, C., Boneca, I.G., Cardona, A., Girardin, S.E., Moran, A.P., *et al* (2004) Nod1 responds to peptidoglycan delivered by the Helicobacter pylori cag pathogenicity island. *Nat Immunol.* **5**: 1166-1174.
- Voss, E., Wehkamp, J., Wehkamp, K., Stange, E.F., Schroder, J.M. and Harder, J. (2006) NOD2/CARD15 mediates induction of the antimicrobial peptide human beta-defensin-2. *J Biol Chem.* **281**: 2005-2011.
- Vucic, D., Franklin, M.C., Wallweber, H.J., Das, K., Eckelman, B.P., Shin, H., *et al* (2005) Engineering ML-IAP to produce an extraordinarily potent caspase 9 inhibitor: implications for Smac-dependent anti-apoptotic activity of ML-IAP. *Biochem J.* **385**: 11-20.
- Wai, S.N., Lindmark, B., Soderblom, T., Takade, A., Westermarck, M., Oscarsson, J., *et al* (2003) Vesicle-mediated export and assembly of pore-forming oligomers of the enterobacterial ClyA cytotoxin. *Cell.* **115**: 25-35.
- Welter-Stahl, L., Ojcius, D.M., Viala, J., Girardin, S., Liu, W., Delarbre, C., *et al* (2006) Stimulation of the cytosolic receptor for peptidoglycan, Nod1, by infection with Chlamydia trachomatis or Chlamydia muridarum. *Cell Microbiol.* **8**: 1047-1057.
- Werts, C., le Bourhis, L., Liu, J., Magalhaes, J.G., Carneiro, L.A., Fritz, J.H., *et al* (2007) Nod1 and Nod2 induce CCL5/RANTES through the NF-kappaB pathway. *Eur J Immunol.* **37**: 2499-2508.
- Wilmanski, J.M., Petnicki-Ocwieja, T. and Kobayashi, K.S. (2008) NLR proteins: integral members of innate immunity and mediators of inflammatory diseases. *J Leukoc Biol.* **83**: 13-30.
- Windheim, M., Lang, C., Peggie, M., Plater, L.A. and Cohen, P. (2007) Molecular mechanisms involved in the regulation of cytokine production by muramyl dipeptide. *Biochem J.* **404**: 179-190.
- Wu, G., Chai, J., Suber, T.L., Wu, J.W., Du, C., Wang, X. and Shi, Y. (2000) Structural basis of IAP recognition by Smac/DIABLO. *Nature.* **408**: 1008-1012.
- Yamaguchi, K., Nagai, S., Ninomiya-Tsuji, J., Nishita, M., Tamai, K., Irie, K., *et al* (1999) XIAP, a cellular member of the inhibitor of apoptosis protein family, links the receptors to TAB1-TAK1 in the BMP signaling pathway. *Embo J.* **18**: 179-187.
- Yamamoto-Furusho, J.K., Barnich, N., Xavier, R., Hisamatsu, T. and Podolsky, D.K. (2006) Centaurin beta1 down-regulates nucleotide-binding oligomerization domains 1- and 2-dependent NF-kappaB activation. *J Biol Chem.* **281**: 36060-36070.
- Yang, Q.H. and Du, C. (2004) Smac/DIABLO selectively reduces the levels of c-IAP1 and c-IAP2 but not that of XIAP and livin in HeLa cells. *J Biol Chem.* **279**: 16963-16970.
- Yang, Q.H., Church-Hajduk, R., Ren, J., Newton, M.L. and Du, C. (2003) Omi/HtrA2 catalytic cleavage of inhibitor of apoptosis (IAP) irreversibly inactivates IAPs and facilitates caspase activity in apoptosis. *Genes Dev.* **17**: 1487-1496.

REFERENCES

- Yeretssian, G., Correa, R.G., Doiron, K., Fitzgerald, P., Dillon, C.P., Green, D.R., *et al* (2011) Non-apoptotic role of BID in inflammation and innate immunity. *Nature*. **474**: 96-99.
- Yuan, S., Yu, X., Asara, J.M., Heuser, J.E., Ludtke, S.J. and Akey, C.W. (2011) The holo-apoptosome: activation of procaspase-9 and interactions with caspase-3. *Structure*. **19**: 1084-1096.
- Zamore, P.D., Tuschl, T., Sharp, P.A. and Bartel, D.P. (2000) RNAi: double-stranded RNA directs the ATP-dependent cleavage of mRNA at 21 to 23 nucleotide intervals. *Cell*. **101**: 25-33.
- Zhang, J., Stirling, B., Temmerman, S.T., Ma, C.A., Fuss, I.J., Derry, J.M. and Jain, A. (2006) Impaired regulation of NF-kappaB and increased susceptibility to colitis-associated tumorigenesis in CYLD-deficient mice. *J Clin Invest*. **116**: 3042-3049.
- Zhang, J.H., Chung, T.D. and Oldenburg, K.R. (1999) A Simple Statistical Parameter for Use in Evaluation and Validation of High Throughput Screening Assays. *J Biomol Screen*. **4**: 67-73.
- Zhao, Y., Yang, J., Shi, J., Gong, Y.N., Lu, Q., Xu, H., *et al* (2011) The NLRC4 inflammasome receptors for bacterial flagellin and type III secretion apparatus. *Nature*. **477**: 596-600.
- Zhu, J., Miller, M.B., Vance, R.E., Dziejman, M., Bassler, B.L. and Mekalanos, J.J. (2002) Quorum-sensing regulators control virulence gene expression in *Vibrio cholerae*. *Proc Natl Acad Sci U S A*. **99**: 3129-3134.
- Zurek, B., Proell, M., Wagner, R.N., Schwarzenbacher, R. and Kufer, T.A. (2012) Mutational analysis of human NOD1 and NOD2 NACHT domains reveals different modes of activation. *Innate Immun*. **18**: 100-111.

6 Abstract

Many Members of the intracellular nucleotide binding and oligomerisation domain (NOD)-like receptor (NLR) family have functions in the innate immune system. The NLR NOD1 acts as pattern recognition receptor and confers immune responses against a broad range of bacteria by triggering NF- κ B and MAPK signalling cascades upon detection of bacterial peptidoglycan. This contributes to bacterial clearance, to the onset of a pro-inflammatory immune response and the release of anti-microbial peptides. As overwhelming inflammatory responses can be detrimental to the host, inflammatory signalling cascades have to be tightly controlled. Even though the main components of the NOD1 signalling cascade are identified, little is known about the regulation and fine-tuning so far.

In this project, we identified novel components of the NOD1 signalling pathway by an automated high-throughput siRNA screen using a cell based NF- κ B reporter system in epithelial HEK293T cells. To this end, we screened the human druggable genome siRNA library for NOD1-mediated NF- κ B activation upon stimulation with the elicitor Tri-DAP. Hits specifically involved in NOD1-mediated NF- κ B activation were identified using TNF- α -stimulation as differential read-out. Finally, these hits were validated in myeloid THP1 cells. Beside the established NOD1 pathway component RIP2, the combined screening steps identified the BIRC family member XIAP as the strongest inhibiting hit. Follow-up experiments confirmed XIAP as an essential component of NOD1-mediated responses to the minimal NOD1 elicitor and to *Shigella flexneri*. We also revealed that XIAP contributes to responses mediated by the closely related NOD2 protein. In line with a recent report, we provide evidence that XIAP acts upstream of the IKK complex in the NOD1 signalling cascade.

Strikingly, the screen revealed that the type II BMP receptor BMPR-2 is specifically involved in NOD1 signalling. Further experiments confirmed these findings and revealed that BMPR-2 positively regulates NOD1 signalling, likely by contributing to stabilisation of XIAP.

Furthermore, we analysed the contributions of the BIRC proteins BIRC2 and BIRC3, which are closely related to XIAP, and of the other human BIRC proteins to NOD1-mediated responses. By using siRNA-mediated gene knock-down, we confirmed that BIRC2 positively regulates NOD1 signalling. Furthermore, we provide evidence that also BIRC5 and BIRC8, which have not been linked to innate immunity so far, positively contribute to NOD1-mediated inflammatory responses.

ABSTRACT

Another event in NOD signalling that is still not fully understood is how bacterial peptidoglycan is translocated to the cytoplasm of host cells, as extracellular bacteria are known to activate NOD1 as well as NOD2. In the second part of this project, we analysed if bacterial outer-membrane vesicles (OMVs) might serve as carriers for peptidoglycan. We provide clear evidence that OMVs derived from the extracellular pathogen *Vibrio cholerae* are internalised by host cells, contain peptidoglycan and trigger NOD1- and NOD2-dependent inflammatory responses. OMVs derived from bacteria deficient for HapR, a master regulator of quorum sensing that represses the expression of virulence genes, induced markedly lower NOD-mediated inflammatory responses than OMVs derived from WT bacteria. In contrast, the overall peptidoglycan composition and the inflammatory potential of bacterial lysates derived from $\Delta hapR$ compared to WT bacteria did not change. We conclude that *V. cholerae* uses quorum sensing to influence the peptidoglycan content of OMVs, to prevent detection by the host innate immune system under virulent conditions.

7 Zusammenfassung

Viele Mitglieder der intrazellulären Nukleotid-binde und oligomerisierungsdomäne (NOD) ähnlichen Rezeptor (NLR) Familie erfüllen Funktionen im angeborenen Immunsystem. Das NLR Protein NOD1 fungiert als Mustererkennungs-Rezeptor und vermittelt Immunantworten gegen ein breites Spektrum von Bakterien durch Erkennen von bakteriellem Peptidoglykan und anschließender Aktivierung von NF- κ B und MAP-Kinase Signaltransduktionskaskaden. Dies trägt zur Beseitigung der Bakterien, zur Induktion einer entzündlichen Immunantwort sowie zur Expression von antimikrobiellen Peptiden bei. Da überbordende Immunantworten schädlich für den Wirt sein können, müssen derartige inflammatorische Signaltransduktionskaskaden strikt reguliert werden. Obwohl die Hauptkomponenten der NOD1 Signaltransduktionskaskade bekannt sind, ist wenig über die Regulation und die Feinabstimmung dieses Signalweges bekannt.

In diesem Projekt haben wir mittels eines automatisierten Hochdurchsatz siRNA Screens unter Verwendung eines zellbasierten NF- κ B Reportersystems in epithelialen HEK293T Zellen neue Komponenten des NOD1 Signalweges identifiziert. Zu diesem Zweck wurde eine humane „Druggable Genome“ siRNA Bibliothek im Hinblick auf NOD1-vermittelte NF- κ B Aktivierung induziert durch den Elicitor Tri-DAP untersucht. Kandidaten, die spezifisch im NOD1 Signalweg eine Rolle spielen, wurden durch ein differentielles Auslesen mittels TNF- α -Stimulation identifiziert. Abschließend wurden diese Kandidaten in myeloiden THP1 Zellen bestätigt. Neben der Komponente RIP2, welche bekannt dafür ist, eine regulatorische Funktion im NOD1 Signalweg auszuüben, haben wir XIAP, ein Mitglied der BIRC Familie, als stärksten Kandidaten identifiziert. Anschließende Experimente konnten XIAP als essentielle Komponente für NOD1-vermittelte Antworten auf den minimalen NOD1-Elicitor sowie auf *Shigella flexneri* Infektion bestätigen. Darüber hinaus konnten wir zeigen, dass XIAP oberhalb des IKK Komplexes im NOD1 Signalweg agiert und dass XIAP auch in Immunantworten vermittelt durch das verwandte Protein NOD2 eine wichtige Rolle spielt.

Interessanterweise hat der Screen auch gezeigt, dass der Typ II BMP Rezeptor BMPR-2 spezifisch in den NOD1 Signalweg involviert ist. Diese Hinweise wurden durch anschließende Experimente bestätigt: Es erscheint sehr wahrscheinlich, dass BMPR-2 eine positive regulatorische Funktion im NOD1 Signalweg ausübt, wahrscheinlich durch einen Beitrag zur Stabilisierung von XIAP.

Darüber hinaus haben wir die Einflüsse der BIRC Proteine BIRC2 und BIRC3, welche eine enge Verwandtschaft zu XIAP aufweisen, sowie der anderen humanen BIRC Proteine auf NOD1-vermittelte Antworten untersucht. Durch siRNA-vermittelte Depletion konnten wir

ZUSAMMENFASSUNG

bestätigen, dass BIRC2 eine positive regulatorische Funktion auf NOD1-vermittelte Signalwege ausübt. Ausserdem liefern wir Hinweise dafür, dass auch BIRC5 und BIRC8, die bisher noch nicht mit angeborener Immunität in Verbindung gebracht wurden, zur Positivregulation von NOD1-vermittelten Antworten beitragen.

Ein weiterer wichtiger Prozess in NOD-vermittelten Immunantworten, der bisher nicht vollständig verstanden ist, ist die Aufnahme von bakteriellem Peptidoglykan in Wirtszellen, da auch extrazelluläre Bakterien bekannt dafür sind, NOD1- sowie NOD2-vermittelte Immunantworten auszulösen. Im zweiten Teil dieses Projektes haben wir untersucht, ob bakterielle Vesikel der äußeren Membran („outer-membrane Vesicles“ (OMVs)) als Überträger von Peptidoglykan dienen können. Wir haben klare Hinweise dafür gefunden, dass OMVs, die aus dem extrazellulären Pathogen *Vibrio cholerae* gewonnen wurden, von Wirtszellen aufgenommen werden, Peptidoglykan enthalten sowie NOD1- und NOD2-vermittelte entzündliche Antworten auslösen. OMVs von *V. cholerae* Bakterien defizient für HapR, einen Hauptregulator des Quorum Sensings welcher die Expression von Virulenzgenen unterdrückt, hingegen lösten deutlich geringere NOD-vermittelte entzündliche Antworten aus als OMVs von Wildtyp Bakterien. Im Gegensatz dazu waren die gesammte Zusammensetzung des Peptidoglykans und das entzündliche Potential von bakteriellen Lysaten von $\Delta hapR$ Bakterien im Vergleich zu Lysaten von Wildtyp Bakterien nicht verändert. Wir schließen daraus, dass *Vibrio cholerae* den Quorum Sensing Prozess verwendet, um den Peptidoglykangehalt von OMVs zu beeinflussen und damit einer Entdeckung durch das angeborene Immunsystem des Wirtes zu entgehen.

Danksagung

Mein besonderer Dank gilt Dr. Thomas Kufer für die ausgezeichnete Betreuung, seine stete Hilfsbereitschaft und Einsatzbereitschaft, die vielen interessanten Diskussionen und Anregungen, das Korrekturlesen meiner Arbeit und für die Möglichkeit, in seiner Arbeitsgruppe meine Doktorarbeit anzufertigen.

Ich danke meinem Doktorvater Prof. Dr. Jonathan Howard für hilfreiche Diskussionen und Ratschläge und für die Erstkorrektur und Begutachtung meiner Arbeit.

Prof. Dr. Mats Paulsson danke ich für hilfreiche Diskussionen und Ratschläge sowie für die Zweitkorrektur und Begutachtung meiner Arbeit.

Prof. Dr. Hans-Günther Schmalz danke ich für Übernahme des Vorsitzes bei meiner mündlichen Prüfung und für die gute Zusammenarbeit.

Bei Dr. Peter Braun bedanke ich mich für die angenehme Zusammenarbeit, die erfolgreiche Durchführung des Screens, für hilfreiche Diskussionen über Datenanalyse und die gute Betreuung während meiner Zeit in Berlin. Prof. Dr. Thomas Meyer danke ich für die Betreuung des Projektes.

Dr. Hamid Kashkar und Maria Andree danke ich für die gute Zusammenarbeit während des XIAP Projektes.

Prof. Dr. Sun Nyunt Wai danke ich für die erfolgreiche Zusammenarbeit während des OMV Projektes.

Der AG Kufer - Andi, Maureen, Birte, Anna D. und Christine - danke ich für die gute gemeinsame Zeit, das angenehme Arbeitsumfeld, die gute Zusammenarbeit und die große Hilfsbereitschaft. Ausserdem möchte ich mich bei meinen ehemaligen Kolleginnen Katja, Helen, Anna K. und Katharina für die gute Zusammenarbeit bedanken.

Meinem Bruder Torsten danke ich für das Korrekturlesen meiner Arbeit und meinen Eltern und meiner Freundin Bettina für ihre stete Unterstützung.

Erklärung

Ich versichere, dass ich die von mir vorgelegte Dissertation selbstständig angefertigt, die benutzten Quellen und Hilfsmittel vollständig angegeben und die Stellen der Arbeit – einschließlich Tabellen, Karten und Abbildungen –, die anderen Werken im Wortlaut oder dem Sinn nach entnommen sind, in jedem Einzelfall als Entlehnung kenntlich gemacht habe; dass diese Dissertation noch keiner anderen Fakultät oder Universität zur Prüfung vorgelegen hat; dass sie – abgesehen von unten angegebenen Teilpublikationen – noch nicht veröffentlicht worden ist sowie, dass ich eine solche Veröffentlichung vor Abschluss des Promotionsverfahrens nicht vornehmen werde.

Die Bestimmungen der Promotionsordnung sind mir bekannt. Die von mir vorgelegte Dissertation ist von Prof. Dr. Jonathan Howard und Prof. Dr. Mats Paulsson betreut worden.

Teilpublikationen:

A role for quorum sensing in regulating innate immune responses mediated by bacterial outer membrane vesicles (OMVs). **Bielig H**, Dongre M, Zurek B, Wai SN and Kufer TA. *Gut Microbes*. 2011 Sep 1;2(5). [Epub ahead of print]

Cell-Based Reporter Assay to Analyze Activation of Nod1 and Nod2. Zurek B, **Bielig H**, Kufer TA. *Methods Mol Biol*. 2011;748:107-119. PMID: 21701969

NOD-like receptor activation by outer-membrane vesicles (OMVs) from non-O1 non-O139 *Vibrio cholerae* is modulated by the quorum sensing regulator HapR. **Bielig H**, Rompikuntal PK, Mitesh D, Zurek B, Lindmark B, Ramstedt M, Wai SN and Kufer TA. *Infect Immun*. 2011 Apr;79(4):1418-27. Epub 2011 Jan 24.

Kollaborationserklärung

Das siRNA Screening-Projekt wurde in Kollaboration mit dem Max Planck Institut für Infektionsbiologie (MPIIB) in Berlin, Abteilung Molekulare Biologie (Prof. Dr. Thomas F. Meyer), durchgeführt. Die Beiträge der Kollaborationspartner sind in den jeweiligen Textpassagen kenntlich gemacht.

Das *Vibrio cholerae* Projekt wurde in Kollaboration mit dem Department of Molecular Biology and Umeå Centre for Microbial Research (Prof. Sun Nyunt Wai) der Umeå University, Schweden, durchgeführt. Die Beiträge der Kollaborationspartner sind in den jeweiligen Textpassagen kenntlich gemacht.

Lebenslauf

Harald Bielig

Geburtstag und -ort: 20.02.1981, Neuss

Gottesweg 23
50969 Köln

Telefon: 0176-22382796

E-mail: harald.bielig@hotmail.de

Ausbildung

Promotionsstudium

November 2007- April 2012

Institut für Medizinische Mikrobiologie, Immunologie und Hygiene des Klinikums der Universität zu Köln (PD Dr. Thomas A. Kufer).

Note: Magna Cum Laude

Dissertationsthema: Screening for components involved in NLR-mediated immune signalling.

Studium

Oktober 2001-März 2007

Biologiestudium an der Heinrich-Heine-Universität Düsseldorf

Note: Ausgezeichnet (1,26)

Diplomarbeitsthema: Identifizierung und Charakterisierung von Proteinen, die mit dem Ubiquitin-ähnliche (UBL)-Domäne Protein Mdy2 von *Saccharomyces cerevisiae* interagieren.

Schulbildung

August 1991-Juni 2000

Gymnasium Norf, Neuss. Abiturnote: 2,2

Auslandsaufenthalte / Praktika

September 2005-Dezember 2005

Praktikum am Turku Centre for Biotechnology, University of Turku and Åbo Akademi University, Turku, Finnland.

Mai 2004- August 2004

Praktikum an der Université de Nantes, Frankreich.

September 2003- Mai 2004

ERASMUS-Studium an der Université de Nantes, Frankreich.

Wissenschaftliche Beiträge

Publikationen

A role for quorum sensing in regulating innate immune responses mediated by bacterial outer membrane vesicles (OMVs). **Bielig H**, Dongre M, Zurek B, Wai SN and Kufer TA. *Gut Microbes*. 2011 Sep 1;2(5).

Cell-Based Reporter Assay to Analyze Activation of Nod1 and Nod2.
Zurek B, **Bielig H**, Kufer TA. *Methods Mol Biol*. 2011;748:107-119. PMID: 21701969

NOD-like receptor activation by outer-membrane vesicles (OMVs) from non-O1 non-O139 *Vibrio cholerae* is modulated by the quorum sensing regulator HapR. **Bielig H**, Rompikuntal PK, Mitesh D, Zurek B, Lindmark B, Ramstedt M, Wai SN and Kufer TA. *Infection and Immunity*. 2011 Apr;79(4):1418-27.

Anti-inflammatory Arene--Chromium Complexes Acting as Specific Inhibitors of NOD2 Signalling. **Bielig H**, Velder J, Saiai A, Menning M, Meemboor S, Kalka-Moll W, Krönke M, Schmalz HG, Kufer TA. *ChemMedChem*. 2010 Dec 3;5(12):2065-71.

The yeast ubiquitin-like (UBL)-domain protein Mdy2 is required for microtubule-directed nuclear migration and localizes to cytoplasmic granules in response to heat stress. Cohnen A, **Bielig H**, Hollenberg CP, Hu Z, Ramezani-Rad M. *Cytoskeleton*. 2010 Oct;67(10):635-49.

A function for AAMP in Nod2-mediated NF-kappaB activation. **Bielig H**, Zurek B, Kutsch A, Menning M, Philpott DJ, Sansonetti PJ, Kufer TA. *Molecular Immunology*. 2009 Aug;46(13):2647-54.

Patent

EPO patent: EP 10 150 691.3; „Arene chromium-carbonyl complexes, a method for the preparation of and use of as pharmaceutical“. **Bielig H**, Velder J, Krönke M, Schmalz HG, Kufer TA, 13.01.2010 (laufendes PCT-Verfahren)

Konferenzen

Tag der Molekularen Medizin (Ulm, April 2012). Vortrag mit dem Titel „High-throughput siRNA screening reveals XIAP as essential factor for NOD1-mediated innate immune signalling“.

Molecular Life Science 2011 (Frankfurt am Main, September 2011). Kurzvortrag und Poster mit dem Titel „High-throughput siRNA screening reveals XIAP as essential factor for NOD1-mediated innate immune signalling“.

Keystone Symposium *Innate Immunity: Mechanisms linking with adaptive immunity* (Dublin, Juni 2010). Präsentation eines Posters mit dem Titel „Quorum sensing controls NOD1/2 activation by *Vibrio cholerae* outer-membrane vesicles“.

International Symposium *Signal Transduction and Disease* (Aachen, September 2009). Präsentation eines Posters mit dem Titel „Identification of chemical inhibitors of Nod2 signalling“.

Luminy Advanced Course in Immunology der Université Marseille-Luminy, sowie EMBO-workshop *Visualizing Immune System Complexity* (Marseille, Januar 2009). Präsentation eines Posters mit dem Titel „Identification of chemical modulators of Nod1 and Nod2 signalling“.

Jahrestagung des Vereins für Allgemeine und Angewandte Mikrobiologie (VAAM) (Osnabrück, April 2007). Präsentation eines Posters mit dem Titel: „Mdy2, a ubiquitin-like (UBL)-domain protein, is involved in regulation of microtubular dynamics and nuclear movement in budding yeast“.